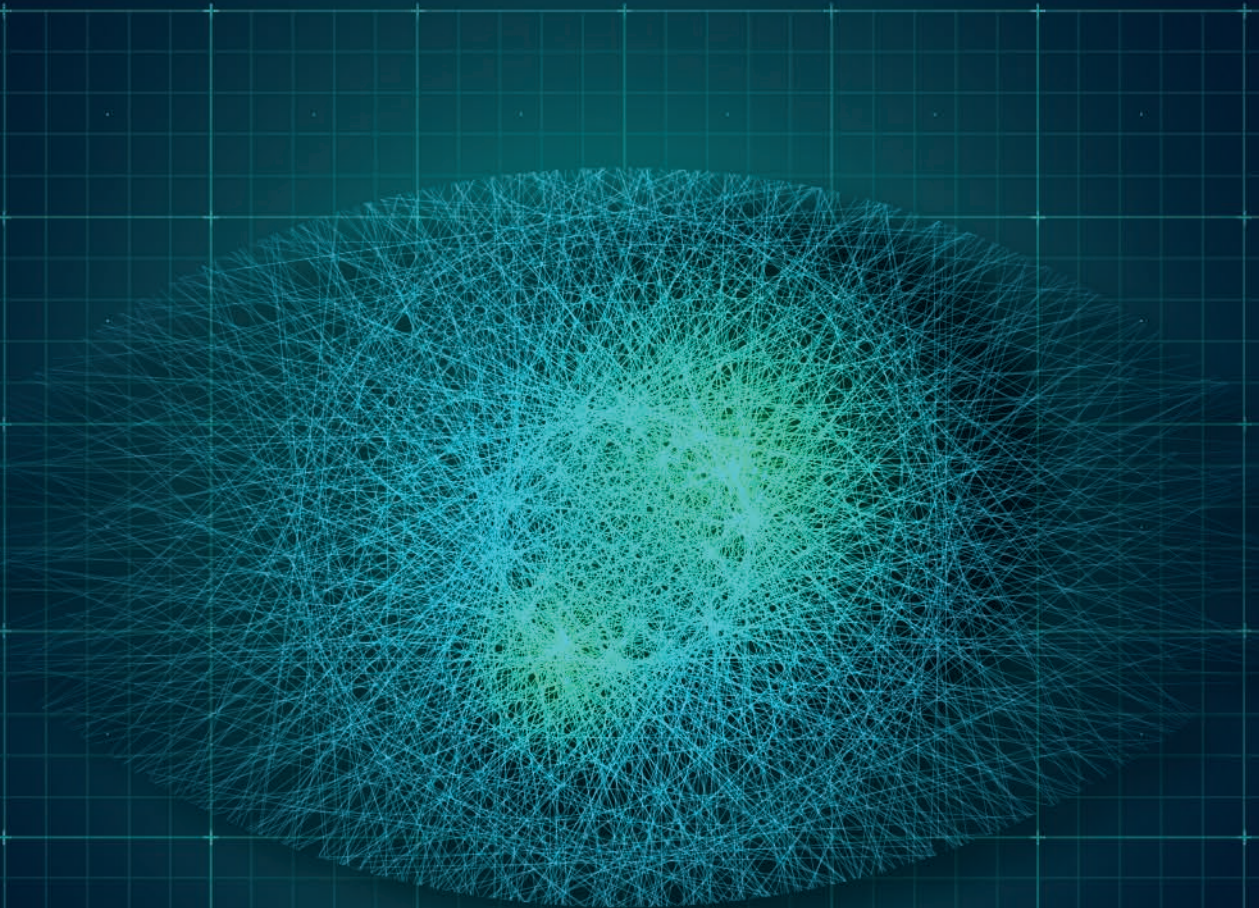


Multimodal Imaging in DME

An update on biomarkers for clinical practice



Mariacristina Parravano - Stela Vujosevic
Gilda Cennamo - Luca Di Antonio - Maria Oliva Grassi - Marco Lupidi
Marco Rispoli - Maria Cristina Savastano - Daniele Veritti

Multimodal Imaging in DME

An update on biomarkers for clinical practice

MULTIMODAL IMAGING IN DME

ISBN: 9788897719519

Health Publishing & Services S.r.l.

Milan, Piazza Duca d'Aosta 12; Rome, Piazza di San Silvestro 8

Copyright © 2022 Health Publishing & Services S.r.l. All rights reserved. www.hpsitaly.healthcare

Editor in Chief: Giulio Zuanetti

Printed by Geca S.r.l. (San Giuliano Milanese - MI) on August 2022

Graphic Project

Marco Marsala

Layout

The Graphic Forge

This publication and its contents are protected by copyright and may not be reproduced, whether in whole or in part and in any format, language and country without specific written consent by the copyright holder.

Editor's note: highest editorial and production standards have been applied for this publication. Nevertheless the publisher declines any responsibility for errors, omissions and/or inaccuracies, and for any consequences derived from the information contained. For any image included in this publication for which permission has not been obtained, the publisher is available to recognize the copyright.

The statements, opinions and data contained in this publication are solely those of the individual authors and contributors and do not reflect the opinion of the editor and the publisher. The editor and publisher disclaim responsibility for any injury to persons or property resulting from any idea or products referred to in this publication. The information presented in this publication does not replace the Summary of Product Characteristics which the reader should refer to.

This publication is addressed to medical professionals only and not for the general public.

This special edition has been published for distribution at congress venues

This publication was supported by an unrestricted grant from *Novartis Farma S.p.A.*

NVR239-21_LIB

Authors

Mariacristina Parravano

IRCCS Fondazione G.B. Bietti, Rome

Stela Vujosevic

University of Milan, IRCCS MultiMedica, Milan

Gilda Cennamo

University of Naples Federico II, Naples

Luca Di Antonio

ASL-1 Avezzano-Sulmona, L'Aquila

Maria Oliva Grassi

AOU Policlinico, University of Bari, Bari

Marco Lupidi

S. Maria della Misericordia Hospital, University of Perugia, Perugia

Marco Rispoli

Eye Hospital, Rome

Maria Cristina Savastano

Fondazione Policlinico Universitario A. Gemelli IRCCS, Catholic University "Sacro Cuore", Rome

Daniele Veritti

University of Udine, Udine

Multimodal Imaging in DME

An update on biomarkers for clinical practice

Summary

Foreword	IX
1. Introduction	1
Treatment of diabetic macular edema	4
Evolution of diabetic macular edema classification in clinical practice	7
References	11
2. Non-invasive imaging of diabetic macular edema	14
Optical coherence tomography	14
Patterns of diabetic macular edema	14
Hyperreflective foci	14
Disorganization of retinal inner layers	16
Integrity of the ellipsoid zone	18
Optical coherence tomography angiography	18
Overview	18
Non-perfusion areas	22
Foveal avascular zone	24
Microaneurysms	24
Correlation between retinal capillary plexuses and the inner/outer retina	28
References	29
3. Ultrawide-field imaging evaluation of diabetic macular edema	32
Multicolor fundus imaging and ultrawide-field color fundus photography	32
Ultrawide-field fluorescein angiography	32
Ultrawide-field optical coherence tomography angiography	34
References	39
4. Clinical cases	40
Clinical case 1	40
Clinical case 2	42
Clinical case 3	44
5. Future perspectives	47
Artificial Intelligence applications for diabetic retinopathy and diabetic macular edema	47
References	51

Foreword

Our understanding of diabetic retinopathy (DR) has evolved, over the past few decades, from the concept of purely microvascular disease to the recognition that events including neurovascular dysfunction and chronic local inflammation underly the pathogenesis of diabetic macular edema (DME). Remarkable technological advances in retina imaging have played a crucial role. Fundus fluorescein angiography (FA), wide-field (WF) and ultrawide-field (UWF) techniques, optical coherence tomography (OCT), and OCT angiography (OCTA) are the milestones of this fascinating journey. FA has highlighted the role of peripheral non-perfusion and ischemia and has shown that non-perfusion correlates with neovascularization. WF and UWF techniques have made peripheral regions of the retina accessible to investigation. OCT has revealed novel structural features of DME that correlates with disease severity, response to treatment and visual prognosis. OCTA has further refined our knowledge of diabetes related vascular abnormalities.

These advances have been paralleled by the development of multiple treatment options for DME, including the intravitreal injection of anti-VEGF agents and corticosteroids, leading to considerable improvements of vision outcomes. As for developments that we can expect soon, artificial intelligence (AI) based tools for the evaluation of retinal images are attracting great interest for the speed, efficiency, and accuracy of their performance.

This book, coauthored by nine retina experts, is directed to ophthalmologists, diabetologists and general practitioners and aims to provide an overview of the major achievements of retinal imaging in the management of DME. Chapter 1 reviews current knowledge of DR and DME and describes the ongoing efforts to define and classify DME. Chapter 2 presents DME-related retinal features visualized by OCT/OCTA, while Chapter 3 reviews the findings of studies using WF/UWF techniques applied to FA and OCTA. The emphasis of Chapters 2 and 3 is on the studies that have tested the predictive and/or prognostic values of the identified parameters and their ability to assess the response to anti-VEGF treatment. Chapter 4 presents three cases of patients with long-standing diabetes treated with anti-VEGF agents and assessed by multimodal imaging in the authors' clinical practice. Finally, Chapter 5 discusses the application of machine-learning to DR screening and management.

I believe this book will offer to clinicians useful and updated information about current imaging techniques for retina assessment in DR and DME. The comprehensive collection of images throughout the book will be greatly appreciated by readers.

Francesco Bandello

Department of Ophthalmology, Scientific Institute,
Vita-Salute San Raffaele University, Milan, Italy

1. Introduction

In the first chapter we will review current knowledge of diabetic retinopathy and diabetic macular edema. Focusing attention on the pathogenesis, diagnosis, classification, and treatment algorithm for patients with diabetic macular edema

D iabetic macular edema (DME) is a common sight-threatening disease. It is the major cause of central vision loss in working-age individuals affected by diabetic retinopathy (DR) and particularly in those with type 2 diabetes. It has been estimated that about 30 million people are affected by DME worldwide, a number that will likely grow as the prevalence of DR is steadily increasing. The global prevalence of DME has been estimated to 6.8%^[1]. DME prevalence increases with the duration and severity of DR: in adults with a ≥ 20 -year history of diabetes it is approximately 30%, while in adults with proliferative DR it increases to 71%^[2].

DME is the intraretinal accumulation of fluid caused by the disruption of the blood-retinal barrier. The Early Treatment Diabetic Retinopathy Study (ETDRS) defined DME as a retinal thickening, or presence of hard exudates, within one disk diameter of the center of the macula^[3]. Furthermore, the ETDRS defined DME severity and issued treatment guidelines^[3]. Modifiable systemic risk factors, including elevated blood levels of glycosylated hemoglobin (HbA1c) and high blood pressure, are associated with the development of DR and DME^[4,5]. It has been hypothesized that the early and tight control of systemic risk factors may reduce the occurrence of both DR and DME, particularly in type 1 diabetes. The pathogenesis of DME is complex and multifactorial, with the hyperglycemic state associated with diabetes playing a pivotal role in inducing microangiopathy. Hyperglycemia activates different metabolic pathways leading to increased hypoxia, reactive oxygen species formation, and inflammation^[6]. Inflammation is a key player in the pathogenesis and persistence of DME through the release of cytokines, chemokines, and growth factors from retinal pigment epithelium cells, retinal glial Müller cells, and activated microglia. These inflammatory mediators cause

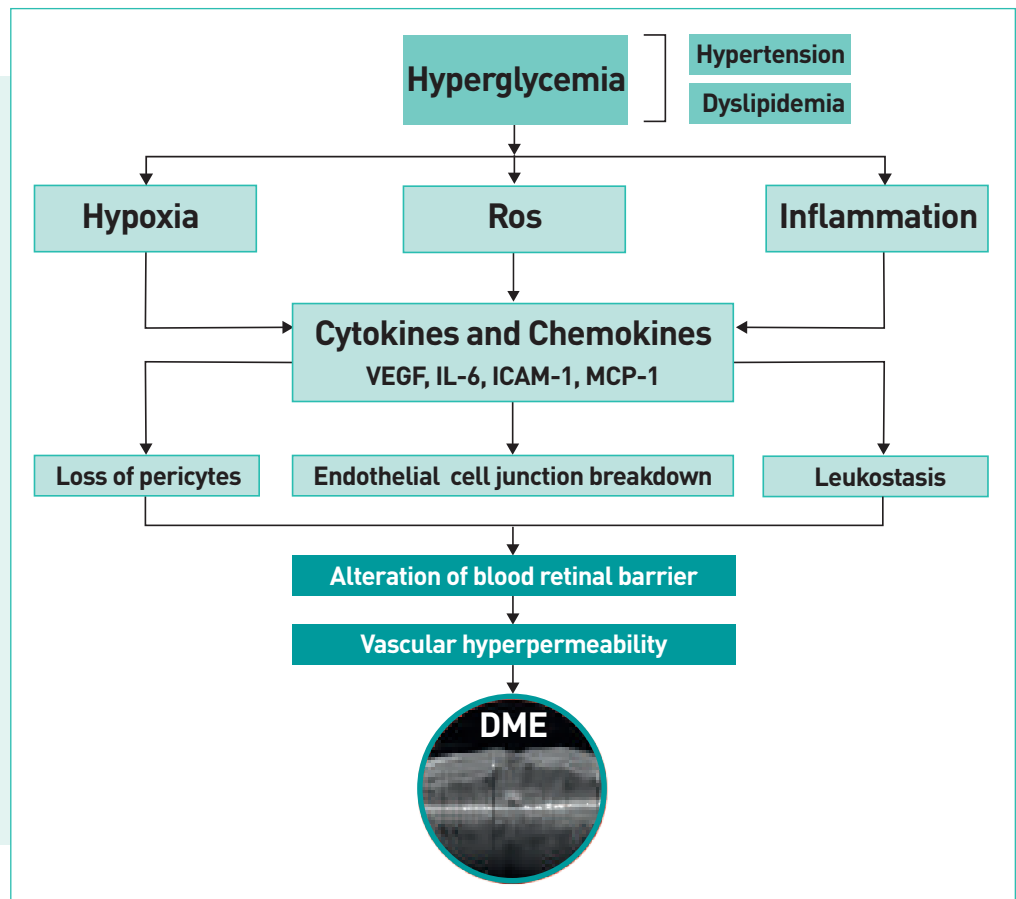
endothelial cell junction breakdown, loss of pericytes, and leukostasis resulting in alterations of the blood-retinal barrier and vascular hyperpermeability due to the increased production of vascular endothelial growth factor (VEGF), which eventually leads to DME formation (Figure 1).

Early screening for DR may facilitate timely referral to an ophthalmologist; it is therefore recommended for the prevention and/or timely treatment of DR and DME. Technical advances in retinal imaging have significantly contributed to the early diagnosis and management of DME. Color fundus photography is helpful for screening patients with DR and DME and monitoring disease progression. This technique visualizes typical disease features including microaneurysms, retinal hemorrhages, intraretinal microvascular abnormalities, venous dilation and beading, and soft and/or hard exudates.

Fluorescein angiography (FA) is a dye-based invasive technique able to detect areas of capillary non-perfusion, neovascularization, macular ischemia, and to differentiate between focal and diffuse macular edema^[7]. Focal macular edema is characterized by the presence of localized areas of retinal thickening associated with focal leakage of clusters of microaneurysms. Diffuse macular edema is a more generalized and chronic form of edema caused by widespread macular leakage and evidenced by the pooling of dye in retinal cystoid spaces. FA examination has long been considered the gold standard for assessing DR and DME severity and for guiding appropriate and targeted laser treatment^[7]. However, FA is an invasive and time-consuming examination and an increasing number of ophthalmologists base DME treatment decisions on optical coherence tomography (OCT) scans only^[8].

Since its introduction, OCT has made DME evaluation faster, more precise and more re-

Figure 1. Pathophysiology of DME. Hyperglycemia activates different pathways leading to increased hypoxia, reactive oxygen species formation, and inflammation with production of cytokines and chemokines. These mediators cause endothelial cell junction breakdown, loss of pericytes, and leukostasis, resulting in alterations of the blood-retinal barrier and retinal vascular hyperpermeability, and DME formation. Hypertension and dyslipidemia may also contribute to the pathogenesis of DME. DME, diabetic macular edema; ICAM-1, intercellular adhesion molecule-1; IL-6, interleukin-6; MCP-1, monocyte chemoattractant protein-1; ROS, reactive oxygen species; VEGF, vascular endothelial growth factor.



liable^[9]. The OCT technique allows to measure central retinal thickness (CRT), a quantitative parameter that has proven useful for assessing DME severity and response to treatment. CRT is however not a surrogate marker of visual acuity (VA), because of the poor correlation between CRT and VA changes over time. OCT also allows to see relevant morphological features such as hyporeflective cavities caused by intraretinal and/or subretinal fluid accumulation, and hard exudates, which appear as hyperreflective spots.

Advances in OCT software have increased imaging resolution, leading to the identification of different DME patterns, namely: i) diffuse retinal thickening type; ii) cystoid macular edema type; iii) serous retinal detachment type^[10]. More recently, the OCT technique has allowed to identify two DME phenotypes that differ both for the presence of characteristic biomarkers and for distinct responses to treatment^[11]. These are the vascular DME phenotype and the inflammatory DME phenotype. The vascular DME phenotype is predominantly due the dysfunction of the inner blood-retinal barrier and responds to anti-VEGF therapy (Figure 2A and B). The inflammatory

DME phenotype seems to respond better to steroids (Figure 2C and D). This phenotype has been associated with increased levels of cytokines in the vitreous and aqueous humor of patients with DME^[12], which contribute to functional and structural retinal changes by affecting endothelial cells, pericytes, Müller cells, microglial cells, and cells of the retinal pigment epithelium.

Potential inflammatory biomarkers of DME have been identified using OCT. It has been suggested that the presence of multiple hyperreflective foci (HRF), corresponding to activated microglia, as well as the presence of serous retinal detachment, caused by the dysfunction of the outer blood-retinal barrier and retinal pigment epithelium cells, may be considered as hallmarks of inflammation^[13,14]. The presence of serous retinal detachment was reported in 36.5% of the eyes with DME, and was related to an increased number of HRF^[14] and high levels of interleukin (IL)-6, which supports the role of serous retinal detachment as biomarker of inflammation^[12].

Another potential biomarker of DME outcomes identified via OCT is the disorganization

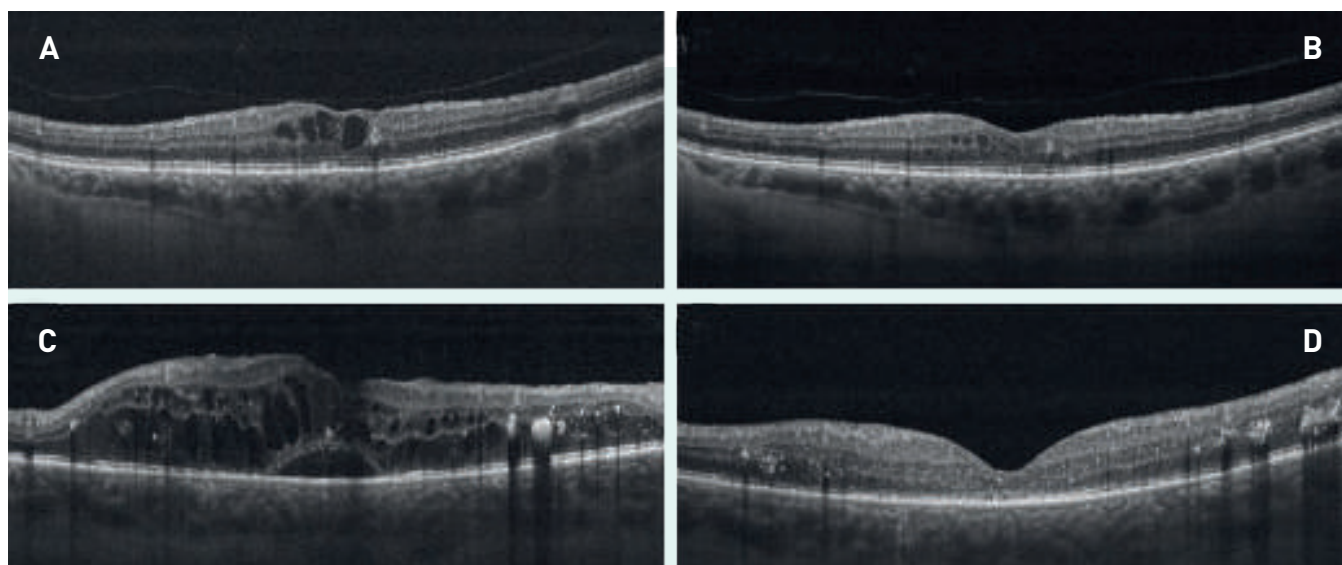


Figure 2. OCT images of the vascular and inflammatory phenotypes of DME before and after treatment. A, Vascular DME phenotype at baseline. B, Resolution of intraretinal fluid in the same patient after intravitreal injection of anti-VEGF. C, Inflammatory DME phenotype. D, Resolution of both intraretinal fluid and subretinal detachment, as well as of several hyperreflective foci, in the same patient after sustained administration of steroids via an intravitreal implant.

of retinal inner layers (DRIL). DRIL, defined as the horizontal extent over which no boundaries between the ganglion cell layer-inner plexiform layer complex, inner nuclear layer, and outer plexiform layer can be identified, has been proposed as a reliable biomarker of VA in patients with ongoing or resolved center-involving DME^[15]. Recently, a correlation between changes in DRIL extension and changes in VA following treatment has been hypothesized. Indeed, a reduction in inflammation may be expected to have a positive effect on the architecture of Müller cells resulting in decreased DRIL extension and, ultimately, VA improvement^[16]. Other retinal morphologic changes have been correlated to visual outcomes: the disruption of the external limiting membrane and the photoreceptor layers (ellipsoid zone) have been associated with poor VA improvement^[17]. Thus, the evaluation of pre-treatment VA and photoreceptor status may predict potential restoration of photoreceptor integrity and subsequent visual recovery in DME patients. In addition, OCT has improved the visualization of vitreomacular traction, another relevant factor in the development and/or persistence of DME.

The introduction of OCT angiography (OCTA) and wide-field/ultrawide-field (WF/UWF) imaging has also contributed to the identifica-

tion of new clinical biomarkers that can identify disease at an early stage and predict response to treatment of DME. OCTA is a fast, safe, and non-invasive method for imaging retinal and choroidal microcirculation^[18]. This technique is based on motion contrast imaging and it detects the normal movement of red blood cells in the retinal capillaries by distinguishing flow signals in the vessels from static tissues. Motion contrast is measured by decorrelation signals (differences in the back-scattered OCT signal intensity or amplitude) between sequential OCT B-scans performed in the same retinal location^[19]. OCTA is a valuable tool for assessing the reliability of foveal avascular zone (FAZ) area measurement^[20], as a well as the severity and progression of DR^[21]. Although FA is able to detect a greater number of microaneurysms than OCTA, OCTA allows the visualization of microaneurysms that appear as focally dilated saccular or fusiform capillaries of the superficial capillary plexus as well as the deep capillary plexus, and of areas of retinal non-perfusion. In addition, OCTA has proven reliable for assessing the density of the superficial and deep capillary plexuses^[21], showing early vessel density reduction in the deep capillary plexus compared to the superficial capillary plexus^[22]. It has been highlighted that the deep capillary plexus may

be more vulnerable to ischemic injury than the superficial capillary plexus. Therefore, the deep capillary plexus may undergo greater dilation and rarefaction, leading to a poorer and slower response to DME treatment^[23]. More recently, a committee of retinal experts of the European Vision Clinical Research network reviewed the available evidence on the use of OCTA as imaging biomarker in DR and DME^[24]. The committee pointed out the need to standardize the OCTA nomenclature and the use of qualitative and quantitative parameters for improving the measurement accuracy. Although OCTA has extensively validated the use of biomarkers for assessing DR (early diagnosis, disease progression, and treatment response), its use in DME presents several limitations due to the high rates of segmentation errors caused by changes in retinal architecture and artifacts on the vascular network caused by the presence of intra/subretinal fluid^[24]. Nevertheless, OCTA has identified macular ischemia as an important cause of VA loss and as a marker of poor response to any kind of treatment. Currently, OCTA parameters that can be considered as biomarkers of response to DME treatment are: FAZ size^[21], microaneurysm features (internal reflectivity, number, and location)^[25], vessel density in superficial capillary plexus and deep capillary plexus^[21], and extent of non-perfusion areas. In conclusion, the integration of both OCT and OCTA data is highly recommended for the assessment of DME biomarkers.

As for UWF imaging, UWF FA is helpful for detecting peripheral non-perfusion areas and neovascularization. It has been speculated that ischemic areas act as a source of inflammatory cytokines and VEGF, which in turn lead to DME development. The identification of peripheral ischemia should be used as biomarker during treatment. It is well established that targeted laser treatment of non-perfused areas can block cytokines release and improve DME^[26].

Today multimodal retinal imaging is considered the gold standard approach for deciding the treatment protocol and for predicting the outcome of DME patients (**Figure 3**). Furthermore, new technologies, including peripheral OCT, WF OCTA, and artificial intelligence (AI), may provide additional predictive power in the assessment of DR and DME. AI and deep learn-

ing are being increasingly used for detecting eye disease in patients with diabetes and for guiding therapeutic decisions^[27].

Treatment of diabetic macular edema

Recent advances in the management of DME have revolutionized our daily clinical practice. In the early pioneering studies, laser treatment emerged as the best therapeutic option compared to sham treatment. Treatment according to the ETDRS consisted of a combination of focal treatment of individual leaking microaneurysms and grid treatment of areas of diffuse leakage and capillary non-perfusion. The ETDRS introduced the definition of clinically significant macular edema and demonstrated a 50% reduction in the risk of moderate visual loss in patients with clinically significant macular edema treated by focal photocoagulation^[28]. However, only 3% of the patients achieved an improvement of VA. Another randomized clinical trial, conducted by the Diabetic Retinopathy Clinical Research (DRCR) Network, showed that laser treatment was more effective than intravitreal injection of triamcinolone acetonide in phakic patients^[29]. In this study, 21% of laser-treated patients achieved VA improvement at 2 years, suggesting a delayed benefit of photocoagulation^[29]. The introduction of sub-threshold grid laser treatment, which avoids retinal damage caused by thermal spreading, was shown to achieve similar functional and morphological outcomes while minimizing the destructive effects of conventional photocoagulation^[30]. Furthermore, laser treatment may also have the advantage of reducing the burden of frequent intravitreal injections. Currently, retinal specialists reserve laser treatment only to DME with no center involvement of the macula and, in particular, to the vasogenic subtype of DME, which is characterized by the presence of focally grouped microaneurysms and leaking capillaries.

The advent of intravitreal agents for the treatment of center-involving macular edema with VA impairment has changed considerably DME management. In detail, intravitreal agents

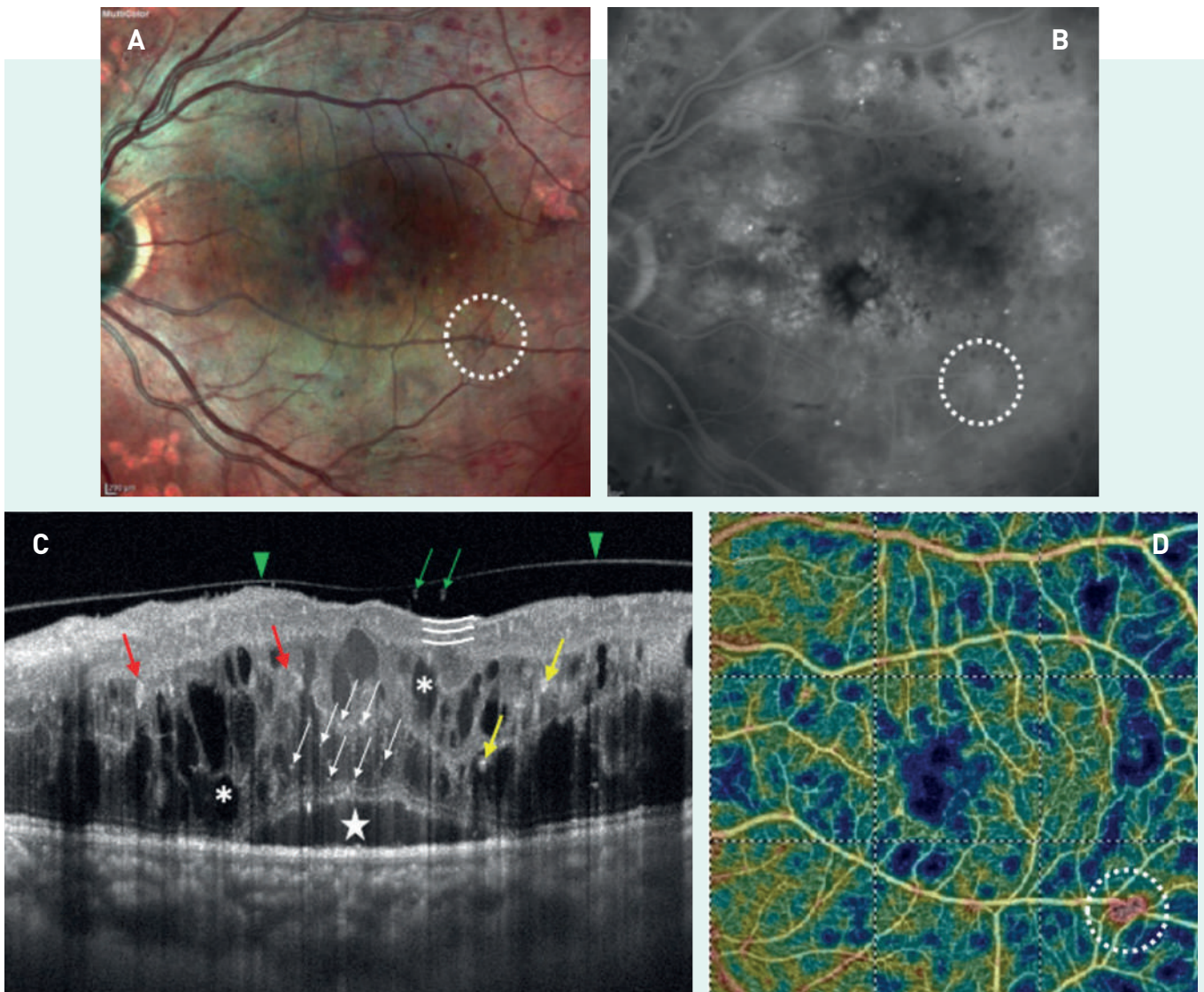
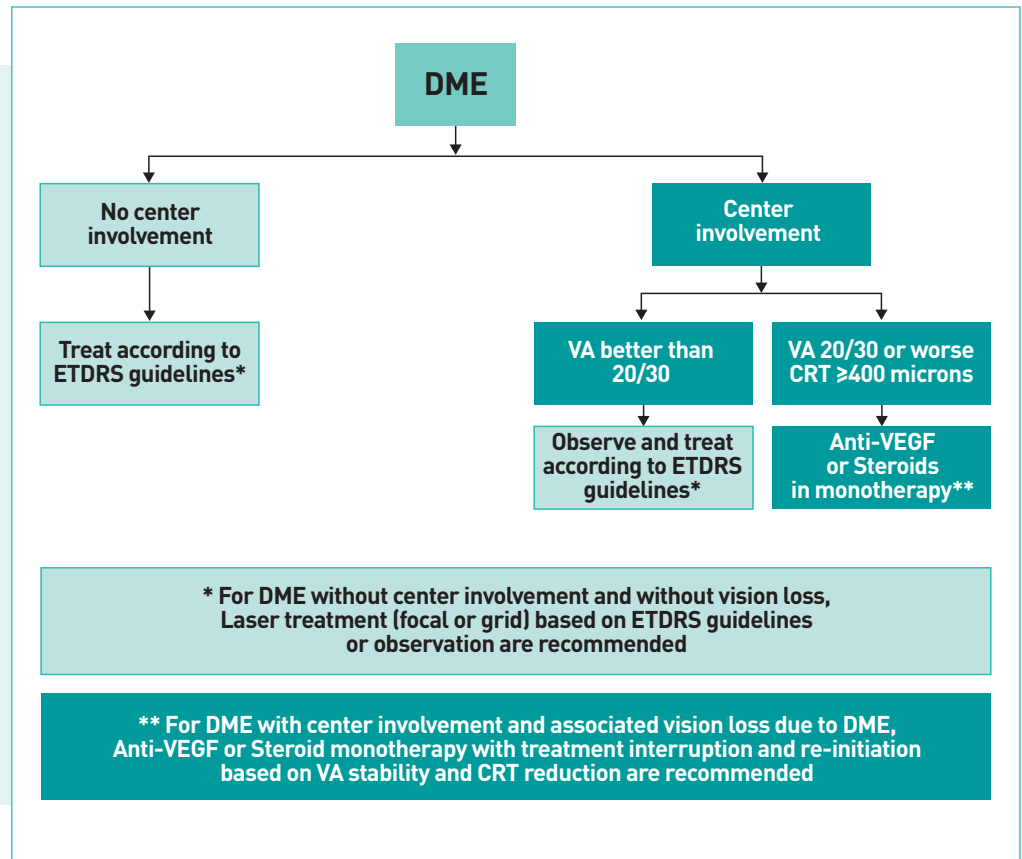


Figure 3. Multimodal retinal imaging of a patient affected by DME. A, Color fundus photography showing severe proliferative diabetic retinopathy with neovascularization elsewhere (dotted circle), laser scarring, and DME. B, FA showing diffuse leakage and pooling of dye with the typical “petaloid” feature of DME. C, Spectral-domain OCT showing inflammatory DME findings such as: posterior hyaloid detachment (green arrowheads); vitreous highly-reflective dots (green arrows); disorganization of retinal inner layers (white lines); hard exudates with shadowing effect (yellow arrows); microaneurysms (red arrows); cystoid spaces (asterisks); hyperreflective foci (white arrows); and subretinal detachment (star). D, Color coded OCTA showing enlargement of the foveal avascular zone, non-perfused areas (the colder the color the lower the flow), and neovascularization elsewhere missed on FA (dotted circle).

targeting VEGF include three agents; of note, one of them is not licensed for intravitreal injection and its use in patients with DME is therefore off-label. Agents acting on the inflammatory cascade include sustained-release steroid intravitreal implants such as dexamethasone (first- or second-line treatment) and fluocinolone acetonide (third-line treatment). Clinical trials evaluating these agents have shown good functional and anatomical responses in selected patients with DME^[31-34]. Based on a review of the published literature, an international panel of experts developed an algorithm

for the treatment of DME with or without center involvement (Figure 4)^[35]. The DRCR.net Protocol T study showed that all three anti-VEGF drugs quickly improved VA in eyes with DME at 1 year^[36]. In eyes with better baseline VA (Snellen 20/40 or better) no statistically significant differences among the three agents were reported. However, in eyes with worse baseline VA (Snellen 20/50 or worse), an anti-VEGF achieved greater improvement of VA compared to the other two agents. The safety profile of the three agents was similar, but several estimates of cardiovascular events and mortality

Figure 4. Treatment algorithm for DME (modified from ref.^[35]). DME, diabetic macular edema; ETDRS, Early Treatment Diabetic Retinopathy Study; VA, visual acuity; CRT, central retinal thickness; anti-VEGF, anti-vascular endothelial growth factor.



may have been inaccurate. Studies comparing the three anti-VEGF agents in the long-term are needed. It should also be reminded that about 50% of diabetic patients die because of a cardiovascular event. Prior to starting any pharmacologic treatment, a careful medical history evaluation (including diabetes control, recent stroke or cardiovascular events, and other comorbidities) is recommended (Table 1). A comprehensive ophthalmologic examination is also recommended (to detect glaucoma or other eye diseases, evaluate the lens status, grade DR, and enquire about a possible history of vitrectomy), along with the careful eval-

uation of previous treatments, particularly in DME patients with a poor response to current treatment (Table 1).

According to international guidelines for the management of DME, treatment with anti-VEGF should start with a loading phase (4-6 monthly injections of anti-VEGF), followed by a maintenance phase with monthly or bimonthly intravitreal injections. In the maintenance phase, the treatment can be administered as needed (pro re nata [PRN] regimen), or according to a treat-and-extend regimen (TER)^[37].

With regard to intravitreal steroids, dexamethasone intravitreal implant is suitable for

Table 1. Emerging strategies for DME management: when and how to use anti-VEGFs or steroids. *In non-responders to anti-VEGF (after 4-6 injections) it is reasonable to shift to steroids (consider as a suboptimal response to anti-VEGF a VA gain of 5 letters or less, or a less than 20% CRT reduction).

ANTI-VEGFs	STEROIDS
No recent cardiovascular events (3-6 months)	Recent cardiovascular events (3-6 months)
Younger patients	Vitrectomized eyes
Clear lens or aphakia	Pseudophakia
Advanced or uncontrolled glaucoma	Patient with risk of non-compliance
History of ocular infection (herpes, toxoplasmosis)	Non-responder* to anti-VEGFs
Proliferative diabetic retinopathy with DME	

treatment-naïve DME, according to recent guidelines^[38]; the treatment can be repeated on average every 5 months or it can be administered as needed^[38]. Fluocinolone acetonide is indicated for chronic DME, particularly in patients insufficiently responsive to the available treatments^[38]. Although fluocinolone acetonide intravitreal implant has an extended durability (about 3 years), additional intravitreal injections of anti-VEGF may be required in some patients. However, intravitreal steroids are associated with increased rates of cataract progression and glaucoma. They may be considered for patients with ocular hypertension if this is controlled by topical treatment. Advantages of steroids over anti-VEGF agents include the reduction of treatment burden, as well as a predictable pharmacokinetics even in vitrectomized eyes.

The presence of vitreomacular traction, as an effective tangential or anterior-posterior vector force (detected using OCT), usually leads to worsening of DME. Patients with vitreomacular traction can be treated with anti-VEGF or steroids. If DME and traction persist, pars plana vitrectomy with or without peeling of the internal limiting membrane should be performed. However, no statistically significant differences in VA gain have been reported between the two surgical interventions^[39].

Given the complexity of DME, only a tailored approach will provide the best treatment strategy to each patient. Although anti-VEGF agents and steroids are the current standard of care in DME, several important unmet needs remain, including the burden of frequent intravitreal injections and the maintenance of VA gains in the long-term. New drugs, with an improved pharmacokinetic profile compared to conventional anti-VEGFs, or targeting other pathways involved in the pathogenesis of DME, are currently evaluated in clinical trials and will be available soon.

Evolution of diabetic macular edema classification in clinical practice

Over the past decades considerable efforts have been devoted to the definition and classification

of DR, as both processes are crucial for deciding when and how to treat affected eyes, and for predicting outcomes. DME is the most relevant DR-related retinal lesion. Indeed, DME is the main cause of vision loss in patients with DR and one of the few targets of available treatments. The initial attempts to find a consensus on DR among retina specialists date back to more than fifty years ago. These attempts were prompted by the growing number of diabetes patients living long enough to develop vision loss, a consequence of the increased life expectancy of the diabetic population achieved thanks to the improved efficacy of systemic therapies for diabetes control. The development of FA leading to the visualization and measurement of the typical DR-related lesions (capillary occlusion, leakage, neovascularization) also contributed to the need for a shared definition and classification of DR.

The Airlie House Symposium held in 1969 was the first meeting of DR specialists. Its objectives included the classification of DR based on stereoscopic fundus photography, the description of the natural history of DR, the identification of a relationship between DR and metabolic control, and the evaluation of the efficacy of photocoagulation^[40]. The first classification of DR was published in 1984 by the Wisconsin Epidemiology Study of DR (WESDR) research group. The WESDR group defined DME as “thickening of the retina with or without partial loss of transparency, within one disc diameter from the center of the macula” and provided the first grading of DME based on fundus photographs^[41]. In 1985, the ETDRS published Report 1 describing the results of a prospective study evaluating the efficacy of photocoagulation in the treatment of DME^[3]. Based on stereoscopic fundus photography, macular edema was considered clinically significant (CSME) if one of the following features was present: retinal thickening at or within 500 μm of the center of the macula; hard exudates at or within 500 μm of the center of the macula, if associated with thickening of adjacent retina; a zone or zones of retinal thickening one disc area or larger, any part of which is within one disc diameter of the center of the macula^[3]. Based on FA, the study also identified the areas to be targeted by photocoagulation treatment and provided indications on how to administer treatment (focal or grid laser photocoagulation)^[3]. Finally,

the study demonstrated that patients with CSME had significant benefits in terms of VA with early treatment. A review published in 1986 provided a classification of DME based on the leakage seen with FA and distinguished between focal and diffuse leakage^[42]. This review also suggested distinct origins of macular edema (clusters of microaneurysms and hard exudates for focal edema, and damage of the blood-retinal barrier for diffuse edema), requiring distinct treatment strategies (focal and grid laser treatment, respectively); a third form of edema (diffuse edema that develops or worsens following panretinal photocoagulation) was also recognized. Furthermore, the concept of macular ischemia (the extensive occlusion of capillaries and arterioles), which can complicate macular edema and limit the functional recovery following treatment, was introduced. In 1991, the ETDRS published Report 7, which provided a new definition of macular edema (thickening of the retina within one disc diameter of the center of the macula; and/or hard exudates in a standard 30° photographic field centered on the macula [field 2], with some hard exudates within one disc diameter of the center of the macula) and refined the definition of CSME provided in Report 1^[43]. In Report 11, also published in 1991, the ETDRS introduced FA parameters for the classification of DR and for guiding treatment choices^[44]. Following parameters were considered: size and outline of the FAZ; capillary loss; increased capillary visibility; abnormalities of the arterioles; defects in the retinal pigment epithelium; fluorescein leakage; source of leakage; cystoid changes^[44]. In a following ETDRS report, FA parameters were used to differentiate between focal and diffuse DME as follows: $\geq 67\%$ of leakage from microaneurysms was classified as focal DME; microaneurysm leakage between 33% and 66%, as intermediate DME; and microaneurysm leakage $\leq 33\%$ as diffuse DME^[45].

The early 2000s were characterized by the introduction of high-resolution digital cameras and the development of UWF techniques, which provided significantly improved fundus images^[46-48]. Despite these advances, a generally accepted, international classification of DR that would be straightforward to use in clinical practice and easy to convey to patients was still missing. To address this unmet need, the American

Academy of Ophthalmology published in 2003 a new, international clinical classification of DR and DME^[49]. Based on three-dimensional eye assessment using a slit lamp or stereoscopic fundus photography, DME was classified as absent (“no apparent retinal thickening or hard exudates in the posterior pole”) or present (“some apparent retinal thickening or hard exudates in the posterior pole”)^[49]. In addition, based on its location with respect to the fovea, DME could be graded as mild (distant from the center of the macula), moderate (approaching the center of the macula but not involving the center), and severe (involving the center of the macula)^[49].

A breakthrough in DR characterization and management was brought about by the introduction of OCT for the non-invasive, cross-sectional imaging of the retina with a 10 μm -resolution^[50]. OCT made it possible to monitor the course of retinal thickness over time and contributed significantly to improve our understanding of DME etiology and pathogenesis. Based on the etiopathogenesis and using OCT, Bandello et al. classified DME as: prevalently retinovascular; tractional; and with taut attached posterior hyaloid^[51]. In a previous study, Otani et al. had provided the first OCT-based classification of retinovascular DME into three morphological patterns of edema, namely sponge-like retinal swelling, cystoid macular edema, and serous retinal detachment^[9]. In a later study, this classification was integrated with FA data to provide four morphologic types that correlated with VA: thickening of the fovea with homogeneous optical reflectivity throughout the whole layer of the retina (type 1); thickening of the fovea with markedly decreased optical reflectivity in the outer retinal layers (type 2); foveal detachment without traction (type 3); foveal detachment with apparent vitreofoveal traction (type 4)^[52].

OCT also allowed to assess DME quantitatively. Panozzo et al. provided the first morphologic classification and grading of DME based on OCT measurements, with the involvement of five parameters: retinal thickness in three points; volume; morphology (three categories of increasing severity, namely, simple thickening, cystoid thickening, and neuroepithelial detachment); diffusion; epiretinal traction^[53]. Taking into account the quantitative classification by Panozzo et al., a subsequent study tried to correlate the vari-

ous DME grades with the following five OCT patterns: diffuse retinal thickening; cystoid macular edema; posterior hyaloidal traction; subretinal fluid/serous retinal detachment; traction retinal detachment^[10]. This classification proved useful because a good correlation of retinal thickening with VA could be demonstrated.

The application of the spectral domain method to OCT imaging improved the visualization of outer retinal layers, that is the external limiting membrane (ELM) and the ellipsoid zone (EZ). The extent of EZ disruption was shown to correlate with VA changes in DME patients^[54], while ELM damage was found to occur before EZ disruption^[55]. As a consequence, ELM assessment was introduced in the OCT-based classifications proposed by several authors, including the staging system by Helmy et al. for cystoid macular edema and the VA-correlated DME patterns described by Kothari et al.^[56,57].

All the OCT-based classifications discussed above did not include the location of edema, and thus foveal involvement, among the parameters considered. The LET classification (LET for Location, Extent, and Traction) included three different locations (central, peripheral, and marginal) among the extent of retinal thickness and the presence or absence of vitreofoveal traction^[58].

The SAVE classification combined OCT and FA parameters and introduced a new form of CSME, namely atrophic edema^[8]. SAVE stands for Subretinal fluid (present or absent), Area (ETDRS fields that show thickening), Vitreoretinal interface abnormalities, Etiology. The etiology item included four different events: focal or multi-focal leakage (seen with FA) with a definable source; non-focal capillary leakage without a definable source; macular or peripheral ischemia; atrophic edema. Atrophic edema was defined as retinal cystoid degeneration without Müller cells and/or disruption of the horizontal layer centrally^[8].

Macular ischemia can be associated with DME. Before the introduction of OCT, this feature was visualized by FA as enlargement of the FAZ and changes in its shape. OCT allowed to detect ischemia indirectly, by revealing the thinning of the ganglion cell layer^[59]. However, this OCT feature may be unreliable if edema is present.

The development of UWF angiography en-

abled the concomitant view of central macular edema, peripheral ischemia, and leakage leading to a new pathogenetic classification of DME into three types: DME arising from leakage associated with parafoveal microaneurysms alone (type A); DME associated with significant peripheral retinal ischemia (>10%) seen as areas of capillary non-perfusion on early- to mid-phase (20-50 seconds) images (type B); DME associated with active perivascular leakage from neovascularization on late-phase (5-7 minutes) images (type C)^[60]. Notably, all three DME types responded to anti-VEGF treatment. A new pathogenetic classification was attempted in 2018, based on fundus photographs and OCT^[61]. Following parameters were considered: CRT, subretinal fluid, intraretinal cysts, and HRF. Four categories of DME were recognized: vasogenic DME, non-vasogenic DME, tractional DME, mixed DME^[61]. Based exclusively on spectral domain OCT, Arf et al. proposed a classification of DME that took retinal cystoid degeneration into account leading to three DME types: diffuse macular edema; cystoid macular edema; cystoid degeneration^[62]. Each type was further subdivided according to the presence of OCT findings including serous macular detachment, vitreomacular interface abnormalities, and hard exudates. The state of ELM and EZ was also considered.

The latest DME classification was published in 2020 by the European School for Advanced Studies in Ophthalmology (ESASO)^[63]. This classification includes seven quantitative and qualitative OCT parameters to stage DME according to four degree of increasing severity, namely early DME, advanced DME, severe DME, and atrophic maculopathy. The seven OCT parameters considered include: foveal thickness; intraretinal cysts; status of the EZ and/or ELM; presence of DRIL; number of HRF; subfoveal fluid, and vitreoretinal relationship. Only the first four parameters are used for DME staging. Early DME is defined by the presence of small intraretinal cysts associated with well-recognizable and detectable inner retinal layers, EZ, and ELM, and increases in central subfoveal thickness and/or macular volume <30% of maximum normal values. This stage of DME is usually associated with good VA and a shorter duration of the hyperglycemic state. Advanced and severe DME are both characterized by the presence of

intraretinal cysts and a central subfoveal thickness $>30\%$ of maximum normal values. The two stages differ however in the EZ/ELM state, with advanced DME having a still visible EZ/ELM and a preserved inner retinal layers segmentation, while severe DME is characterized by mostly undetectable inner retinal segmentation and/or EZ/ELM. The two categories may differ considerably in treatment response and visual outcomes. Finally, macular atrophy is characterized by the complete disruption of the EZ/ELM and by DRIL. Macular atrophy is usually a consequence of long-standing macular edema.

This overview of the most relevant DME classification systems developed over the past fifty years clearly illustrates how the multimodal approach to the visualization of retinal changes induced by diabetes has contributed to advance our understanding of DR. DME classification continues to evolve along with the improvements in retinal imaging to provide tools that combine comprehensiveness and ease-of-use in clinical practice.

In this book, some of the major retina experts (and friends) joined to share their experiences in the field of DR, and DME in particular. In the following chapters, diagnostic and therapeutic aspects, as well as clinical biomarkers, will be discussed in detail and documented with examples of multimodal retinal imaging from clinical practice. This will hopefully improve the accessibility to and usability of clinical information that is often difficult to interpret when attempting to formulate the correct diagnosis and make the appropriate treatment decision.

REFERENCES

- Ogurtsova K, da Rocha Fernandes JD, Huang Y, et al. IDF Diabetes Atlas: global estimates for the prevalence of diabetes for 2015 and 2040. *Diabetes Res Clin Pract* 2017;128:40-50
- Varma R, Bressler NM, Doan QV, et al. Prevalence of risk factors for diabetic macular edema in the United States. *JAMA Ophthalmol* 2014;132:1334-40
- Early Treatment Diabetic Retinopathy Study Research Group. Photocoagulation for diabetic macular edema. Early Treatment Diabetic Retinopathy Study Report Number 1. *Arch Ophthalmol* 1985;103:1796-806
- Aiello LP, DCCT/EDIC Research Group. Diabetic retinopathy and other ocular findings in the Diabetes Control and Complications Trial/Epidemiology of Diabetes Interventions and Complications Study. *Diabetes Care* 2014;37:17-23
- Kohner EM. Microvascular disease: what does the UKPDS tell us about diabetic retinopathy? *Diabet Med* 2008;25(Suppl 2):20-4
- Tangand J, Kern TS. Inflammation in diabetic retinopathy. *Prog Retin Eye Res* 2011;30:343-58
- Kylstra JA, Brown JC, Jaffe GJ, et al. The importance of fluorescein angiography in planning laser treatment of diabetic macular edema. *Ophthalmology* 1999;106:2068-73
- Bolz M, Lammer J, Deak G, et al. SAVE: a grading protocol for clinically significant diabetic macular oedema based on optical coherence tomography and fluorescein angiography. *Br J Ophthalmol* 2014;98:1612-7
- Otani T, Kishi S, Mauyama Y. Patterns of diabetic macular edema with optical coherence tomography. *Am J Ophthalmol* 1999;127:688-93
- Kim BY, Smith SD, Kaiser PK. Optical coherence tomographic patterns of diabetic macular edema. *Am J Ophthalmol* 2006;142:405-12
- Chung YR, Kim YH, Ha SJ, et al. Role of inflammation in classification of diabetic macular edema by optical coherence tomography. *J Diabetes Res* 2019;2019:8164250
- Sonoda S, Sakamoto T, Yamashita T, et al. Retinal morphologic changes and concentrations of cytokines in eye with diabetic macular edema. *Retina* 2014;34:741-8
- Vujosevic S, Bini S, Midena G, et al. Hyperreflective intraretinal spots in diabetics without and with nonproliferative diabetic retinopathy: an in vivo study using spectral domain OCT. *J Diabetes Res* 2013;2013:491835
- Vujosevic S, Torresin T, Berton M, et al. Diabetic macular edema with and without subfoveal neuroretinal detachment: two different morphological and functional entities. *Am J Ophthalmol* 2017;181:149-55
- Sun JK, Lin MM, Lammer J, et al. Disorganization of the retinal inner layers as a predictor of visual acuity in eyes with center-involved diabetic macular edema. *JAMA Ophthalmol* 2014;132:1309-16
- International Retina Group (IRG). Disorganization of retinal inner layers as a biomarker in patients with diabetic macular oedema treated with dexamethasone implant. *Acta Ophthalmol* 2020;98:e217-e223
- Shin HJ, Lee SH, Chung H, Kim HC. Association between photoreceptor integrity and visual outcome in diabetic macular edema. *Graefes Arch Clin Exp Ophthalmol* 2012;250:61-70
- Mastropasqua R, Di Antonio L, Di Staso S, et al. Optical coherence tomography angiography in retinal vascular diseases and choroidal neovascularization. *J Ophthalmol* 2015;2015:343515
- Jia Y, Tan O, Tokayer J, et al. Split-spectrum amplitude-decorrelation angiography with optical coherence tomography. *Opt Express* 2012;20:4710-25
- Carpineto P, Mastropasqua R, Marchini G, et al. Reproducibility and repeatability of foveal avascular zone measurements in healthy subjects by optical coherence tomography angiography. *Br J Ophthalmol* 2016;100:671-6
- Mastropasqua R, Toto L, Mastropasqua A, et al. Foveal avascular zone area and parafoveal vessel density measurements in different stages of diabetic retinopathy by optical coherence tomography angiography. *Int J Ophthalmol* 2017;10:1545-5
- Simonetti JM, Scarinci F, Picconi F, et al. Early microvascular retinal changes in optical coherence tomography angiography in patients with type 1 diabetes mellitus. *Acta Ophthalmol* 2017;95:e751-e755
- Mastropasqua R, Toto L, Di Antonio L, et al. Optical coherence tomography angiography microvascular findings in macular edema due to central and branch retinal vein occlusions. *Sci Rep* 2017;7:40763
- Vujosevic S, Cunha-Vaz J, Figueira J, et al. Standardization of optical coherence tomography angiography imaging biomarkers in diabetic retinal disease. *Ophthalmic Res* 2021;64:871-87
- Parravano M, De Geronimo D, Scarinci F, et al. Progression of diabetic microaneurysms according to the internal reflectivity on structural optical coherence tomography and visibility on optical coherence tomography angiography. *Am J Ophthalmol* 2019;198:8-16
- Wessel MM, Nair N, Aaker GD, et al. Peripheral retinal ischaemia, as evaluated by ultra-widefield fluorescein angiography, is associated with diabetic macular oedema. *Br J Ophthalmol* 2012;96:694-8
- Wu Q, Zhang B, Hu Y, et al. Detection of morphologic patterns of diabetic macular edema using a deep learning approach based on optical coherence tomography images. *Retina* 2021;41:1110-7
- Early Treatment Diabetic Retinopathy Study Research Group. Treatment techniques and clinical guidelines for photocoagulation of diabetic macular edema. Early Treatment Diabetic Retinopathy Study Report Number 2. *Ophthalmology* 1987;94:761-74
- Elman MJ, Bressler NM, Qin H, et al. Diabetic Retinopathy Clinical Research Network. Expanded 2-year follow-up of ranibizumab plus prompt or deferred laser or triamcinolone plus prompt la-

- ser for diabetic macular edema. *Ophthalmology* 2011;118:609-14
30. Lavinsky D, Cardillo JA, Melo LA Jr, et al. Randomized clinical trial evaluating mETDRS versus normal or high-density micropulse photocoagulation for diabetic macular edema. *Invest Ophthalmol Vis Sci* 2011;52:4314-23
 31. Nguyen QD, Brown DM, Marcus DM, et al. Ranibizumab for diabetic macular edema: results from 2 phase III randomized trials: RISE and RIDE. *Ophthalmology* 2012;119:789-801
 32. Heier JS, Korobelnik JF, Brown DM, et al. Intravitreal aflibercept for diabetic macular edema: 148-week results from the VISTA and VIVID Studies. *Ophthalmology* 2016;123:2376-85
 33. Boyer DS, Yoon YH, Belfort R Jr, et al. Three-year, randomized, sham-controlled trial of dexamethasone intravitreal implant in patients with diabetic macular edema. *Ophthalmology* 2014;121:1904-14
 34. Campochiaro PA, Brown DM, Pearson A, et al; FAME Study Group. Sustained delivery fluocinolone acetonide vitreous inserts provide benefit for at least 3 years in patients with diabetic macular edema. *Ophthalmology* 2012;119(10):2125-32
 35. Bandello F, Cunha-Vaz J, Chong NV, et al. New approaches for the treatment of diabetic macular oedema: recommendations by an expert panel. *Eye* 2012;26:485-93
 36. Diabetic Retinopathy Clinical Research Network, Wells JA, Glassman AR, Ayala AR, et al. Aflibercept, bevacizumab, or ranibizumab for diabetic macular edema. *N Engl J Med* 2015;372:1193-203
 37. Schmidt-Erfurth U, Garcia-Arumi J, Bandello F, et al. Guidelines for the Management of Diabetic Macular Edema by the European Society of Retina Specialists (EURETINA). *Ophthalmologica* 2017;237:185-222
 38. Kodjikian L, Bellocq D, Bandello F, et al. First-line treatment algorithm and guidelines in center-involving diabetic macular edema. *Eur J Ophthalmol* 2019;29:573-84
 39. Bahadir M, Ertan A, Mertoglu O. Visual acuity comparison of vitrectomy with and without internal limiting membrane removal in the treatment of diabetic macular edema. *Int Ophthalmol* 2005;26:3-8
 40. Goldberg MF, Jampol LM. Knowledge of diabetic retinopathy before and 18 years after the Airlie House Symposium on Treatment of Diabetic Retinopathy. *Ophthalmology* 1987;94(7):741-6
 41. Klein R, Klein BE, Moss SE, et al. The Wisconsin epidemiologic study of diabetic retinopathy. IV. Diabetic macular edema. *Ophthalmology* 1984;91(12):1464-74
 42. Bresnick GH. Diabetic macular edema. A review. *Ophthalmology* 1986;93(7):989-97
 43. Early Treatment Diabetic Retinopathy Study design and baseline patient characteristics. ETDRS report number 7. *Ophthalmology* 1991;98(5 Suppl):741-56
 44. Classification of diabetic retinopathy from fluorescein angiograms. ETDRS report number 11. Early Treatment Diabetic Retinopathy Study Research Group. *Ophthalmology* 1991;98(5 Suppl):807-22
 45. Focal photocoagulation treatment of diabetic macular edema. Relationship of treatment effect to fluorescein angiographic and other retinal characteristics at baseline: ETDRS report no. 19. Early Treatment Diabetic Retinopathy Study Research Group. *Arch Ophthalmol* 1995;113(9):1144-55
 46. Fransen SR, Leonard-Martin TC, Feuer WJ, Hildebrand PL; Inveon Health Research Group. Clinical evaluation of patients with diabetic retinopathy: accuracy of the Inveon diabetic retinopathy-3DT system. *Ophthalmology* 2002;109(3):595-601
 47. Rudnisky CJ, Hinz BJ, Tennant MT, et al. High-resolution stereoscopic digital fundus photography versus contact lens biomicroscopy for the detection of clinically significant macular edema. *Ophthalmology* 2002;109(2):267-74
 48. Neubauer AS, Kernt M, Haritoglou C, et al. Nonmydriatic screening for diabetic retinopathy by ultra-widefield scanning laser ophthalmoscopy [Optomap]. *Graefes Arch Clin Exp Ophthalmol* 2008;246(2):229-35
 49. Wilkinson CP, Ferris FL 3rd, Klein RE, et al; Global Diabetic Retinopathy Project Group. Proposed international clinical diabetic retinopathy and diabetic macular edema disease severity scales. *Ophthalmology* 2003;110(9):1677-82
 50. Hee MR, Puliafito CA, Wong C, et al. Quantitative assessment of macular edema with optical coherence tomography. *Arch Ophthalmol* 1995;113(8):1019-29
 51. Bandello F, Pognuz R, Polito A, et al. Diabetic macular edema: classification, medical and laser therapy. *Semin Ophthalmol* 2003;18(4):251-8
 52. Kang SW, Park CY, Ham DI. The correlation between fluorescein angiographic and optical coherence tomographic features in clinically significant diabetic macular edema. *Am J Ophthalmol* 2004;137(2):313-22
 53. Panozzo G, Parolini B, Gusson E, et al. Diabetic macular edema: an OCT-based classification. *Semin Ophthalmol* 2004;19(1-2):13-20
 54. Maheshwary AS, Oster SF, Yuson RM, et al. The association between percent disruption of the photoreceptor inner segment-outer segment junction and visual acuity in diabetic macular edema. *Am J Ophthalmol* 2010;150(1):63-67.e1
 55. Jain A, Saxena S, Khanna VK, et al. Status of serum VEGF and ICAM-1 and its association with external limiting membrane and inner segment-outer segment junction disruption in type 2 diabetes mellitus. *Mol Vis* 2013;19:1760-8
 56. Helmy YM, Atta Allah HR. Optical coherence tomography classification of diabetic cystoid macular edema. *Clin Ophthalmol* 2013;7:1731-7
 57. Kothari AR, Raman RP, Sharma T, et al. Is there a correlation between structural alterations and retinal sensitivity in morphological patterns of diabetic macular edema? *Indian J Ophthalmol* 2013;61(5):230-2
 58. Dolz-Marco R, Abreu-González R, Alonso-Plasencia M, Gallego-Pinazo R. Treatment decisions in diabetic macular edema based on optical coherence tomography retinal thickness map: LET classification. *Graefes Arch Clin Exp Ophthalmol* 2014;252(10):1687-8

59. Byeon SH, Chu YK, Lee H, et al. Foveal ganglion cell layer damage in ischemic diabetic maculopathy: correlation of optical coherence tomographic and anatomical changes. *Ophthalmology* 2009;116(10):1949-59.e8
60. Xue K, Yang E, Chong NV. Classification of diabetic macular oedema using ultra-widefield angiography and implications for response to anti-VEGF therapy. *Br J Ophthalmol* 2017;101(5):559-63
61. Parodi Battaglia M, Iacono P, Cascavilla M, et al. A pathogenetic classification of diabetic macular edema. *Ophthalmic Res* 2018;60(1):23-8
62. Arf S, Sayman Muslubas I, Hocaoglu M, et al. Spectral domain optical coherence tomography classification of diabetic macular edema: a new proposal to clinical practice. *Graefes Arch Clin Exp Ophthalmol* 2020;258(6):1165-72
63. Panozzo G, Cicinelli MV, Augustin AJ, et al. An optical coherence tomography-based grading of diabetic maculopathy proposed by an international expert panel: The European School for Advanced Studies in Ophthalmology classification. *Eur J Ophthalmol* 2020;30(1):8-18

2. Non-invasive imaging of diabetic macular edema

In the present Chapter we will describe diabetic macular edema (DME)-related retinal changes that have been extensively studied using optical coherence tomography (OCT) and have emerged in recent years as useful imaging biomarkers, including hyperreflective retinal foci and the disorganization of inner retinal layers and outer retinal layers (ellipsoid zone). Microvascular changes visualized by OCT angiography (OCTA) will also be addressed

Optical coherence tomography

PATTERNS OF DIABETIC MACULAR EDEMA

Over the past two decades OCT has seen a remarkable development and is now an essential imaging technique for the rapid and non-invasive assessment of retinal morphology. More than twenty years ago, Otani et al. identified three distinct patterns of structural change in DME on OCT scans, namely sponge-like retinal swelling, cystoid macular edema, and serous retinal detachment^[1]. Sponge-like retinal swelling was the most common structural alteration and was reported in 88% of the eyes analyzed, followed by cystoid macular edema (47%) and serous retinal detachment (15%); more than one pattern could coexist in a patient^[1]. Later studies have suggested that the three DME patterns may have distinct underlying pathophysiologic mechanisms and may therefore respond differently to treatment, making OCT a crucial assessment tool also for therapeutic decisions^[2]. A key mechanism in the pathogenesis of DME is the breakdown of the inner and outer blood-retinal barriers. Breakdown of the inner membrane appears to be involved mainly in sponge-like and cystoid DME, while breakdown of the outer membrane appears to be responsible for neuroretinal detachment^[2]. Evidence suggests that inflammatory processes are implicated in the development of the DME pattern with neuroretinal detachment^[3].

The DME patterns identified by Otani et al. continue to be relevant for DME manage-

ment. However, our knowledge of the structural changes associated with diabetic retinopathy (DR) and DME has tremendously improved over the years leading to continuous updates of OCT-based grading. In 2020 the European School for Advanced Studies in Ophthalmology (ESASO) published an updated classification of DME^[4], which is discussed in Chapter 1.

HYPERREFLECTIVE FOCI

Hyperreflective foci (HRF), which are known in the literature also as hyperreflective spots or hyperreflective dots, were first described in the early '80 in patients with age-related macular degeneration^[5]. HRF are visible on OCT scans as small, punctiform, hyperreflective elements distributed across all retina layers^[5,6]. The origin of HRF is still debated. According to a few authors, these OCT features are due to the extravasation of lipoproteins and proteins following the breakdown of the blood-retinal barrier and are the precursors of hard exudates^[6]. Other authors have suggested that HRF represent activated microglia cells and are therefore the result of an inflammatory process^[7,8]. According to recently published evidence, hyperreflective OCT elements constitute a family and can be classified according to their size, location in the retina, and reflectivity^[9]. More in detail, elements with a diameter >30 μm , located to the inner retina, with back-shadowing are classified as retinal vessels and may represent microaneurysms, while elements >30 μm , located to the outer retina, with back-shadowing and reflectiv-

ity similar to that of the retinal pigment epithelium are classified as hard exudates^[8]. Solitary hyperreflective spots with a diameter $\leq 30 \mu\text{m}$, located mostly to the inner retina but also to the outer retina, with no back-shadowing and with reflectivity similar to that of the retinal nerve fiber layer correspond to the HRF discussed here. According to the prevailing hypothesis, these spots represent aggregates of activated microglia cells and have been proposed as biomarkers of retinal inflammation^[8].

Several studies have been performed to investigate the impact of HRF presence on retinal integrity and function, and visual acuity^[7,8,10]. A study evaluated the presence of HRF

in patients with diabetes, with or without DR, and without DME; the study also included a control group without diabetes (control)^[7]. The number of HRF was higher in patients with diabetes versus control patients, and progressively increased with increasing severity of DR (Figure 1). HRF were mainly located to the inner retinal layers, where microglia cells are located prior to activation^[7]. Upon activation, as for example in diabetes mellitus, microglia cells migrate to the outer retinal layers, undergo morphological changes and aggregate^[7]. As no patient enrolled in this study had DME (including subclinical signs of DME), and no hard exudates or disrupted photoreceptors were detected, the authors conclud-

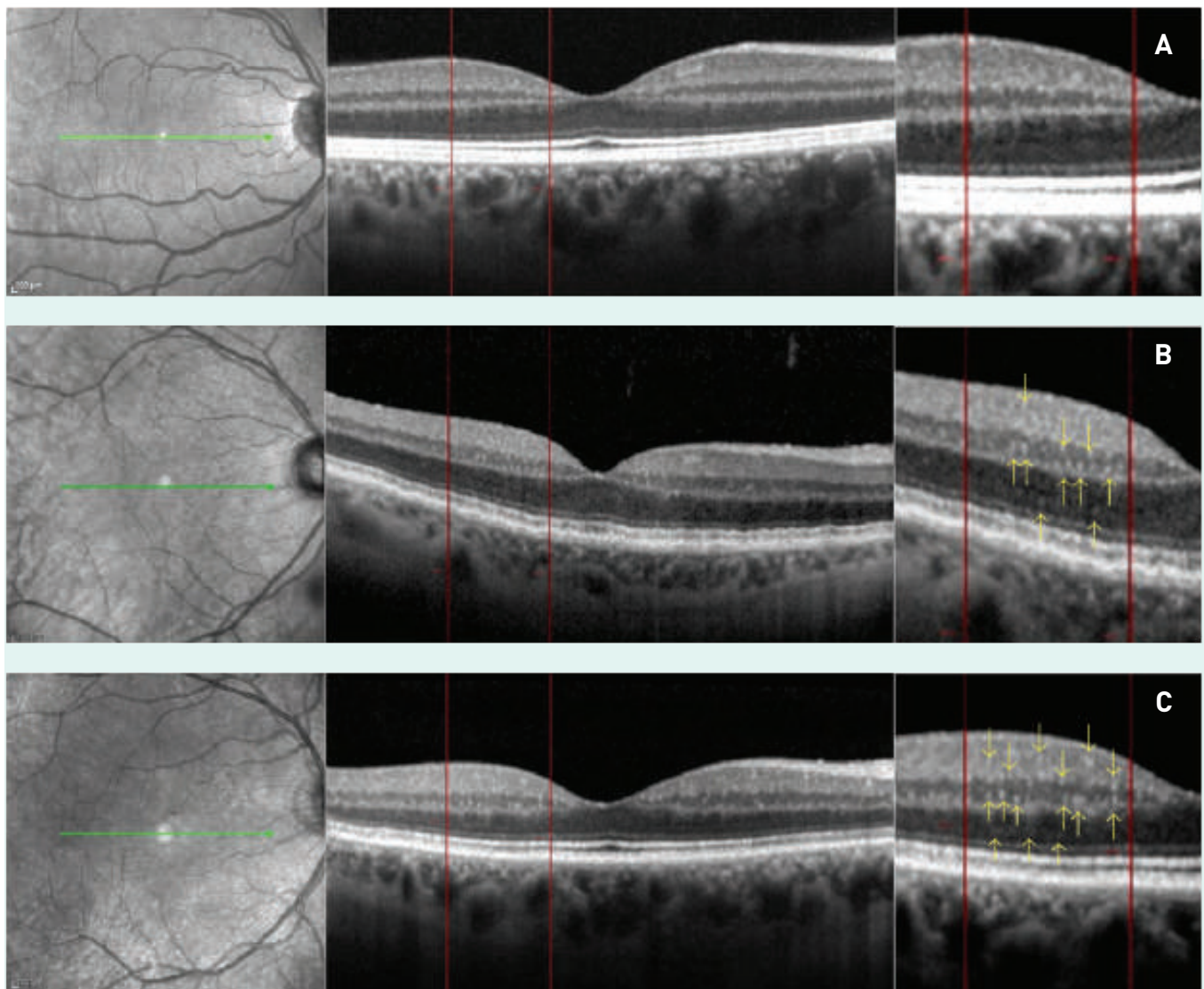


Figure 1. Detection of HRF in the macula of: A a control subject (no HRF are seen), B a patient with diabetes and no retinopathy, and C a patient with diabetes and non-proliferative DR. Left panels: fundus photographs; central and right panels: spectral domain OCT linear scans. HRF, indicated by yellow arrows, were counted in the region between the two red lines that were drawn at $500 \mu\text{m}$ and $1500 \mu\text{m}$ from the center of the fovea in the temporal region. (Reproduced with permission from Hindawi Publishing Corporation from ref.^[7]).

ed that the observed HRF were likely due to aggregates of activated microglia cells.

The potential of HRF as biomarker for evaluating the response to treatment has been investigated in several small studies^[10-13]. Overall, these studies found that treatment with intravitreal anti-vascular endothelial growth factor (VEGF) agents, or with intravitreal steroids, was associated with a significant decrease in the number of HRF, with the greater decrease being reported after treatment with steroids^[13]; this decrease correlated with the improvement of visual functional parameters^[11,13]. A retrospective analysis of OCT scans and patient charts of patients with DME treated with intravitreal steroids or anti-VEGF therapy found that both treatments improved significantly central macular thickness and visual acuity^[11]. Both treatments were associated with a significant decrease in the number of HRF, while subfoveal neuroretinal detachment resolved significantly more in eyes treated with steroids than in eyes treated with anti-VEGF (resolution rates, respectively, 85.7% and 50%). In the group treated with intravitreal steroids, high number of HRF and larger areas of increased foveal autofluorescence were correlated with greater improvements in retinal sensitivity, while eyes with neuroretinal detachment had more substantial decreases in central macular thickness compared with those without neuroretinal detachment. According to these findings, high number of HRF, along with areas of increased foveal autofluorescence and subfoveal neuroretinal detachment, suggest the presence of an inflammatory condition underlying DME, and may guide treatment choices towards steroids, at least as initial treatment^[11]. More recent studies have further confirmed that HRF and other parameters of retinal inflammation can help improve the evaluation of treatment response and thus the selection of personalized treatment^[12,13]. Given the steadily increasing availability of therapies for DR and DME, the ability to predict response accurately will further improve patient management and outcomes.

Further research is required to improve our understanding of HRF and their role as biomarkers in the management of DR and DME. An open issue concerning HRF is that their detection and manual counting on OCT scans are time-demanding and require expertise. The introduction

of artificial intelligence-based systems for the automated, standardized, and reliable assessment of OCT scans^[2,9] will certainly contribute to the implementation of these markers in real-world ophthalmology (see also Chapter 5).

DISORGANIZATION OF RETINAL INNER LAYERS

OCT of eyes with DR and DME has revealed and visualized the disorganization of retinal inner layers (DRIL), among other relevant morphological alterations of the retina. DRIL is defined as the absence of visible boundaries between the ganglion cell-inner plexiform layer complex, the inner nuclear layer, and the outer plexiform layer, within 1.5 mm from the macula (**Figure 2**)^[14]. This OCT parameter has attracted considerable interest because of its well-documented and consistent association with visual acuity^[14,15]. The potential of DRIL as predictor of visual acuity was first described by Sun et al. in a retrospective study published in 2014^[14]. In eyes with center-involving DME, greater DRIL extent was found to correlate significantly with worse visual acuity at baseline, and DRIL changes at 4 months were shown to be predictive of changes in visual acuity at 8 months^[14]. A further study by the same authors not only confirmed these findings but also showed that DRIL was able to predict visual acuity in eyes that had been previously affected by DME and in which edema had resolved^[15]. The study showed that DRIL affecting more than 50% of the 1-mm foveal area was associated with decreased visual acuity in eyes with current DME and in eyes with resolved DME^[15]. Consistent with the results of the first study^[14], early changes in DRIL extent accurately predicted changes in visual acuity from baseline to 1 year^[15]. According to the authors, the strong association between foveal DRIL and visual outcomes in eyes with DME might be explained by the fact that the disorganized structures defining this OCT parameter contain the key elements involved in the transmission of visual signals from photoreceptors to ganglion cells^[15]. This damage to transmission might be irreversible, at least in part, and may account for the observed association between DRIL and loss of visual acuity also in eyes with resolved edema. Finally, the authors pointed out that foveal DRIL was the first non-invasive parameter to correlate significantly and

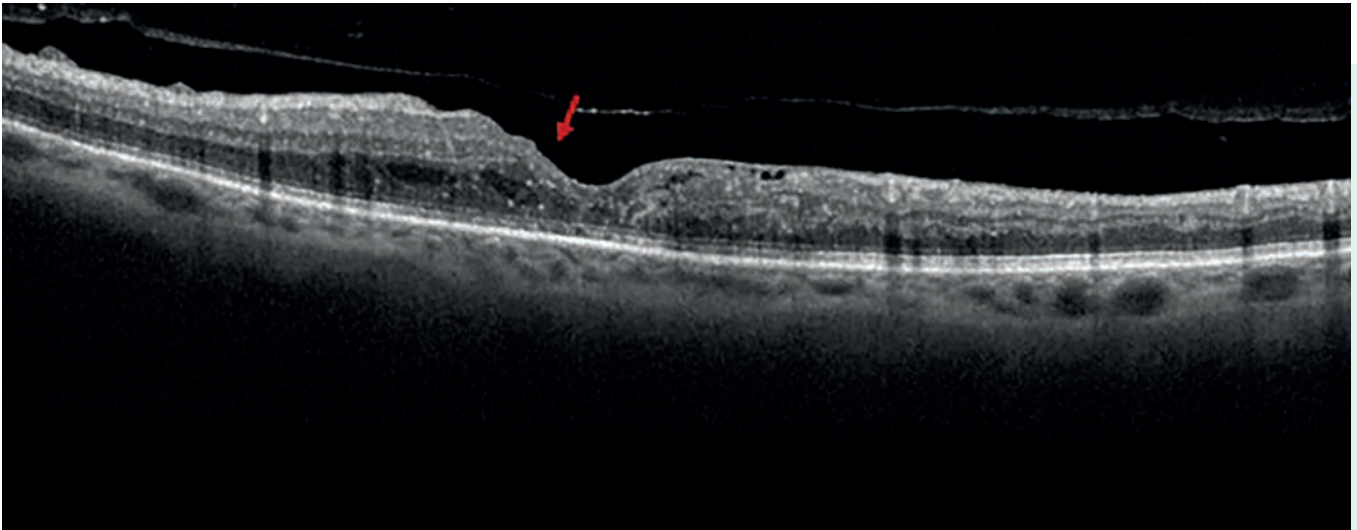


Figure 2. Spectral domain OCT scan showing a case of DME with DRIL in the central millimeter. The arrow point shows to the absence of visible boundaries between inner retinal layers.

consistently with visual acuity, while attempts to demonstrate the association with other parameters, including central retinal thickness and ellipsoid zone (EZ) integrity, had provided inconsistent results or weak correlations^[15].

The potential of DRIL as biomarker of visual acuity has been extensively investigated in other studies. A retrospective analysis of the charts of patients with center-involving diabetic and non-diabetic macular edema investigated whether changes in DRIL and other OCT variables were associated with visual acuity after edema resolution^[16]. DRIL was the variable with the best correlation with visual acuity. Furthermore, DRIL resolution was associated with an improvement of visual outcomes, while persistent DRIL correlated with a worsening. Based on the hypothesis that DRIL may represent non-perfusion areas, a study evaluated the ability of DRIL to predict macular capillary non-perfusion in eyes with DR^[17]. The study confirmed that DRIL can predict the presence of non-perfusion. However, non-perfusion was observed also in eyes with no DRIL. In an observational case series, disrupted external limiting membrane, disorganized EZ, the presence of epiretinal membrane, and higher central retinal thickness were all associated with increased likelihood of DRIL^[18]. DRIL correlated positively with disruption of the outer retina and with DR severity, while DRIL improvements were associated with improved visual outcomes. According

to the authors of this study, mechanical stress caused by edema to inner layer cells underlines the occurrence of DRIL. In detail, when neurons of the inner nuclear layer are stretched by edema to the limit of their elasticity, they break leading to the disruption of the retinal inner layer. However, other mechanisms, including non-perfusion of the macular area, have been implicated in the pathogenesis of DRIL^[19,20].

OCTA has allowed to quantify microvasculature changes occurring in eyes with DR and has significantly contributed to improving our understanding of DRIL development; OCTA also visualizes areas of retinal ischemia. A recent study using OCTA compared the morphology of the foveal avascular zone (FAZ) in patients with resolved DME, in the presence or absence of DRIL^[19]. The study found that the extension of the FAZ was significantly greater in patients with DRIL and that a larger FAZ correlated with a worse visual acuity. This association suggested that retinal ischemia and microvasculature changes may lead to DRIL. More recently, a study used OCTA to compare retinal vessel density and the FAZ extension in eyes, with and without DRIL, of patients with resolved DME and in eyes of healthy controls^[20]. Consistent with the conclusions of the previous study using OCTA^[19], this comparison suggested that non-perfusion of the macular region may have a role in the development of DRIL. Eyes with resolved DME, regardless of the presence of DRIL, had lower vascular

density in the superficial capillary plexus and in the deep capillary plexus and a greater FAZ extension compared with healthy eyes (Figure 3). In eyes with DRIL, vascular density was lower and FAZ extension was greater compared with eyes without DRIL (Figure 3B and C), suggesting that lower vascular density, along with non-perfusion, may also contribute to the disruption of retinal architecture. In eyes with DRIL, the study reported a significant correlation between OCTA variables (vascular density of the superficial capillary plexus and the deep capillary plexus, and FAZ extension) and visual outcomes, with lower vascular density and larger FAZ being both correlated with worse visual acuity^[20].

INTEGRITY OF THE ELLIPSOID ZONE

The EZ, which corresponds to the hyper-reflective line above the retinal pigment epithelium, was formerly known as photoreceptor inner segment/outer segment junction. The EZ has long been used for assessing the integrity of photoreceptors in retinal disease^[21,22]. Evidence of a correlation between photoreceptor status and visual outcomes is available for several retinal diseases, while studies evaluating the biomarker potential of EZ changes in DME are more limited^[23]. An early study in patients with DME suggested that the percentage of EZ disruption evaluated using spectral domain OCT might predict visual acuity^[21]. A retrospective study investigating the possible correlation between photoreceptor integrity and visual acuity in patients with DME following treatment found that EZ intactness and the preservation of the external limiting membrane were markers of photoreceptor integrity^[23]. In addition, these two OCT parameters were closely associated with visual acuity.

More recently, the prospective observational study CHARTRES performed to determine baseline OCT parameters able to predict visual outcomes following anti-VEGF therapy, identified EZ disruption and a great extent of DRIL as predictors of limited visual recovery^[24]. A post-hoc analysis of OCT parameters from the VISTA-DME phase III study evaluating the efficacy and safety of intravitreal anti-VEGF reported an improvement of EZ integrity with treatment and the association of this OCT parameter with visual outcomes^[25]. Finally, a

study in patients with DME addressed long-term (up to five years) changes in OCT parameters (including EZ) and visual acuity during intravitreal anti-VEGF therapy^[26]. EZ reflectivity ratio (an indicator of photoreceptor cell vitality) was found to improve with treatment and to correlate significantly with visual acuity over 5 years of anti-VEGF therapy.

Taken together the available data in DME suggest the association of EZ integrity with visual acuity and the potential of these OCT feature as biomarker for the assessment of response to treatment. Further research is however needed for the validation of this biomarker in DME.

Optical coherence tomography angiography

OVERVIEW

The perfusion of retinal and choroidal vasculature is usually visualized and evaluated using dye-based angiography (for example, fluorescein angiography, indocyanine green angiography). This technique provides morphological information comparable to that obtained with histological exams and continues to play a central role in the detection and diagnosis of retinal disease^[27]. Fluorescein angiography (FA) has long been the gold-standard of fundus imaging as it allows to view the retinal capillary bed, especially in the macular area, the leakage from abnormal vessels, and/or newly formed vessels, one of the most important signs of DR. However, FA is a two-dimensional examination that visualizes superficial retinal vessels, while the deeper capillary network is not optimally shown by this technique, possibly due to light scattering by the retina^[28]. Another important drawback of dye-based angiography is the need to inject the fluorescent dye intravenously, which may be associated with adverse events^[29].

OCTA is non-invasive and allows a clear, three-dimensional visualization of the retinal and choroidal microvasculature, across all layers, by calculating the decorrelation of signal between static and non-static tissue^[30,31]. The superficial capillary plexus is shown by en-face OCTA (also called C-scan OCTA) as a fine cap-

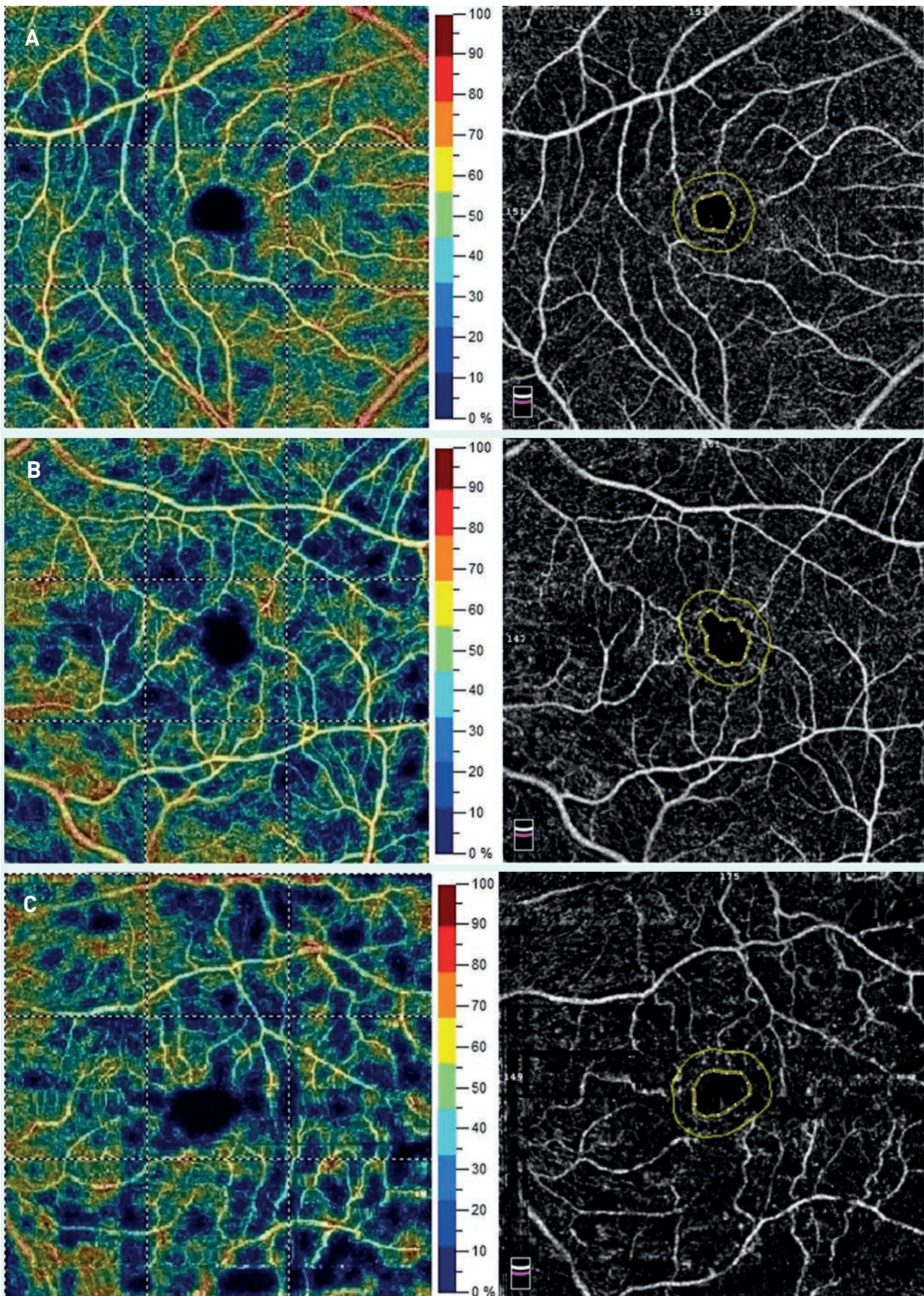


Figure 3. Vascular density in the superficial capillary plexus and FAZ in eyes from: A a healthy control, B a patient with resolved DME without DRIL, and C a patient with resolved DME and DRIL. Left panels: multicolor OCTA imaging of the superficial capillary plexus; right panels: OCTA imaging of the FAZ.

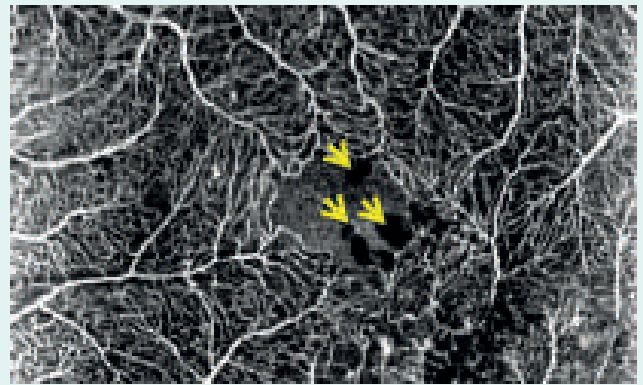
illary network with a hyperintense signal at the level of the ganglion cell layer, while the deep capillary plexus is visualized by en-face OCTA images taken at the level of the inner nuclear layer. In DR, the architecture of the superficial and deep capillary plexuses is often disrupted; the presence of DME may contribute to these structural changes. Since OCTA closely correlates with structural OCT^[32], this technique provides a simultaneous picture of retinal vasculature and macular edema and allows to monitor progressive vascular changes (Figures 4 and 5). The comprehensive OCTA assessment of eyes with DME requires C-scans (en-face images) taken at the level of the ganglion cell layer (to visualize the superficial capillary plexus) and at the level of the inner nuclear layer (to visualize the deep capillary plexus). The corresponding B-scan (cross-sectional image) may be useful for evaluating the potential misalignment of segmented retinal boundaries.

Similar to what has been reported with other imaging techniques, distinct patterns of exudative macular edema can be recognized also with OCTA. These include: hypointense intraretinal spaces, grayish intraretinal spaces, and focal hyperintense clumps (Figure 4). The characterization and clinical relevance of these patterns are the object of current research.

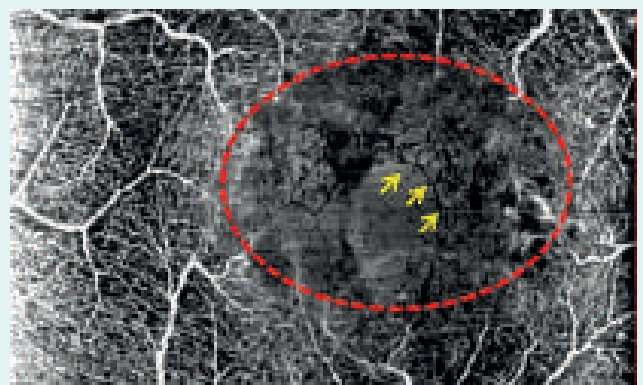
Hypointense intraretinal spaces appear on OCTA C-scans as dark, roundish areas devoid of signal, with variable size and location, depending on the depth of the section^[33,34]. They are the most common OCTA pattern of DME, notably in case of intraretinal fluid accumulation; they are due to the presence of intraretinal cystoid spaces and are usually found close to areas with altered perfusion, intraretinal microvascular abnormality, or microaneurysms (Figure 4). Large hypointense intraretinal spaces are usually located in the sub-foveal and para-foveal regions, while small spaces are usually seen in the macular and extra-macular regions.

Greyish intraretinal spaces of OCTA images (Figure 4) are often misinterpreted as they have a signal intensity similar to that of intervascular spaces and, in some cases, of non-perfused areas (NPAs)^[34]. However, since NPAs are usually not visible on OCTA scans due to the absence of blood flow and, thus, of a decorrelation signal,

Hypointense intraretinal spaces



Greyish intraretinal spaces



Focal hyperintense clumps

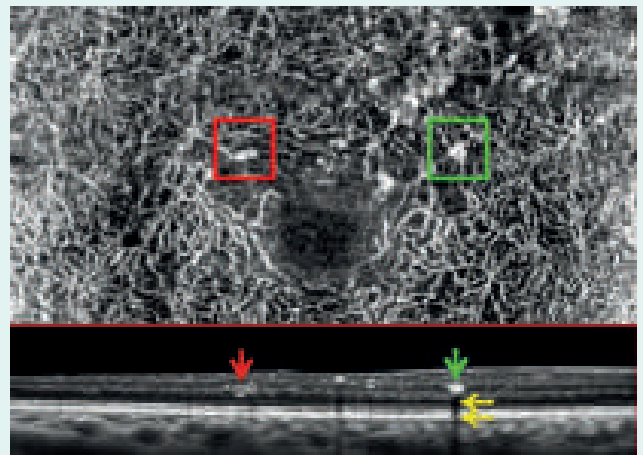


Figure 4. Patterns of DME on OCTA. Top and middle images: C-scan OCTA images taken at the level of the ganglion cell layer and showing the superficial capillary plexus. Yellow arrows indicate hypointense intraretinal spaces in the top image. In the middle C-scan image, the dashed red line includes a greyish intraretinal space; the yellow arrows point to dark tubular structures corresponding to non-perfused vessels. Bottom image: C-scan OCTA image taken at the level of the inner nuclear layer and showing the deep capillary plexus; the corresponding B-scan including the foveal depression is shown below. The red square indicates a fusiform hyperintense structure with the typical appearance of a microaneurysm. The hyperintense lesion indicated by the green box is due to the focal accumulation of hard exudates. In the B-scan OCT image, the hyperreflective lesion (green arrow) is associated with back-shadowing (yellow arrows), which is due to the high reflectivity of hard exudates.

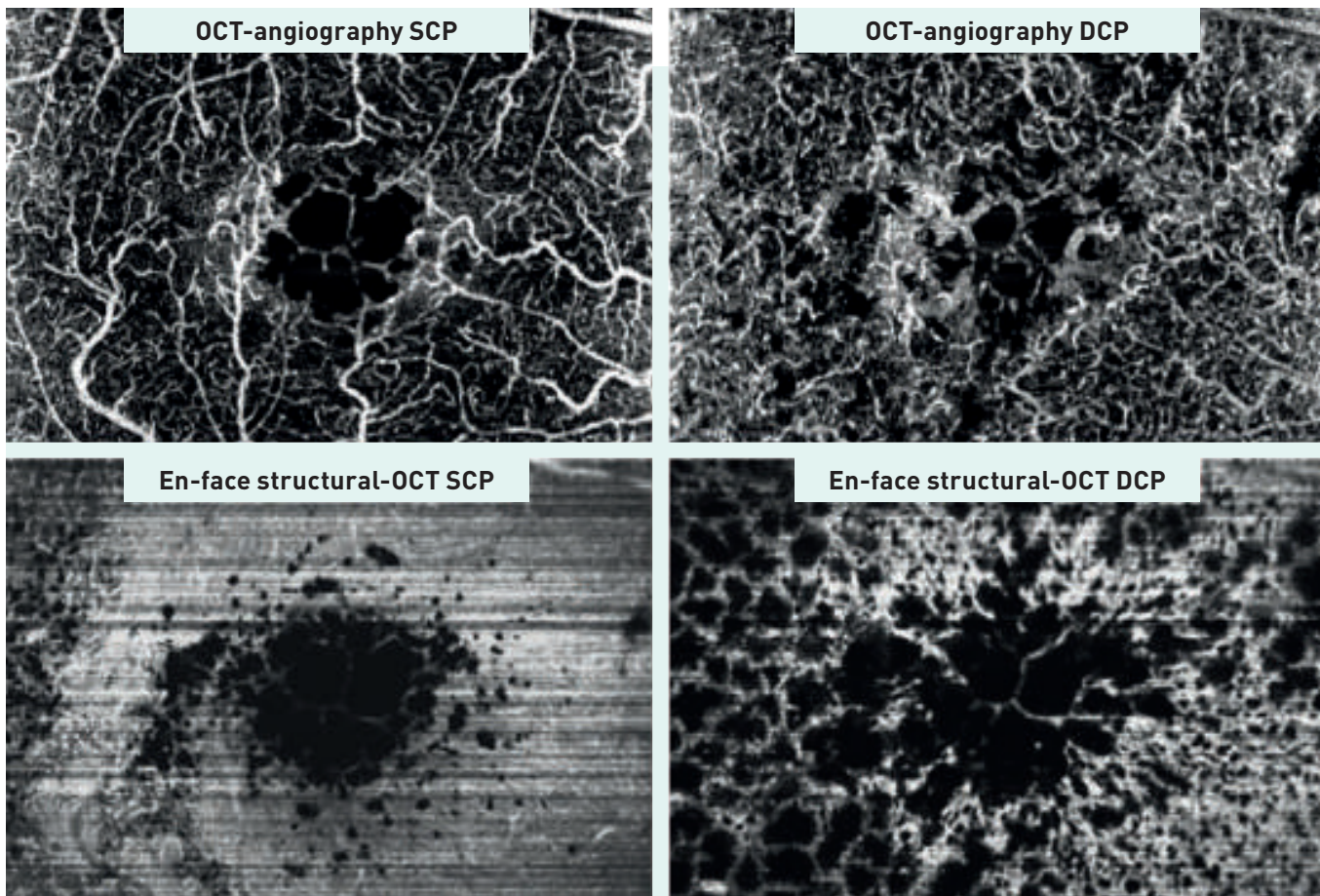


Figure 5. Assessment of DME using OCTA and OCT. Left panels: superficial capillary plexus; right panels: deep capillary plexus. The images show the distinct contributions of OCTA (top images) and en-face structural OCT (bottom images) to the definition of DME extension. Since DME is merely a structural rather than a functional finding, it should be primarily investigated by structural imaging.

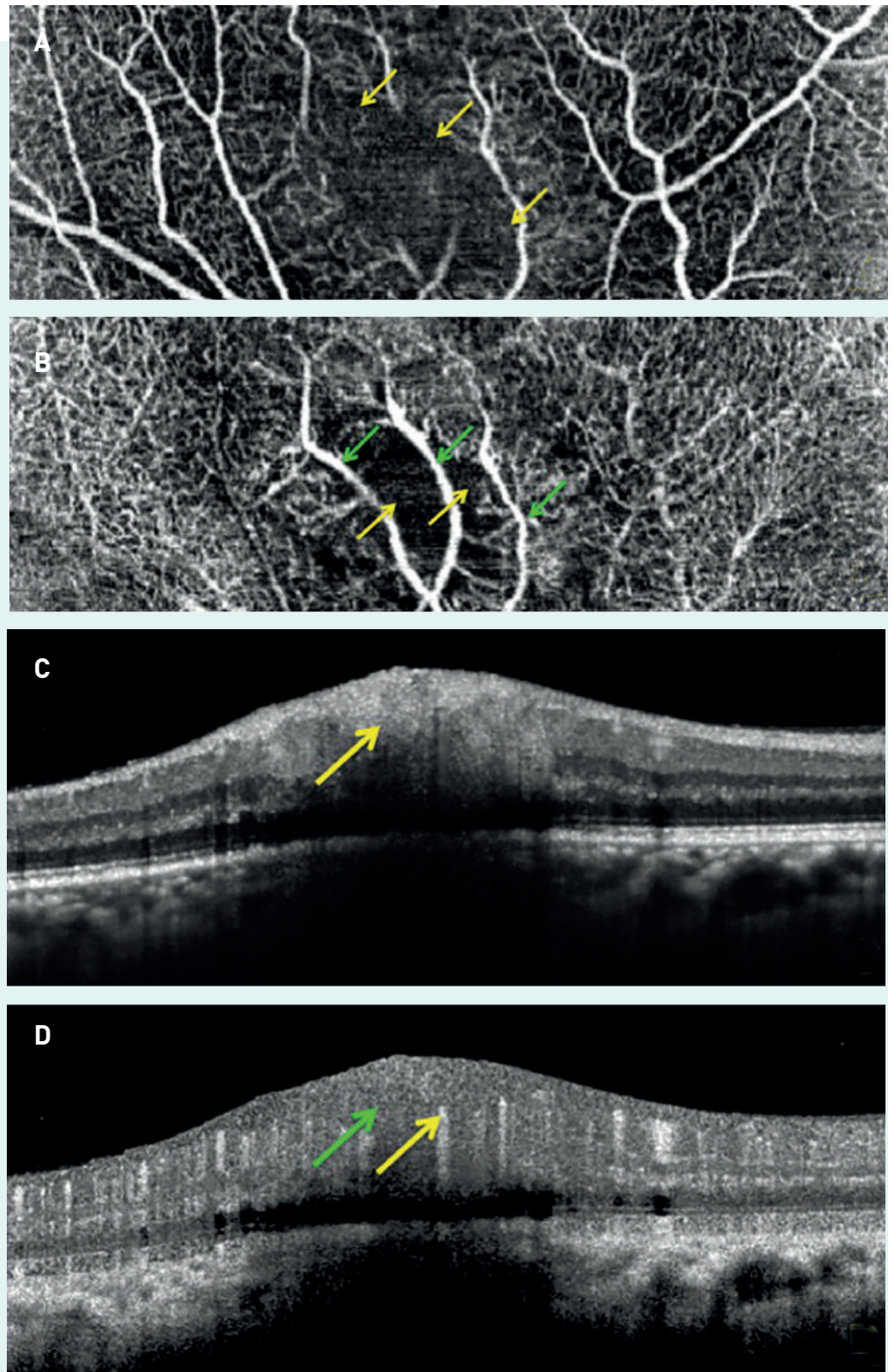
non-perfused vessels that appear as tubular structures without a signal can be easily distinguished from greyish cystoid spaces^[33]. The origin of greyish cystoid spaces is not entirely understood. According to some authors, the weak decorrelation signal of these spaces may be the result of the active motion of molecules caused by intense intraretinal exudation^[33,34]. Other authors have explained this OCTA feature by the presence of “suspended scattering particles in motion” (SSPIM)^[35]. In some cases, SSPIM have been associated with hard exudates^[35].

Focal hyperintense clumps appear on OCTA images as highly decorrelated roundish or elongated structures (Figure 4). They are often misinterpreted as microaneurysms and intraretinal microvascular abnormalities, and hard exudates. To help distinguish between focal hyperintense clumps and hard exudates it is useful to note that hard exudates are hyperreflective structures on OCT and hyperintense structures

on OCTA. The hyperintensity on OCTA is caused by the fact that hard exudates completely reflect the refracted signal coming from the perfused vessels above. In contrast with truly perfused lesions, hard exudates display back shadowing on OCTA B-scans, as the light that reaches them is almost completely reflected^[36].

Finally, OCTA can also visualize retinal lesions associated with ischemic DME, including cotton-wool spots (Figure 6). These lesions represent axoplasmic debris in the axons of ganglion cells caused by the interruption of axoplasmic flow due to vascular or mechanical events. At the biomicroscopic analysis, cotton-wool spots appear as whitish, fluffy retinal patches that fade with time. FA assessment may reveal reduced blood flow, while OCT scans typically show marked retinal thickening at the lesion site, confined at the level of the retinal nerve fiber layer. On OCTA scans, cotton-wool spots appear as areas with no flow signal from the

Figure 6. Cotton-wool spots visualized by OCT and OCTA. A, OCTA of the superficial capillary plexus; the yellow arrows point to an area with no hyperintense signals coming from perfused vessels. B, OCTA of the deep capillary plexus; the yellow arrows point to an area with no decorrelated (i.e., perfused) structures. Large retinal vessels (green arrows) are visible due to the inward displacement caused by the thickening of the nerve fiber layer, and due to the absence of decorrelation signal from the inner vascular layers. C, B-scan OCT; the yellow arrow shows a focal thickening of the ganglion cell layer. D, in the corresponding B-scan OCTA no hyperintense signals are visible in the involved area indicated by the green arrow, while large retinal vessels are displaced deeper in the retina. This phenomenon is caused by focal capillary ischemia.



superficial and deep capillary plexuses, which may be simultaneously involved (Figure 6).

NON-PERFUSION AREAS

Retinal NPAs and the enlargement of the FAZ are common features of DR detected by

OCTA. NPAs can affect both the superficial and deep capillary plexuses to a variable extent^[37]. On OCTA scans, NPAs appear as regions with a grey hue, surrounded by adjacent capillaries (Figure 7). OCTA allows the quantitative assessment of vascular perfusion in the different

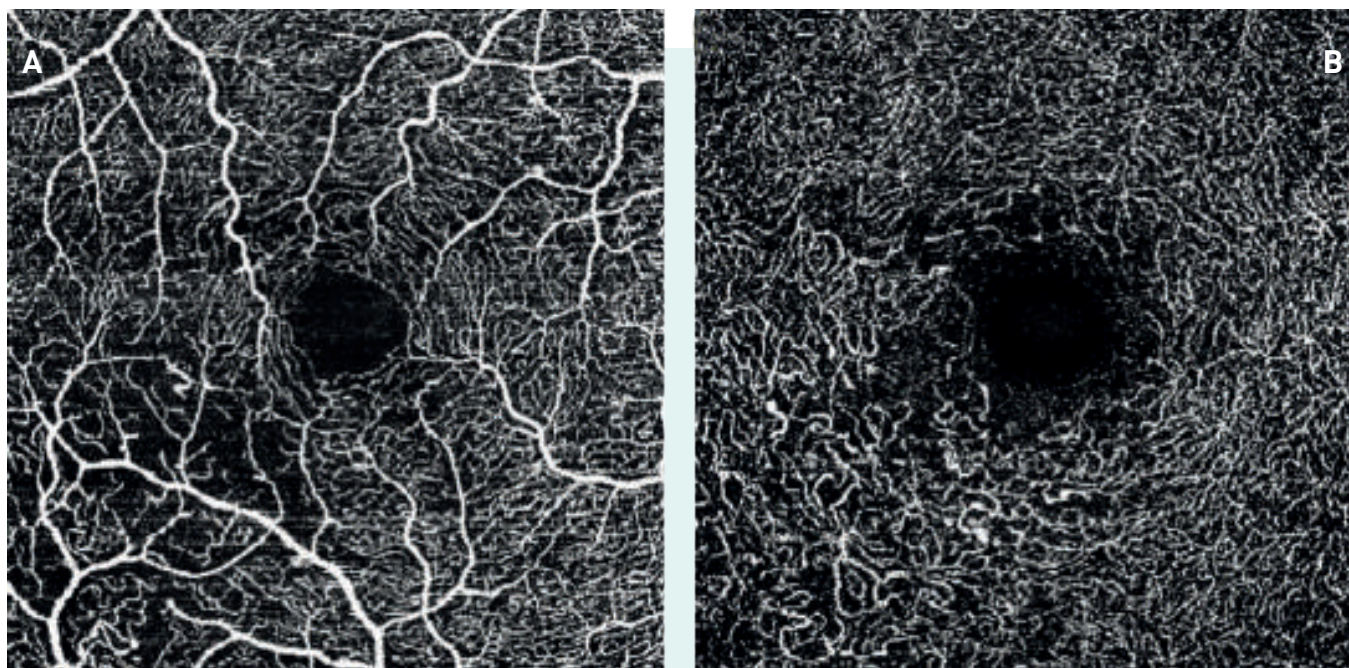


Figure 7. NPAs in DR evaluated using OCTA. A, OCTA of the superficial capillary plexus. The perifoveal arcade appears preserved. B, OCTA of the deep capillary plexus. Several NPAs, where the capillary network is undetectable, are visible in the inferior-temporal quadrants in both capillary plexuses.

retinal layers^[38-41]. However, OCTA devices are not interchangeable in the classification of signals from cystoid spaces and NPAs in eyes with DME. Indeed, there is a strong need for standardized image acquisition and assessment^[34]. For example, in the study by Parravano et al. mentioned above, swept source OCT technology proved more reliable than spectral domain OCT for the detection of NPAs in DME^[34].

Several studies were performed to quantify capillary damage in different stages of diabetic disease. Coscas et al. initially assessed NPAs qualitatively on OCTA scan, based on perfusion damage in focal, moderate, and severe macular ischemia^[42]. A study by Carnevali et al. showed that OCTA can visualize early impairment of perfusion in diabetic patients with no biomicroscopic evidence of DR^[38]. A statistically significant difference in the density of capillary perfusion between the superficial and the deep capillary plexuses was reported, and the damage to vascular perfusion increased progressively with worsening DR^[39,43]. In contrast with these findings, Lupidi et al. reported no statistically significant difference in the total surface of superficial and deep capillary plexuses both in diabetic patients and healthy controls^[41]. Based on these results, both retinal layers may be simultaneously

affected by non-perfusion. Of note, the vascular density in each layer was significantly different in diabetic patients versus healthy controls^[41].

Studies addressing the effects of anti-VEGF therapy on macular ischemia in patients with DME have reported conflicting results. A few studies assessing macular ischemia with fundus FA showed no significant changes in perfusion following treatment with anti-VEGF agents in patients with DR and DME^[44,45]. Other studies reported a worsening of macular non-perfusion following anti-VEGF treatment in patients with DME, DR, or proliferative DR, with an enlargement of the FAZ as assessed by fundus FA^[46,47]. As previously pointed out, OCTA is a more reliable tool than FA for the assessment of macular ischemia and can be used for quantifying FAZ area and vascular density. Studies using OCTA to quantify FAZ area and vascular density changes during treatment with anti-VEGF agents have also yielded conflicting results. In a study in patients with DR, no change in FAZ area and vascular density, in both the superficial and deep capillary plexuses was reported following treatment with an anti-VEGF agent^[48]. On the other hand, and in agreement with previous studies using fundus FA for the assessment of ischemia^[46,47] a significant en-

largement of the FAZ area and a decrease in vascular density following anti-VEGF treatment have been reported, raising concern about the potential risk of worsening macular perfusion in eyes with DR^[49].

As we will see in Chapter 3, thanks to the use of swept source (SS) wide-field (WF) OCTA peripheral retinal ischemia can now be assessed. Using WF SS OCTA and ultrawide-field (UWF) fundus FA, Couturier et al. evaluated peripheral perfusion in patients with DR, after treatment with anti-VEGF therapy^[50] (see Chapter 3 for a detailed description of the study). The study concluded that anti-VEGF therapy does not reverse non-perfusion.

FOVEAL AVASCULAR ZONE

The FAZ is a region at the center of the macula with no blood vessels. It corresponds to the point of fixation and its diameter is approximately 0.5 mm, although a great size variability has been reported in healthy eyes^[51]. The FAZ is a relevant feature of fundus FA. In eyes with DR, the FAZ increases in size and this increase appears to correlate with disease progression^[30,41]. Traditionally, the FAZ has been examined using fundus FA; however, due to the invasiveness of FA, this technique is not routinely used in the early stages of DR. OCTA provides a valuable, non-invasive tool for FAZ examination^[30,41]. In addition, and in contrast with FA, with OCTA the different layers of the FAZ can be visualized individually^[30,52].

The comparison of histological pictures of the FAZ with OCTA images of the same area in healthy eyes has shown that both the superficial and deep capillary plexuses contribute to outline the perifoveal vascular arcade^[53]. OCTA imaging can be associated with artifacts because it relies on segmentation strategies that can result in corrupted images. In DME, which involves retinal infiltration that can cause misalignments between automated segmentation and borders of retinal layers, segmentation strategies often fail. As a consequence, the layers of the vessels are shown together, or partially together, with no visualization of the true anatomy^[54]. However, studies have investigated the superficial and deep capillary plexuses separately and an enlargement of the FAZ in both layers has been reported in eyes of diabetic

patients versus healthy controls (Figure 8). For example, De Carlo et al. showed that the FAZ area was larger in patients with diabetes ($0.35 \pm 0.10 \text{ mm}^2$) compared to healthy individuals ($0.29 \pm 0.14 \text{ mm}^2$; $p=0.04$)^[55]. In a study investigating retinal vascular plexuses and choriocapillaris in patients with type 1 diabetes mellitus, however, Carnevali et al. measured a mean FAZ area of $0.22 \pm 0.10 \text{ mm}^2$ in the superficial capillary plexus in diabetic patients, and of $0.25 \pm 0.10 \text{ mm}^2$ in healthy control individuals ($p=0.34$)^[38]. In the deep capillary plexus, the mean FAZ area was $0.75 \pm 0.20 \text{ mm}^2$ in diabetic patients and $0.76 \pm 0.23 \text{ mm}^2$ in healthy individuals ($p=0.81$)^[38]. Al-Sheikh et al. reported an overall FAZ size increase in both plexuses, with the exception of the superficial capillary plexus in mild and moderate non-proliferative DR^[56]. A few studies have compared FAZ size between the two plexuses, with a statistically significant difference in FAZ size being reported only in one study^[41]. The observation that capillary dropout is more pronounced in the deep capillary plexus than in the superficial capillary plexus^[41] may be explained by the different blood supply to the two layers. In fact, the deep capillaries surrounding the FAZ have a terminal structure, while those of the superficial plexus contribute to the continuity of the ring forming the perifoveal vascular arcade.

Several studies have addressed factors that may influence FAZ area, including age and duration of diabetes, but no consistent correlations could be identified^[57-59]. In a comparison between studies reporting an elevated area of FAZ in diabetes and those that did not, we were unable to find confounding variables like age, duration of diabetes, or number of patients, which may account for such differences^[60,33]. Given that FAZ area shows a great interpersonal variability also in age-matched groups of both healthy individuals and patients with diabetes^[60], this OCTA feature may have some limitations as diagnostic tool in population-based studies.

MICROANEURYSMS

Loss of pericyte cells and proliferation of endothelial cells, which can result in the weakening of vessel walls and the occurrence of microaneurysms (MAs), are among the first signs of DR^[61]. Leaking MAs are implicated in the de-

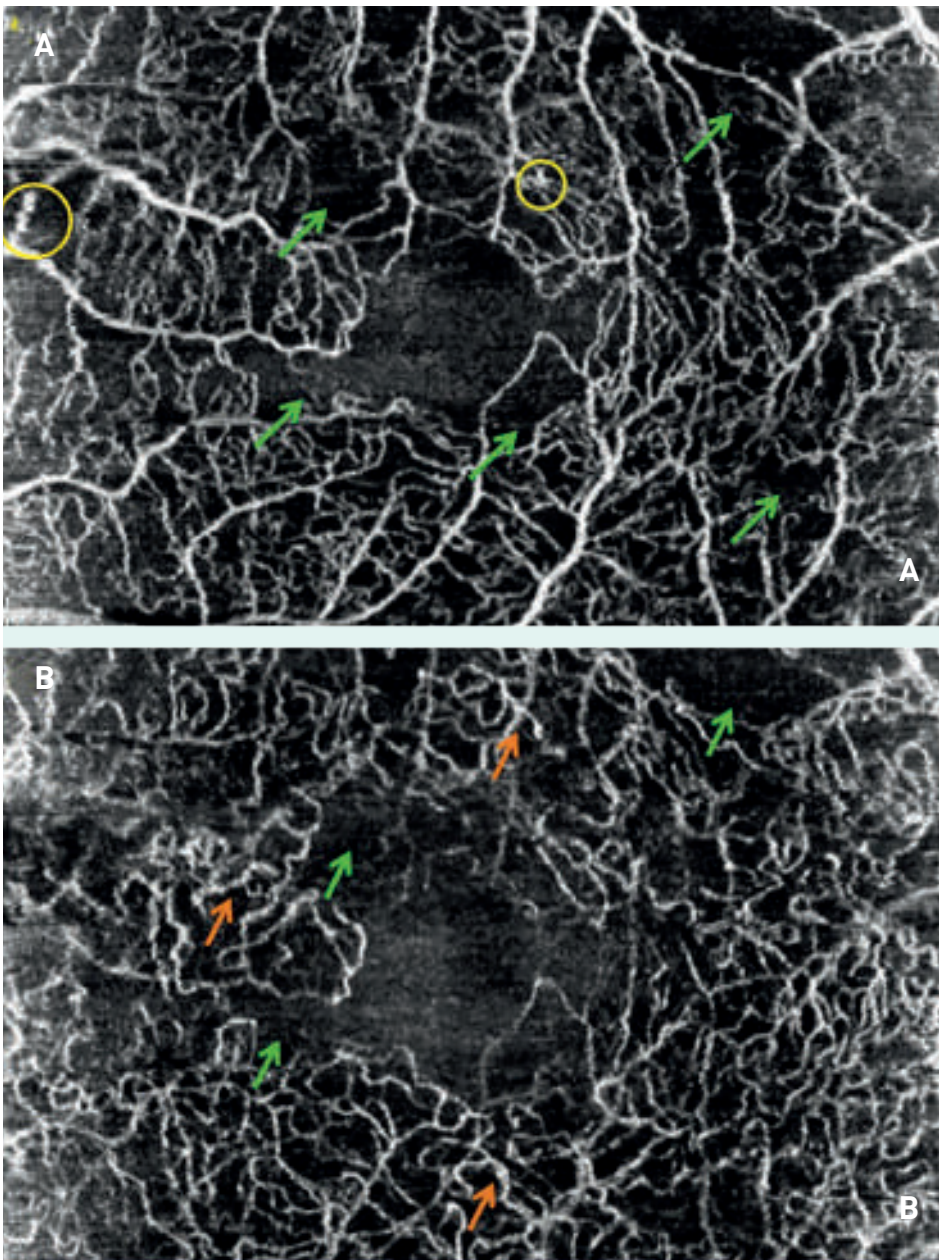


Figure 8. The FAZ in eyes with DR. A, OCTA image of the superficial capillary plexus. The perifoveal vascular arcade, which borders with the FAZ, is interrupted in virtually all quadrants. Focal vascular dilations, mostly due to microaneurysms are visible (yellow circles); green arrows indicate NPAs, where the capillary network is not visible. B, OCTA image of the deep superficial capillary plexus. Orange arrows point to focal vascular dilations, while green arrows point to several NPAs.

velopment of macular edema, a frequent cause of blindness related to DR^[37,62]. Early studies of MAs were based on pathological and histological exams, which described these microvascular abnormalities as protrusions of the retinal capillary network, affecting primarily the deep capillary plexus located in the inner nuclear layer of the retina^[63]. Fundus FA has long played a central role in the detection of MAs and other early signs of DR; however, as previously noted, this technique is invasive, relatively expensive, and time-demanding. The introduction of OCT has considerably advanced the non-invasive imaging of the retina. As seen in the previous sections of this Chapter, the further advance to OCTA has made the detailed observation of

DR-related vascular changes possible and has brought the attention to retinal NPAs, shape and size of the FAZ, MAs, and other morphological features^[39,64]. Furthermore, OCTA is increasing our knowledge of retinal architecture and the morphological alterations associated with the progression of DR. OCTA is currently regarded as an important alternative to FA, especially in patients who are not eligible to the intravenous injection of fluorescent dyes. However, it should be kept in mind that OCTA, unlike FA, does not detect fluid leakage. Therefore, OCTA imaging does not visualize leaking MAs, or late leakage associated with macular edema. On the other hand, OCTA visualizes the different choroidal and retinal capillary plexuses individually, and

vascular changes that in FA images may be masked by the dye.

Several studies using OCTA have addressed morphological changes of the retina, including MAs, at different stages of DR, and compared them to the information provided by FA. A study in 25 patients with DR (47 eyes) compared en-face OCTA and fundus FA in their ability to visualize MAs, retinal NPAs, and neovascularization^[37]. OCTA was able to visualize only 62% of the MAs detected by FA; most MAs were found in the deep capillary plexus and the average extension of NPAs in the superficial capillary plexus was slightly greater than in the deep capillary plexus. Couturier et al. also reported the superiority of FA versus OCTA in detecting MAs^[62]. OCTA was however more accurate in detecting NPAs than FA and potentially better suited for evaluating DR progression. The study by Couturier et al. confirmed that the number of MAs was greater in the deep than in the superficial capillary plexus, with most MAs being located on the edge of NPAs on OCTA images.

A study investigating the correlation between MAs distribution, detected using OCTA, and DME revealed a significantly greater density of MAs inside the edema in the deep capillary plexus than outside the edema^[65]. The density of MAs in the superficial capillary plexus was similar outside and inside the edema. These findings highlighted that MA density in the deep capillary plexus correlated significantly with macular volume and that MAs may be involved in the pathogenesis of DME and especially of cystoid macular edema.

Parravano et al. investigated the correlation between the appearance of MAs on structural spectral domain (SD) OCT and their detection on OCTA in patients with non-proliferative DR (16 patients, 145 MAs assessed)^[66]. MAs were classified based on their internal reflectivity on SD OCT as hyperreflective if their reflectivity was similar to that of the MA wall, as hyporefective if their reflectivity was similar to that of the cystic intraretinal fluid, and moderately reflective if their reflectivity was intermediate. To compare MAs seen on OCTA with MAs seen on SD OCT, OCTA vascular landmarks of the superficial capillary plexus were superimposed to vascular landmarks seen in the near infrared. The ultimate goal of the study was to

establish whether MA reflectivity on SD OCT could influence MA detection in the superficial or deep capillary plexuses, in the corresponding OCTA images. The study found that hyporefective MAs on SD OCT were less detectable on OCTA. These results may contribute to improve our understanding of blood flow patterns in MAs and our interpretation of MAs visualization with OCTA. A possible explanation of these findings is that hyporefective MAs on SD OCT may have a blood flow rate below the threshold required to make the detection by the OCTA system possible. Alternatively, it has been hypothesized that the blood flow inside MAs may be turbulent and therefore difficult to visualize by OCTA^[67]. In addition, MAs may appear hyporefective because they contain plasma without erythrocytes^[68]. Finally, previous histologic studies have shown that some MAs are not perfused and have extensive luminal fibrosis and lipid infiltration^[63]. It is possible that some of the hyporefective MAs described by Parravano et al.^[66] correspond to these sclerosed, fibrotic, poorly perfused MAs.

In another study, Parravano et al. investigated the progression of MAs based on SD OCT and OCTA characteristics with the objective to evaluate the role of MAs in the retinal accumulation of extracellular fluid in patients with non-proliferative DR followed-up for 1 year^[69]. Overall, 127 MAs identified by various techniques were analyzed at baseline and after 1 year of follow-up (26 eyes from 14 patients with type 2 diabetes). Of the 127 MAs detected at baseline, 89 (70%) were still visible on SD OCT after 1 year, while 38 (30%) were not visible. Extracellular fluid accumulation was detected in 44 of 89 MAs (49.4%) after 1 year. MA reflectivity at baseline was strongly associated with extracellular fluid accumulation, with significantly more hyperreflective MAs showing extracellular fluid accumulation compared with hyporefective MAs (**Figures 9 and 10**); this association persisted at 12 months. As for OCTA features, the presence of flow and visibility were both strongly associated with the development of extracellular fluid; this association was also maintained up to 12 months. Furthermore, only MA deep location in the retinal layers was significantly associated with the development of extracellular fluid; this association as well was confirmed at 12

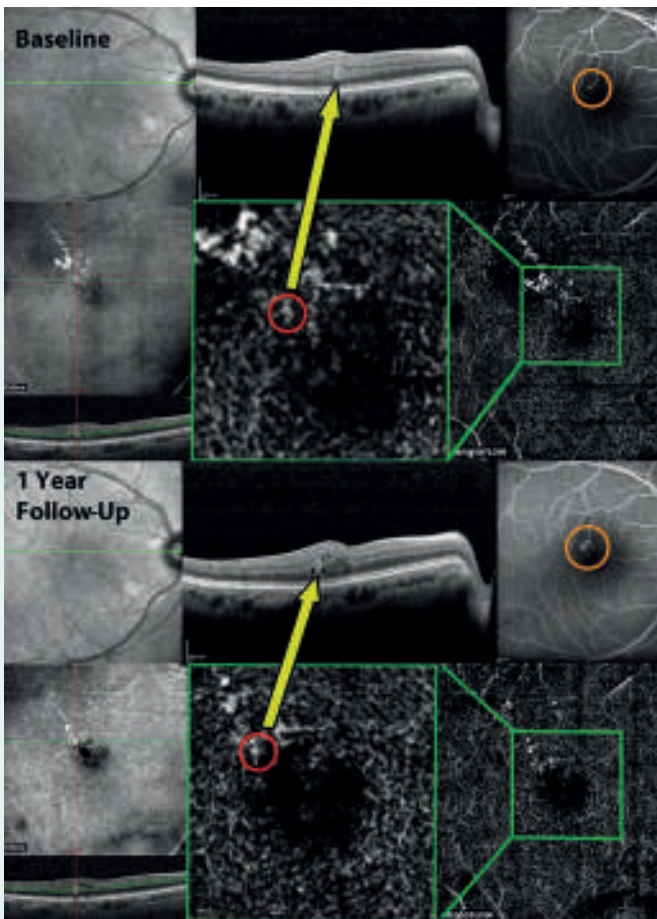


Figure 9. *At baseline:* (Top center) The Spectralis B-scan showing a hyperreflective microaneurysm (yellow arrow) and (Top left) the infrared image with the green line with arrow passing through the microaneurysm. (Top right) The late frame of fluorescein angiography shows the pooling of the dye in correspondence to the microaneurysm, with minimal leakage (orange circle). This exactly corresponds to the focally dilated microaneurysm highlighted by the red circle at the level of the deep capillary plexus (DCP) in the optical coherence tomography (OCTA) imaging (6×6 scanning area) (Bottom right); the inset shows the characteristics of the hyperreflective microaneurysm in detail (Bottom center). (Bottom left) En face imaging with red and green lines indicating the location of B-scans (XR Avanti; Optovue Inc, Fremont, California, USA); the DCP segmentation boundaries (green lines) passing through the microaneurysm are visible. *At 1 year follow-up:* (Top center) The Spectralis B-scan showing the same hyperreflective microaneurysm (yellow arrow) surrounded by new extracellular fluid and (Top left) the infrared image with the green line with arrow passing through the microaneurysm. (Top right) The late frame of fluorescein angiography shows the pooling of the dye in correspondence to the microaneurysm with late leakage (orange circle). This exactly corresponds to the focally dilated microaneurysm highlighted by the red circle at the level of the DCP in the OCTA imaging (6×6 scanning area) (Bottom right); the inset shows the characteristics of the hyperreflective microaneurysm in detail (Bottom center). En face imaging with red and green lines indicating the location of B-scans (Optovue). The DCP segmentation boundaries (green lines) passing through the microaneurysm are visible (Bottom left). (Reproduced with permission from Elsevier Inc. from ref.^[69]).

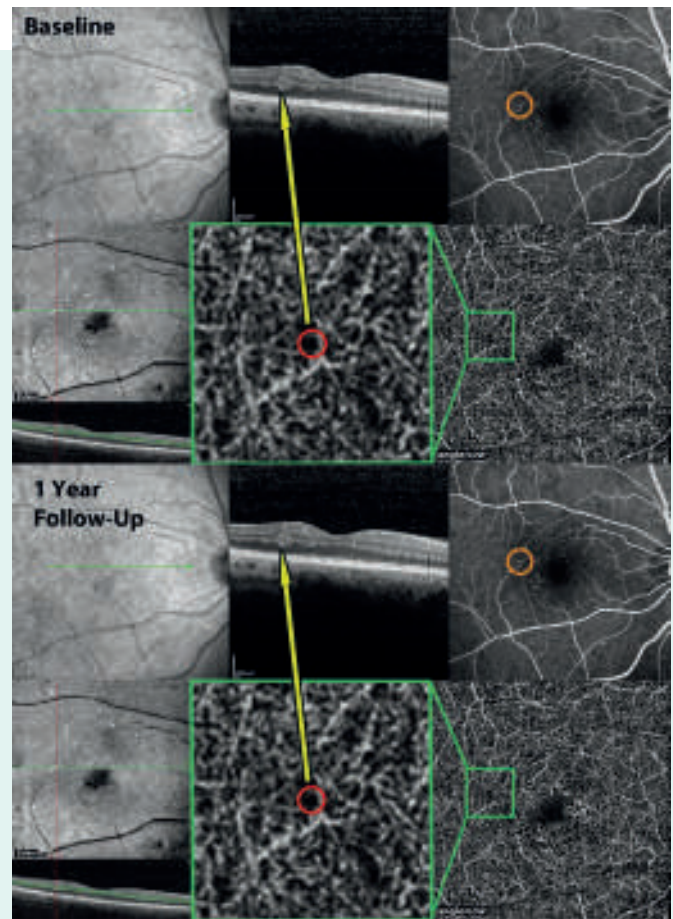


Figure 10. *At baseline:* (Top center) Spectralis B-scan showing a hyporeflective microaneurysm (yellow arrow) and (Top left) the infrared image with the green line with arrow passing through the microaneurysm. (Top right) The late frame of fluorescein angiography shows the pooling of the dye in correspondence to the microaneurysm, with no evident leakage (orange circle). The microaneurysm (red circle) cannot be detected at the level of the deep capillary plexus (DCP) by means of optical coherence tomography angiography (OCTA) imaging (6×6 scanning area) (Bottom right); the inset (green box) shows the area of interest with more detail (Bottom center). (Bottom left) En face imaging with red and green lines indicating the location of B-scans (XR Avanti; Optovue Inc, Fremont, California, USA). The DCP segmentation boundaries (green lines) passing through the microaneurysm are visible. *At 1 year follow-up:* (Top center) The Spectralis B-scan showing the same hyporeflective microaneurysm (yellow arrow) without any new extracellular fluid and (Top left) the infrared image with the green line with arrow passing through the microaneurysm. (Top right) The late frame of fluorescein angiography shows the pooling of the dye in correspondence to the microaneurysm, with still no leakage (orange circle). After 1 year it still appears not visible (red circle) at the level of the DCP by means of OCTA imaging (6×6 scanning area) (Bottom right); the inset (green box) shows the area of interest with more detail (Bottom center). En face imaging with red and green lines indicating the location of B-scans (Optovue). The DCP segmentation boundaries (green lines) passing through the microaneurysm are visible (Bottom left). (Reproduced with permission from Elsevier Inc. from ref.^[69]).

months. The findings of this study suggest a number of baseline MA characteristics that may reliably predict fluid accumulation after 1 year, including: MA reflectivity on SD OCT, presence

of flow on cross-sectional scan, and location in the deep capillary plexus on OCTA. More in detail, hyperreflective MAs with a high blood flow rate appear to correlate with the extracellular

fluid accumulation resulting from disturbances in the blood-retinal barrier in the deep capillary plexus. This OCTA parameter may therefore be a prognostic factor for the onset of macular edema, and DR patients with an elevated number of hyperreflective MAs may be at increased risk of disease progression. At the same time, these patients may be better responders to intravitreal anti-VEGF therapy than patients with hyporefective MAs, a feature that appears to be associated with ischemia. Clearly, the biomarker potential of MAs detected using OCTA for disease prognosis (DR progression and DME onset) and therapy selection needs to be further investigated and validated in larger studies.

CORRELATION BETWEEN RETINAL CAPILLARY PLEXUSES AND THE INNER/OUTER RETINA

The eyes of patients with type 1 and type 2 diabetes are characterized by the presence of microvascular abnormalities affecting the retinal and choroidal vasculature, even in the absence of clinical signs of DR^[67,70,71]. Evidence suggests that early mechanisms of neurovascular dysregulation may play a role in driving the onset of disease^[70]. Neurovascular changes may affect different macular layers, from the inner retina to the choroid. The combination of OCT and OCTA is making the visualization of these changes possible.

The availability of novel imaging techniques has led to the identification of relevant morphological changes including: decrease thickness of the retinal fiber layer and ganglion cell layer; capillary loss in the perifoveal area in the superficial and deep capillary plexuses; presence of dilated capillary ends; presence of NPAs; enlargement of the FAZ in both capillary plexuses, but especially in the deep capillary plexus; damaged photoreceptors; choriocapillaris impairment with an increase in choriocapillaris flow deficit^[67,71-73]. Neuroretinal and microvascular disturbances are key mechanisms in the pathophysiology of DR development. However, the sequence of these changes, or whether these changes occur simultaneously, is currently unknown.

Thinning of the inner retinal layer appears to be the primary OCT finding in diabetic patients who have not developed clinical signs of DR yet. In these patients, Kim et al. described the loss

of macular ganglion cell/inner plexiform layer (mGCIPL) that progressed with time^[70]. These authors demonstrated that the progressive loss of mGCIPL was an independent risk factor for DR progression in early-stage disease and showed that, before DR onset, outer retinal layers were less affected than inner layers^[70]. The capillary network of the superficial capillary plexus is located in the nerve fiber layer or ganglion cell layer, while the capillary network of the deep capillary plexus is located in the inner nuclear layer, which nourishes the middle and outer retina^[70,71].

Very limited data describing the correlation between changes in retinal layer thickness detectable by OCT and microvascular changes detected by OCTA are currently available. Vujosevic et al. reported a robust correlation between perifoveal capillary loss in the superficial capillary plexus and inner retinal layer thickness (ganglion cell layer and nerve fiber layer) in diabetic patients with no signs of DR, confirming that neuronal and microvascular changes take place also in the preclinical stage of DR^[67]. The study by Kim et al. mentioned above reported a progressive loss of mGCIPL thickness that strongly correlated with the decrease of vascular density in the superficial capillary plexus^[70]. More recently, Parravano et al. investigated the structural integrity of photoreceptors in diabetic patients with no DR, by measuring the reflectivity of the EZ on OCTA images^[71]. This novel standardized method had been previously used for quantifying photoreceptor damage in other eye diseases^[74]. When investigating the correlation between EZ normalized reflectivity and the presence of flow deficits in the choriocapillaris slab, a negative correlation was found between these parameters in eyes with no DR^[71]. This finding may support the hypothesis that choriocapillaris vascular drop-out is associated with photoreceptor damage also before the development of DR and confirms the involvement of the choroid in the pathophysiology of diabetes-related events (“diabetic choroidopathy”)^[75].

In conclusion, the available evidence suggests that a correlation between retinal capillary plexuses and the inner/outer retina exists, supporting the hypothesis that neuronal and microvascular changes are interrelated even in the preclinical stage of DR. Further research in this exciting area is warranted.

REFERENCES

1. Otani T, Kishi S, Maruyama Y. Patterns of diabetic macular edema with optical coherence tomography. *Am J Ophthalmol* 1999;127(6):688-93
2. Wu Q, Zhang B, Hu Y, et al. Detection of morphologic patterns of diabetic macular edema using a deep learning approach based on optical coherence tomography images. *Retina* 2021;41:1110-7
3. Sonoda S, Sakamoto T, Yamashita T, et al. Retinal morphologic changes and concentrations of cytokines in eyes with diabetic macular edema. *Retina* 2014;34(4):741-8
4. Panozzo G, Cicinelli MV, Augustin AJ, et al. An optical coherence tomography-based grading of diabetic maculopathy proposed by an international expert panel: The European School for Advanced Studies in Ophthalmology classification. *Eur J Ophthalmol* 2020;30(1):8-18
5. Coscas G, Gaudric A. Natural course of nonrhegmatogenous cystoid macular edema. *Surv Ophthalmol* 1984;28 Suppl:471-84
6. Bolz M, Schmidt-Erfurth U, Deak G, et al. Optical coherence tomographic hyperreflective foci: a morphologic sign of lipid extravasation in diabetic macular edema. *Ophthalmology* 2009;116(5):914-20
7. Vujosevic S, Bini S, Midena G, et al. Hyperreflective intraretinal spots in diabetics without and with nonproliferative diabetic retinopathy: an in vivo study using spectral domain OCT. *J Diabetes Res* 2013;2013:491835
8. Vujosevic S, Bini S, Torresin T, et al. Hyperreflective retinal spots in normal and diabetic eyes: B-scan and en face spectral domain optical coherence tomography evaluation. *Retina* 2017;37(6):1092-103
9. Midena E, Torresin T, Velotta E, et al. OCT hyperreflective retinal foci in diabetic retinopathy: a semi-automatic detection comparative study. *Front Immunol* 2021;12:613051
10. Vujosevic S, Berton M, Bini S, et al. Hyperreflective retinal spots and visual function after anti-vascular endothelial growth factor treatment in center-involving diabetic macular edema. *Retina* 2016;36(7):1298-308
11. Vujosevic S, Torresin T, Bini S, et al. Imaging retinal inflammatory biomarkers after intravitreal steroid and anti-VEGF treatment in diabetic macular edema. *Acta Ophthalmol* 2017;95:464-71
12. Arrigo A, Capone L, Lattanzio R, et al. Optical coherence tomography biomarkers of inflammation in diabetic macular edema treated by fluocinolone acetonide intravitreal drug-delivery system implant. *Ophthalmol Ther* 2020;9:971-80
13. Vujosevic S, Toma C, Villani E, et al. Diabetic macular edema with neuroretinal detachment: OCT and OCT-angiography biomarkers of treatment response to anti-VEGF and steroids. *Acta Diabetol* 2020;57(3):287-96
14. Sun JK, Lin MM, Lammer J, et al. Disorganization of the retinal inner layers as a predictor of visual acuity in eyes with center-involved diabetic macular edema. *JAMA Ophthalmol* 2014;132:1309-16
15. Sun JK, Radwan SH, Soliman AZ, et al. Neural retinal disorganization as a robust marker of visual acuity in current and resolved diabetic macular edema. *Diabetes* 2015;64:2560-70
16. Radwan SH, Soliman AZ, Tokarev J, et al. Association of disorganization of retinal inner layers with vision after resolution of center-involved diabetic macular edema. *JAMA Ophthalmol* 2015;133:820-5
17. Nicholson L, Ramu J, Triantafyllidou I, et al. Diagnostic accuracy of disorganization of the retinal inner layers in detecting macular capillary non-perfusion in diabetic retinopathy. *Clin Exp Ophthalmol* 2015;43:735-41
18. Das R, Spence G, Hogg RE, et al. Disorganization of inner retina and outer retinal morphology in diabetic macular edema. *JAMA Ophthalmol* 2018;136:202-8
19. Moein HR, Novais EA, Rebhun CB, et al. Optical coherence tomography angiography to detect macular capillary ischemia in patients with inner retinal changes after resolved diabetic macular edema. *Retina* 2018;38: 2277-84
20. Cennamo G, Montorio D, Fossataro F, et al. Evaluation of vessel density in disorganization of retinal inner layers after resolved diabetic macular edema using optical coherence tomography angiography. *PLoS One* 2021;16(1):e0244789
21. Maheshwary AS, Oster SF, Yuson RMS, et al. The association between percent disruption of the photoreceptor inner segment/outer segment and visual acuity in diabetic macular edema. *Am J Ophthalmol* 2010;150(1):63-7
22. Itoh Y, Vasanji A, Ehlers JP. Volumetric ellipsoid zone mapping for enhanced visualization of outer retinal integrity with optical coherence tomography. *Br J Ophthalmol* 2016;100(3):295-9
23. Shin HJ, Lee SH, Chung H, Kim HC. Association between photoreceptor integrity and visual outcome in diabetic macular edema. *Graefes Arch Clin Exp Ophthalmol* 2012;250(1):61-70
24. Santos AR, Costa MA, Schwartz C, et al. Optical coherence tomography baseline predictors for initial best-corrected visual acuity response to intravitreal anti-vascular endothelial growth factor treatment in eyes with diabetic macular edema: the CHARTRES study. *Retina* 2018;38(6):1110-9
25. Ehlers JP, Uchida A, Hu M, et al. Higher order assessment of OCT in diabetic macular edema from the VISTA study: ellipsoid zone dynamics and the retinal fluid index. *Ophthalmol Retina* 2019;3(12):1056-66
26. Kessler LJ, Auffarth GU, Bagautdinov D, Khoramnia R. Ellipsoid zone integrity and visual acuity changes during diabetic macular edema therapy: a longitudinal study. *J Diabetes Res* 2021;2021:Article ID 8117650
27. Sulzbacher F, Kiss C, Munk M, et al. Diagnostic evaluation of type 2 (classic) choroidal neovascularization: optical coherence tomography, indocyanine green angiography, and fluorescein angiography. *Am J Ophthalmol* 2011;152(5):799-806 e1

28. Yannuzzi LA, Rohrer KT, Tindel LJ, et al. Fluorescein angiography complication survey. *Ophthalmology* 1986;93(5):611-7
29. Mendis KR, Balaratnasingam C, Yu P, et al. Correlation of histologic and clinical images to determine the diagnostic value of fluorescein angiography for studying capillary detail. *Invest Ophthalmol Vis Sci* 2010;51(11):5864-9
30. Spaide RF, Klanchnik JM Jr, Cooney MJ. Retinal vascular layers imaged by fluorescein angiography and optical coherence tomography angiography. *JAMA Ophthalmol* 2015;133(1):45-50
31. Jia Y, Bailey ST, Wilson DJ, et al. Quantitative optical coherence tomography angiography of choroidal neovascularization in age-related macular degeneration. *Ophthalmology* 2014;121(7):1435-44
32. Mané V, Dupas B, Gaudric A, et al. Correlation between cystoid spaces in chronic diabetic macular edema and capillary nonperfusion detected by optical coherence tomography angiography. *Retina* 2016;36 Suppl 1:S102-S110
33. Coscas G, Lupidi M, Coscas F, et al. Optical coherence tomography angiography in healthy subjects and diabetic patients. *Ophthalmologica* 2018;239(2-3):61-73
34. Parravano M, Costanzo E, Borrelli E, et al. Appearance of cysts and capillary non perfusion areas in diabetic macular edema using two different OCTA devices. *Sci Rep* 2020 Jan 21;10(1):800
35. Kashani AH, Green KM, Kwon J, et al. Suspended scattering particles in motion: a novel feature of OCT Angiography in exudative maculopathies. *Ophthalmol Retina* 2018;2(7):694-702
36. Spaide RF, Fujimoto JG, Waheed NK. Image artifacts in optical coherence tomography angiography. *Retina* 2015;35:2163-80
37. Ishibazawa A, Nagaoka T, Takahashi A, et al. Optical coherence tomography angiography in diabetic retinopathy: a prospective pilot study. *Am J Ophthalmol* 2015;160:35-44
38. Carnevali A, Sacconi R, Corbelli E, et al. Optical coherence tomography angiography analysis of retinal vascular plexuses and choriocapillaris in patients with type 1 diabetes without diabetic retinopathy. *Acta Diabetol* 2017;54(7):695-702
39. Agemy SA, Sripsema NK, Shah CM, et al. Retinal vascular perfusion density mapping using optical coherence tomography angiography in normals and diabetic retinopathy patients. *Retina* 2015;35(11):2353-63
40. Hwang TS, Gao SS, Liu L, et al. Automated quantification of capillary nonperfusion using optical coherence tomography angiography in diabetic retinopathy. *JAMA Ophthalmol* 2016;21:1-7
41. Lupidi M, Coscas G, Coscas F, et al. Retinal microvasculature in non-proliferative diabetic retinopathy: automated quantitative optical coherence tomography angiography assessment. *Ophthalmic Res* 2017;58:131-41
42. Coscas G, Lupidi M, Coscas F. Optical coherence tomography angiography in diabetic maculopathy. *Dev Ophthalmol* 2017;60:38-49
43. Zahid S, Dolz-Marco R, Freund KB, et al. Fractal dimensional analysis of optical coherence tomography angiography in eyes with diabetic retinopathy. *Invest Ophthalmol Vis Sci* 2016;57:4940-7
44. Neubauer AS, Kook D, Haritoglou C, et al. Bevacizumab and retinal ischemia. *Ophthalmology* 2007;114:2096
45. Kook D, Wolf A, Kreutzer T, et al. Long-term effect of intravitreal bevacizumab (avastin) in patients with chronic diffuse diabetic macular edema. *Retina* 2008;28:1053-60
46. Pereira F, Godoy BR, Maia M, Regatieri CV. Microperimetry and OCT angiography evaluation of patients with ischemic diabetic macular edema treated with monthly intravitreal bevacizumab: a pilot study. *Int J Retin Vitreous* 2019;5:24
47. Lee SJ, Koh HJ. Enlargement of the foveal avascular zone in diabetic retinopathy after adjunctive intravitreal bevacizumab (avastin) with pars plana vitrectomy. *J Ocul Pharm Ther* 2009;25:173-4
48. Karst SG, Deak GG, Gerendas BS, et al. Association of changes in macular perfusion with ranibizumab treatment for diabetic macular edema: a subanalysis of the RESTORE (Extension) study. *JAMA Ophthalmol* 2018;136:315-21
49. Barash A, Chui TYP, Garcia P, Rosen RB. Acute macular and peripapillary angiographic changes with intravitreal injections. *Retina* 2020;40:648-56
50. Couturier A, Rey PA, Erginay A, et al. Widefield OCT-angiography and fluorescein angiography assessments of nonperfusion in diabetic retinopathy and edema treated with anti-vascular endothelial growth factor. *Ophthalmology* 2019;126:1685-94
51. Bird AC, Weale RA. On the retinal vasculature of the human fovea. *Exp Eye Res* 1974;19:409-17
52. Samara WA, Shahlaee A, Adam MK, et al. Quantification of diabetic macular ischemia using optical coherence tomography angiography and its relationship with visual acuity. *Ophthalmology* 2017;124:235-44
53. Mammo Z, Balaratnasingam C, Yu P, et al. Quantitative noninvasive angiography of the fovea centralis using speckle variance optical coherence tomography. *Invest Ophthalmol Vis Sci* 2015;56:5074-86
54. Lupidi M, Coscas F, Cagini C, et al. Automated quantitative analysis of retinal microvasculature in normal eyes on optical coherence tomography angiography. *Am J Ophthalmol* 2016;169:9-23
55. De Carlo T, Chin A, Bonini F, et al. Detection of microvascular changes in eyes of patients with diabetes but not clinical diabetic retinopathy using optical coherence tomography angiography. *Retina* 2015;35:2364-70
56. Al-Sheikh M, Akil H, Pfau M, Sadda SR. Swept-source OCT angiography imaging of the foveal avascular zone and macular capillary network density in diabetic retinopathy. *Invest Ophthalmol Vis Sci* 2016;57:3907-13
57. Bhanushali D, Anegondi N, Gadde S, et al. Linking retinal microvasculature features with severity of diabetic retinopathy using optical coherence to-

- mography angiography. *Invest Ophthalmol Vis Sci* 2016;57:519-25
58. Durbin MK, An L, Shemonski ND, et al. Quantification of retinal microvascular density in optical coherence tomography angiography images in diabetic retinopathy. *JAMA Ophthalmol* 2017;135:370-6
 59. Lee H, Lee M, Chung H, Kim HC. Quantification of retinal vessel tortuosity in diabetic retinopathy using optical coherence tomography angiography. *Retina* 2017;38:976-85
 60. Conrath J, Giorgi R, Raccach D, Ridings B. Foveal avascular zone in diabetic retinopathy: quantitative vs qualitative assessment. *Eye (Lond)* 2005;19:322-6
 61. Friberg TR, Lace J, Rosenstock J, Raskin P. Retinal microaneurysm counts in diabetic retinopathy: colour photography versus fluorescein angiography. *Can J Ophthalmol* 1987;22(4):226-9
 62. Couturier A, Mane V, Bonnin S, et al. Capillary plexus anomalies in diabetic retinopathy on optical coherence tomography angiography. *Retina* 2015;35(11):2384-91
 63. Nesper PL, Roberts PK, Onishi AC, et al. Quantifying microvascular abnormalities with increasing severity of diabetic retinopathy using optical coherence tomography angiography. *Invest Ophthalmol Vis Sci* 2017;58(6):BIO307-BIO315
 64. Lee J, Moon BG, Cho AR, Yoon YH. Optical coherence tomography angiography of DME and its association with anti-VEGF treatment response. *Ophthalmology* 2016;123(11):2368-75
 65. Hasegawa N, Nozaki M, Takase N, et al. New insights into microaneurysms in the deep capillary plexus detected by optical coherence tomography angiography in diabetic macular edema. *Invest Ophthalmol Vis Sci* 2016;57(9):OCT348-55
 66. Parravano M, De Geronimo D, Scarinci F, et al. Diabetic microaneurysms internal reflectivity on spectral-domain optical coherence tomography and optical coherence tomography angiography detection. *Am J Ophthalmol* 2017;179:90-6
 67. Vujosevic S, Muraca A, Alkabes M, et al. Early microvascular and neural changes in patients with type 1 and type 2 diabetes mellitus without clinical signs of diabetic retinopathy. *Retina* 2019;39(3):435-45
 68. Dmitriev AV, Henderson D, Linsenmeier RA. Development of diabetes-induced acidosis in the rat retina. *Exp Eye Res* 2016;149:16-25
 69. Parravano M, De Geronimo D, Scarinci F, et al. Progression of diabetic microaneurysms according to the internal reflectivity on structural optical coherence tomography and visibility on optical coherence tomography angiography. *Am J Ophthalmol* 2019;198:8-16
 70. Kim K, Kim ES, Kim DG, Yu SY. Progressive retinal neurodegeneration and microvascular change in diabetic retinopathy: longitudinal study using OCT angiography. *Acta Diabetol* 2019;56(12):1275-82
 71. Parravano M, Ziccardi L, Borrelli E, et al. Outer retina dysfunction and choriocapillaris impairment in type 1 diabetes. *Sci Rep* 2021;11(1):15183
 72. van Dijk HW, Verbraak FD, Kok PH, et al. Early neurodegeneration in the retina of type 2 diabetic patients. *Invest Ophthalmol Vis Sci* 2012;53(6):2715-19
 73. Borrelli E, Abdelfattah NS, Uji A, et al. Postreceptor neuronal loss in intermediate age-related macular degeneration. *Am J Ophthalmol* 2017;181:1-11
 74. Borrelli E, Palmieri M, Viggiano P, et al. Photoreceptor damage in diabetic choroidopathy. *Retina* 2020;40(6):1062-9
 75. Nagaoka T, Kitaya N, Sugawara R, et al. Alteration of choroidal circulation in the foveal region in patients with type 2 diabetes. *Br J Ophthalmol* 2004;88(8):1060-3

3. Ultrawide-field imaging evaluation of diabetic macular edema

Wide-field (WF) and ultrawide-field (UWF) techniques, developed to expand the retinal field of view, have allowed to explore areas of the retina far from the center and to study peripheral lesions. The next sections describe applications of WF and UWF techniques to color fundus photography, fluorescein angiography (FA), and optical coherence tomography angiography (OCTA)

Multicolor fundus imaging and ultrawide-field color fundus photography

Multicolor imaging is a non-invasive imaging procedure, which consists in taking en-face pictures of the retina using three laser lights with different wavelengths (blue, $\lambda = 488$ nm; green, $\lambda = 518$ nm; infrared, $\lambda = 820$ nm) to identify lesions in retinal layers^[1]. The blue laser, with the shortest wavelength, analyzes the inner retinal and vitreoretinal interface. The green laser, thanks to its greater penetration and absorption by hemoglobin, allows to identify retinal vessels and intraretinal exudation. The infrared laser, the most penetrating one, evaluates the deepest layers including the retinal outer layer, retinal pigment epithelium, and choroid^[2,3]. Compared with color fundus photography, multicolor imaging provides higher contrast and resolution. Moreover, thanks to the greater penetration of laser versus visible light, media opacities have less influence than in color fundus photography^[4]. The increased permeability of retinal capillaries in diabetic retinopathy (DR) leads to the extravasation of lipids and lipoproteins into retinal layers, which results in the development of diabetic macular edema (DME) and hard exudates. The presence of hard exudates correlates with a worse prognosis of DME; conversely, the reduction in the number of hard exudates is associated with an improvement in DME. For this reason, analyzing the location, number, and possible pro-

gression of hard exudates is helpful in the evaluation of DME. Multicolor imaging has proven useful for this purpose, as this exam appears to be better and more convenient for the identification of DME than color fundus photography. In addition, hard exudates appear brighter and more visible and are therefore easier to detect with multicolor imaging than with color fundus photography^[4].

When screening for DR/DME, visual acuity measurements and fundus biomicroscopy are generally performed to confirm the fundus condition (**Figures 1 and 2**). This first step provides reproducible measurements for normal eyes and for DR eyes with or without macular edema. However, studies have shown that optical coherence tomography (OCT) is more sensitive for small changes in retinal thickness, compared with biomicroscopy or color fundus photography^[5] (**Figures 1 and 2**). As shown by **Figures 1-3**, with UWF techniques it is possible to increase the fundus field of view and to visualize peripheral areas of the retina.

Ultrawide-field fluorescein angiography

FA, introduced in 1960 by Novotny and Alvis, was the first tool to analyze vascularization in retinal vascular diseases, including DR^[6]. The procedure consists in injecting intravenously a dye, fluorescein, 80% of which binds to serum proteins, mostly albumin, while 20%

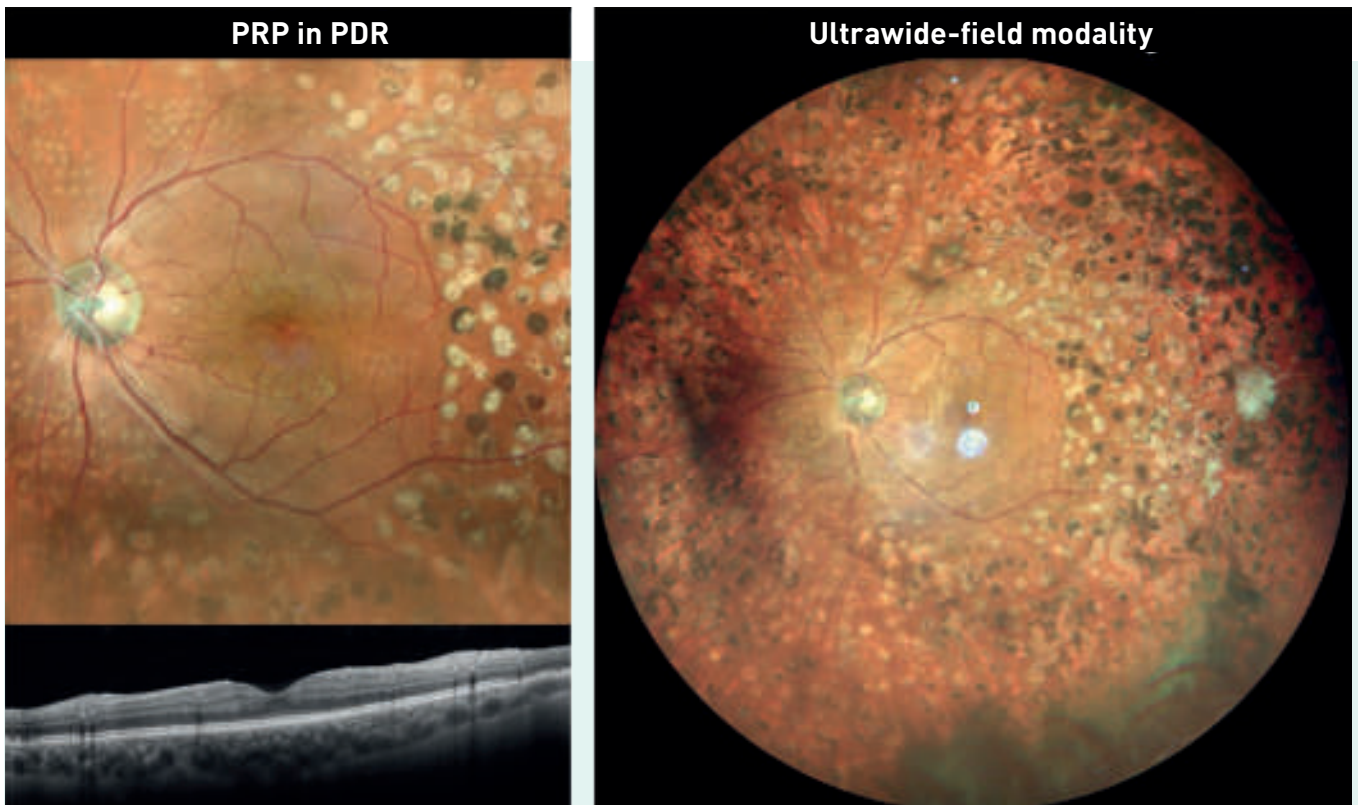


Figure 1. Color fundus photograph at the posterior pole and UWF color fundus photograph of a diabetic eye with panretinal photocoagulation scars. The B-scan OCT reveals the absence of DME. PRP, panretinal photocoagulation; PDR, proliferative diabetic retinopathy.

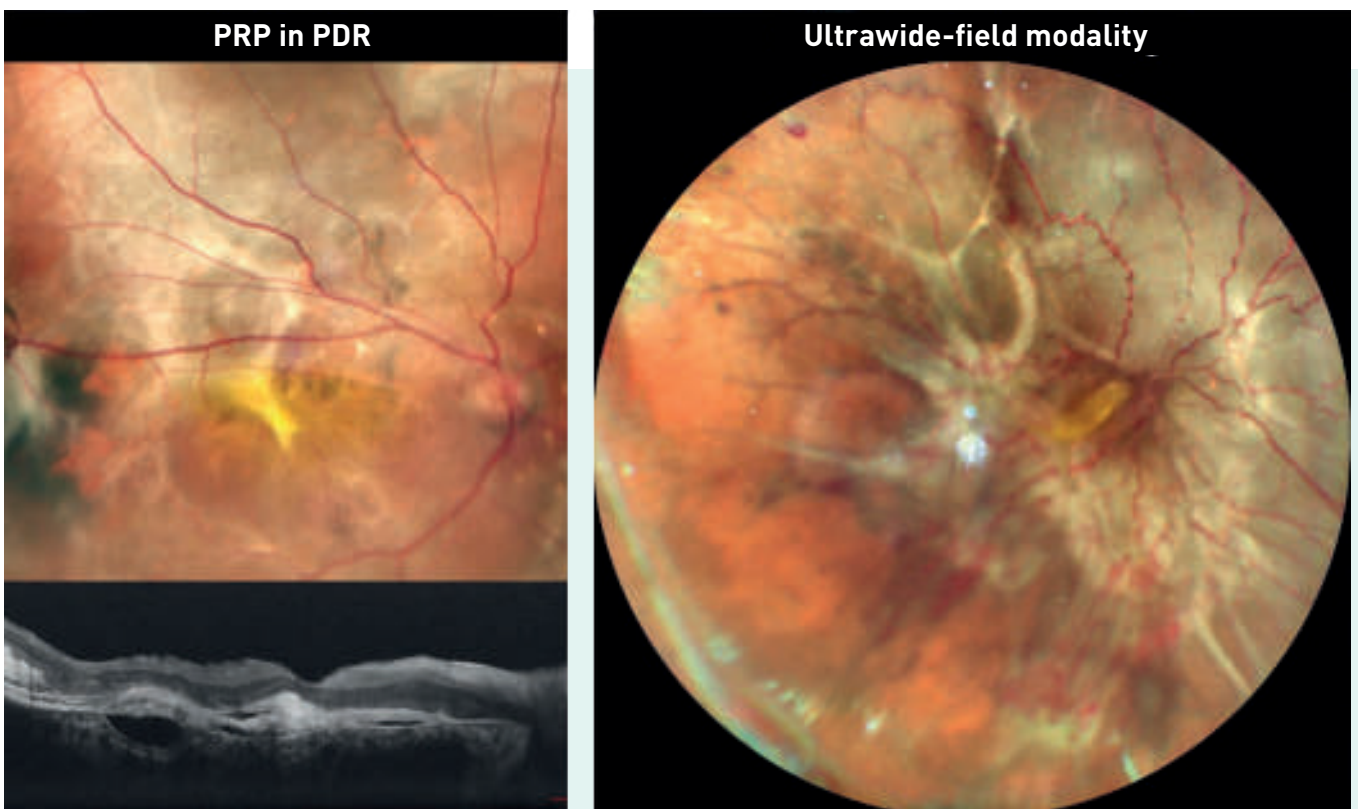


Figure 2. Color fundus photograph at the posterior pole and UWF color fundus photograph of a diabetic eye showing retinal detachment with subretinal proliferation membranes. The OCT B-scan reveals subretinal proliferation. PRP, panretinal photocoagulation; PDR, proliferative diabetic retinopathy.

remains free in the blood. Thanks to the tight junctions between endothelial cells, which establish the inner blood-retinal barrier, and to the apical junctions of the retinal pigmented epithelium, which form the outer retinal barrier, the dye is confined within the retinal vessels. In retinal vascular diseases, including DR, the inner blood-retinal barrier is damaged. Therefore, fluorescein can leak out of vessels giving rise to hyperfluorescence signals. To evaluate the integrity of the blood-retinal barrier, an expert operator takes retinal pictures at early (from the injection of fluorescein to 1 min and 30 seconds), intermediate (from 1 minute and 30 seconds to 5 minutes), and late (from 5 to 10 minutes) time points following fluorescein injection, using a digital fundus camera.

Traditional FA allows to view approximately 30° of the retina in one shot, while about 75° can be analyzed using the Early Treatment for Diabetic Retinopathy Study (ETDRS) seven-standard fields (7SF). UWF FA was introduced in 2000 (Optos PLC, Dunfermline, Scotland, UK). This technique allows to visualize 200° of the retina in a single picture^[7] (Figures 1-3). The advantages of a greater field of visualization have been demonstrated by Wessel et al.: UWF FA was found to highlight non-perfusion areas 3.9 times more than traditional FA, neovascularization 1.9 times more, and panretinal photocoagulation scars 3.8 times more^[8]. Moreover, the identification of a greater proportion of predominantly peripheral lesions was found to correlate with an increased risk of DR progression^[9]. Predominantly peripheral lesions were represented by microaneurysms, hemorrhages, venous beading, intraretinal microvascular abnormalities, and new vascularization elsewhere^[9].

Several studies using UWF FA have evaluated the correlation between peripheral retinal ischemia and DME. Wessel et al. demonstrated that patients with retinal ischemia were 3.75 times more likely to have DME^[10]. Leakage index, ischemic index (which expresses the percentage of ischemia over the total retina), and microaneurysm count resulted higher in diabetic eyes with DME than in diabetic eyes without DME^[7]. Furthermore, Patel et al. highlighted that unresolved DME was

linked to larger ischemic areas in UWF FA and to more severe DR^[11]. Other studies, however, found that non-perfusion areas and ischemic index did not correlate with central macular thickness (CMT) and macular volume^[12]. According to the authors a possible explanation was that in ischemic areas, in the absence of blood supply, the production of vascular endothelial growth factor (VEGF) was decreased, due to retinal cell dysfunction. At the same time, the presence of DME in diabetic eyes with few non-perfusion areas suggested that even a small ischemic area could be sufficient to stimulate VEGF production^[12].

UWF FA may be useful in all stages of DR, from early disease to the advanced neovascularization stage (Figure 3). Furthermore, advances in UWF FA devices allow targeted retinal photocoagulation of non-perfusion areas visualized by UWF FA; this strategy has been applied with good outcomes in terms of neovascularization regression and CMT reduction, with no reported adverse effects^[13]. Therefore, UWF FA may also play a role in identifying DR patients who are likely to benefit from surgical treatment.

Ultrawide-field optical coherence tomography angiography

WF and UWF imaging of the retina allows to capture a greater field of view and to inspect peripheral areas of the retina. Conventional fundus camera cover between 20° and 50° fundus field of view, while UWF techniques cover up to 200° fundus field of view and more^[13,14]. As seen in the previous section, the ability to visualize peripheral retina lesions and to obtain a more comprehensive picture of the retina has significantly changed the assessment and grading of DR. In particular, studies comparing standard-field FA and UWF FA imaging have shown that UWF imaging identifies significantly more neovascularization and non-perfusion areas than standard imaging^[14].

UWF modalities have been applied also to OCTA imaging^[15]. As described in Chapter 2, OCTA is a further development of OCT, which

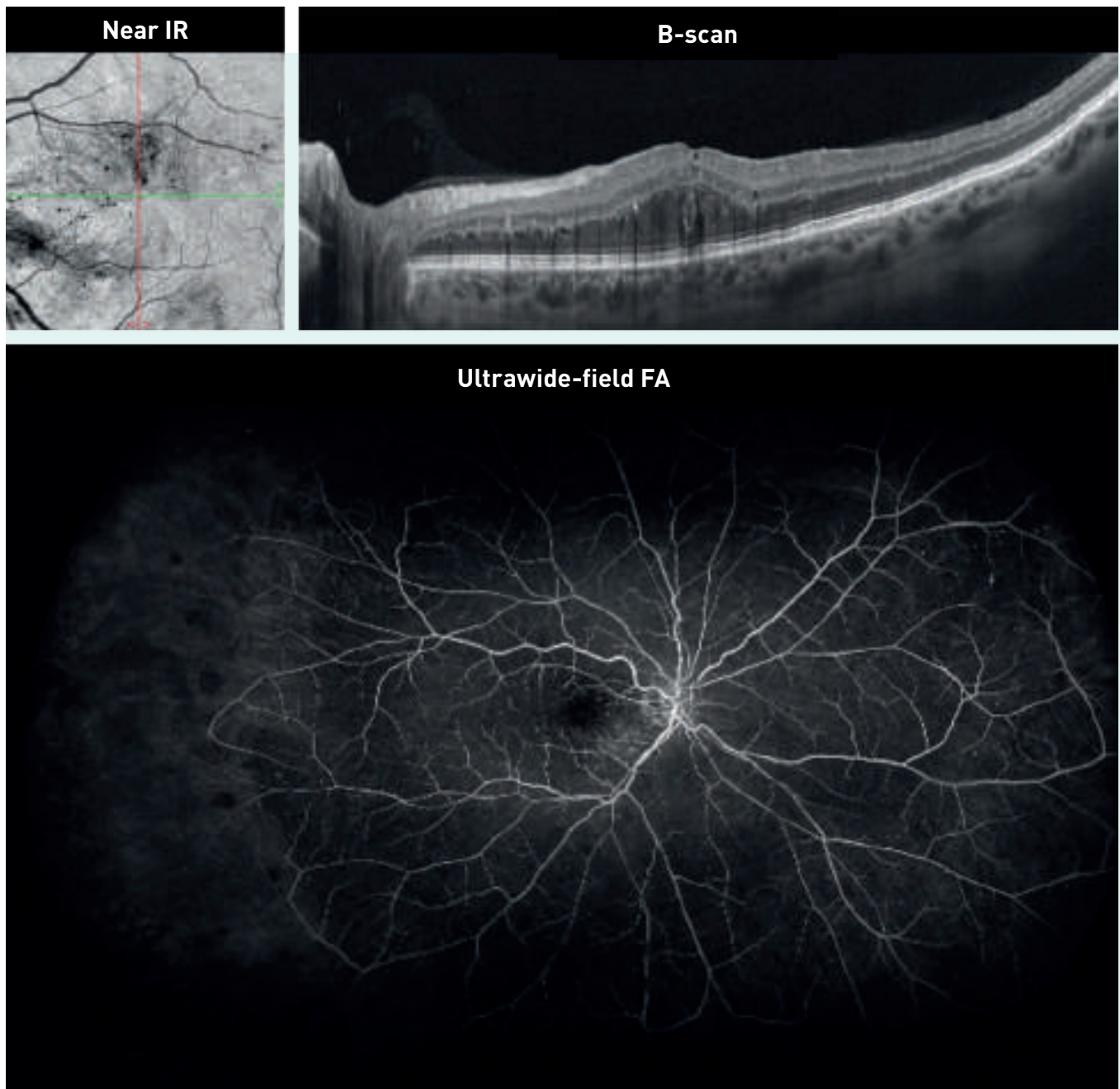


Figure 3. UWF FA using the California-Optos® device. The near infrared (IR) image shows the focal hyporeflective dots suggesting macular involvement of DR; the green horizontal line defines the position of structural OCT. The B-scan OCT shows intraretinal edema involving mainly the outer nuclear layer. UWF FA reveals non-perfusion in the peripheral-temporal area and tiny white dots across all peripheral retina and in the macular region.

evaluates retinal microvasculature by detecting the flow of red blood cells within the vessels. In OCTA, the field of view is limited by the speed of image acquisition^[15]. Standard OCTA systems have an imaging speed of about 70 kHz and fields of view comprised between 3×3 and 6×6 mm²^[15]. Wider fields of view (up to 12×12 mm² and 50°) in a single scan can be achieved with faster (100 kHz), swept source (SS) OCTA systems (**Figure 4A**)^[15]. More than 50° field of view can be achieved with the montage of two 15×9 mm² im-

ages (superior and inferior) (**Figures 4B and 5**). Several small studies have evaluated UWF OCTA, especially in comparison with FA modalities, for the diagnosis of DR and the evaluation of response to treatment, highlighting the potential of this approach for the detection of intraretinal microvascular abnormalities, retinal non-perfusion areas, and neovascularization^[16,17] (**Figures 4-6**).

The first attempt to extend the field of view with OCTA was done with SS OCTA using

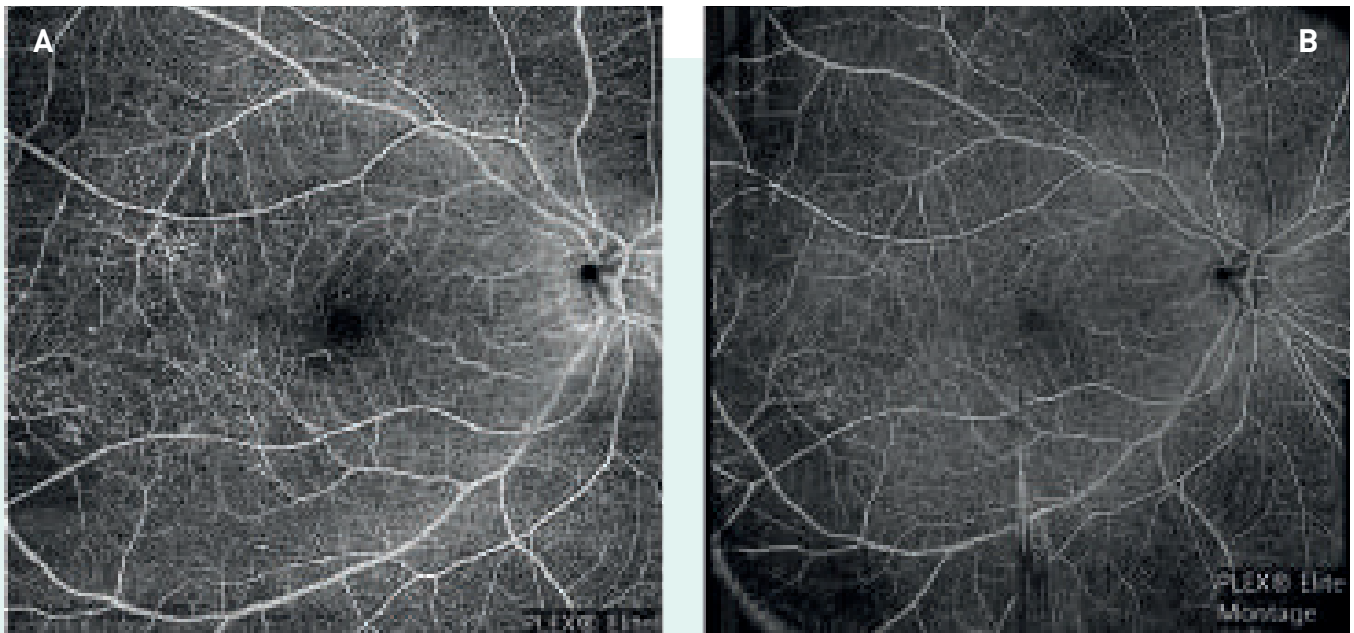


Figure 4. Fields of view that can be achieved with WF OCTA. A, a $12 \times 12 \text{ mm}^2$ WF SS OCTA provides 50° field of view; this image was acquired using SS OCTA PLEX® Elite 9000 (Zeiss) in a patient with non-proliferative DR showing abnormalities in the foveal avascular zone and in the vascularization of the superficial capillary plexus. In the temporal sector non-perfusion areas, microaneurysms, and vascular loops are recognized. B, a $15 \times 9 \text{ mm}^2$ montage provides $>50^\circ$ field of view; this image was obtained in the same patient using the same device as in panel A. The wider field of view extends to the mid periphery. Non-perfusion areas, microaneurysms, and vascular loops are recognized especially in the temporal sector.

the montage of 5 images^[18]. This study in 33 patients (58 eyes) with DR compared the ability of UWF FA and wide-angle OCTA ($12 \times 12 \text{ mm}^2$ fields of five visual fixations) to detect non-perfusion areas and neovascularization. OCTA was found to have elevated sensitivity and specificity for the detection of both markers (0.98 sensitivity and 0.82 specificity for the detection of non-perfusion areas; 1.0 sensitivity and 0.97 specificity for the detection of neovascularization), overlapping with the performance of UWF FA^[18]. Another attempt to extend the field of view was performed by Pellegrini et al.^[19] with a prototype of +20.00-diopter lens designed specifically by Zeiss. The objective of this study was to compare the performance of SS OCTA, with and without the extended field imaging technique (EFI), with standard FA in the setting of clinical practice. The study found that SS OCTA with EFI captured larger areas than SS OCTA without EFI and FA. Without the use of montage techniques, and in a single scan, OCTA was therefore able to obtain more information on the retina.

The superior accuracy of OCTA over FA in delimiting capillary non-perfusion areas is well established^[20]. Several studies have used

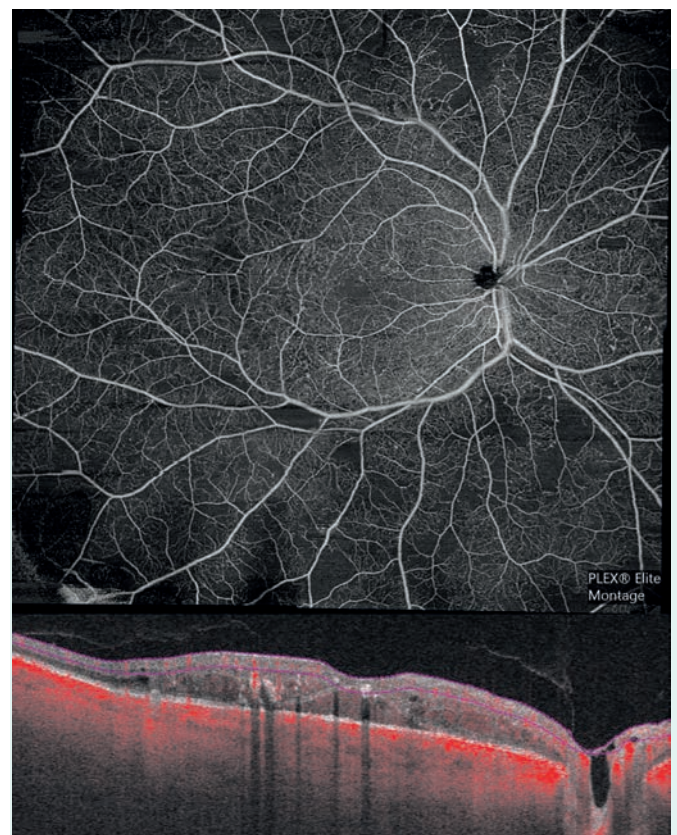


Figure 5. Example of a $15 \times 9 \text{ mm}^2$ montage WF SS OCTA image. The image was acquired using WF SS OCTA PLEX® Elite 9000 (Zeiss) in a patient with non-proliferative DR showing vascularization abnormalities in the superficial capillary plexus. Non-perfusion areas are visible in the mid periphery.

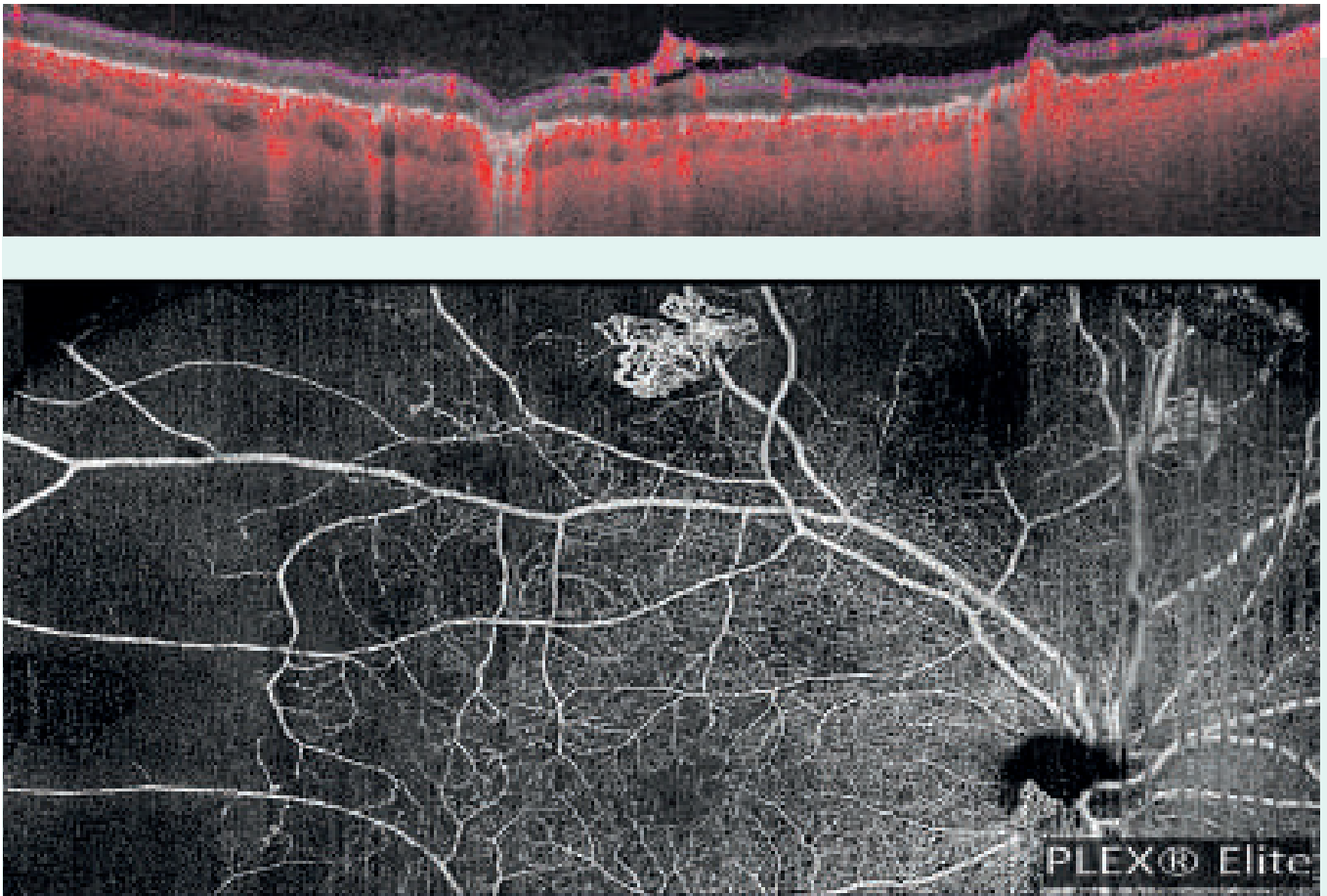


Figure 6. SS OCTA image in a patient with proliferative DR. The image acquired using PLEX® Elite 9000 (Zeiss) shows abnormalities in the foveal avascular zone and in the vascularization of the superficial capillary plexus (lower panel). Neovascularization is visible in the optic disc and the superior mid periphery. Co-recorded OCT with flow overlay OCTA (upper panel) shows advanced retinal neovascularization with a breach in the internal limiting membrane and growth towards the posterior hyaloid.

OCTA to investigate the association between non-perfusion and disease severity. A correlation between the extension of non-perfusion areas and the severity of disease was reported in a study using WF SS OCTA, along with a semiautomatic system for image processing and quantitative analysis of capillary non-perfusion (68 diabetic patients, 73 eyes)^[21]. In the eyes without DR, the mean rate of non-perfusion areas was 0.1%; this rate increased to 2.1% in eyes with non-proliferative DR and to 8.5% in eyes with proliferative disease, with the differences between disease grades being statistically significant. These results suggested that capillary non-perfusion areas in the peripheral retina increase with worsening of retinopathy and that WF OCTA may be suitable for monitoring the course of DR. Of note, no statistically significant difference in mean non-perfusion areas was found between proliferative DR with

and without DME. A study used WF SS OCTA to examine perfusion density of the central and peripheral retina of 94 diabetes patients (94 eyes) with or without DR. Perfusion density was found to correlate significantly with the severity of DR, providing a sensitive and specific marker of disease worsening^[22]. The study also showed that WF SS OCTA is a valuable tool for the evaluation of central and peripheral retinal perfusion in patients with or without DR. Using WF SS OCTA, Russel et al. demonstrated that neovascularization elsewhere in proliferative DR was most prevalent supertemporal, with 99.4% of treatment-naïve eyes showing neovascularization within the simulated WF SS OCTA field of view^[23]. Disc-centered instead of fovea-centered retinal quadrants increased the detection of neovascularization. Combined with the results from previous studies of WF SS OCTA for the identification of neovascularization in pro-

liferative DR, these findings suggested that WF SS OCTA alone may be sufficient for the diagnosis and longitudinal assessment of proliferative DR^[23].

WF OCTA is useful not only for diagnosing and grading DR, but also for assessing response to treatment. Couturier et al. assessed the changes in retinal non-perfusion areas following anti-VEGF therapy in patients with DME, using WF SS OCTA and UWF FA (9 patients, 10 eyes)^[24].

Imaging was performed at baseline and 1 month after the third injection of anti-VEGF. In 80% of the eyes, the DR score improved with treatment by at least 1 stage. WF SS OCTA detected approximately 30% more non-perfusion areas. Neither technique was able to detect reperfusion of retinal vasculature at 3 months of anti-VEGF treatment. In the study by Russell et al. mentioned above, WF SS OCTA and UWF FA were compared in their ability to evaluate changes in neovascularization from baseline to 3 months following panretinal photocoagulation^[23]. The two imaging techniques appeared comparable in their ability to detect and monitor neovascularization at baseline and 3 months after treatment. Based on UWF FA assessment at 3 months from treatment, 47% of the eyes had progressed and 53% had regressed; WF SS OCTA provided similar rates of progression and regression. Notably, at baseline, WF SS OCTA was able to distinguish between intraretinal microvascular retinal abnormalities – one of the features of DR – and neovascularization – the key marker of proliferative DR. WF SS OCTA may therefore be able to detect the subtle vascular changes that cause disease progression^[23]. In a similar study, these authors evaluated retinal non-perfusion areas with the two techniques before and after treatment with panretinal photocoagulation^[25].

Both techniques were comparable in detecting retinal non-perfusion areas at baseline and following treatment. Panretinal photocoagulation did not seem to affect non-perfusion areas that remained stable for up to 1 year following treatment. More recently, Lupidi et al. assessed retinal neovascularization in proliferative DR before and after photocoagulation laser therapy, using OCTA^[26]. The authors confirmed that the quantitative OCTA assessment of laser-induced changes in retinal neovascularization can be a useful, non-invasive approach for determining treatment efficacy. A $\geq 40\%$ reduction of retinal neovascularization areas or vascular perfusion density may help identify eyes that will not require additional treatment. Retinal perfusion impairment seemed to progress independently of treatment^[26].

OCT techniques, which have been traditionally used for the evaluation of DME, provide three-dimensional information and are thereby able to show in detail the layered structure of the retina and to distinguish between neovascularization and intraretinal microvascular retinal abnormalities (see Chapter 2). Unlike FA, which requires the injection of fluorescein, OCTA is not invasive and can be performed at every visit. WF techniques are revolutionizing the evaluation of DR by visualizing the consequences of peripheral retinal ischemia. Evidence shows that WF OCTA can diagnose proliferative DR with accuracy and, in particular cases, this technique may replace FA, which has been for long the mainstay of DR imaging^[17]. In addition, preliminary evidence suggests that WF OCTA may be a valuable tool for monitoring disease progression and assessing the response to treatment of DR. Further effort is needed to standardize image acquisition techniques, increase the field of view, and reduce the occurrence of WF-related artifacts.

REFERENCES

1. Li S, Wang X, Du X, Wu Q. Clinical application of multi-colour scanning laser imaging in diabetic retinopathy. *Lasers Med Sci* 2018;33(6):1371-79
2. Ahmad MSZ, Carrim ZI. Multicolor scanning laser imaging in diabetic retinopathy. *Optom Vis Sci* 2017;94(11):1058-61
3. Tan AC, Fleckenstein M, Schmitz-Valckenberg S, et al. Clinical application of multicolor imaging technology. *Ophthalmologica* 2016;236:8-18
4. Gong R, Han R, Guo J, et al. Quantitative evaluation of hard exudates in diabetic macular edema by multicolor imaging and their associations with serum lipid levels. *Acta Diabetologica* 2021;58(9):1161-7
5. Mookiah MR, Acharya UR, Fujita H, et al. Application of different imaging modalities for diagnosis of Diabetic Macular Edema: A review. *Comput Biol Med* 2015;66:295-315
6. Novotny HR, Alvis DL. A method of photographing fluorescence in circulating blood in the human retina. *Circulation* 1961;24:82-6
7. Sun G, Wang X, Jiang J, et al. Association of subregional quantitative ultra-widefield fluorescence angiography characteristics with the occurrence of diabetic macular edema and proliferative diabetic retinopathy. *Front Med (Lausanne)* 2021;8:720564
8. Wessel MM, Aaker GD, Parlitsis G, et al. Ultra-widefield angiography improves the detection and classification of diabetic retinopathy. *Retina* 2012;32:785e791
9. Silva PS, Cavallerano JD, Haddad NM, et al. Peripheral lesions identified on ultrawide field imaging predict increased risk of diabetic retinopathy progression over 4 years. *Ophthalmology* 2015;122:949e956
10. Wessel MM, Nair N, Aaker GD, et al. Peripheral retinal ischaemia, as evaluated by ultra-widefield fluorescein angiography, is associated with diabetic macular oedema. *Br J Ophthalmol* 2012;96:694e698
11. Patel RD, Messner LV, Teitelbaum B, et al. Characterization of ischemic index using ultra-widefield fluorescein angiography in patients with focal and diffuse recalcitrant diabetic macular edema. *Am J Ophthalmol* 2013;155:1038e1044.e2
12. Fan W, Wang K, Falavarjani KG, et al. Distribution of nonperfusion area on ultra-widefield fluorescein angiography in eyes with diabetic macular edema: DAVE Study. *Am J Ophthalmol* 2017;180:110-6
13. Rabiolo A, Parravano M, Querques L, et al. Ultra-wide-field fluorescein angiography in diabetic retinopathy: a narrative review. *Clin Ophthalmol* 2017 Apr 27;11:803-7
14. Falavarjani KG, Wang K, Khadamy J, Sadda SR. Ultra-wide-field imaging in diabetic retinopathy; an overview. *J Curr Ophthalmol* 2016;28:57-60
15. Zhang Q, Rezaei KA, Saraf SS, et al. Ultra-wide optical coherence tomography angiography in diabetic retinopathy. *Quant Imaging Med Surg* 2018;8(8):743-53
16. Sun Z, Yang D, Tang Z, et al. Optical coherence tomography angiography in diabetic retinopathy: an updated review. *Eye* 2021;35:149-61
17. Vaz-Pereira S, Morais-Sarmento T, Engelbert M. Update on optical coherence tomography and optical coherence tomography angiography imaging in proliferative diabetic retinopathy. *Diagnostics* 2021;11:1869
18. Sawada O, Ichiyama Y, Obata S, et al. Comparison between wide-angle OCT angiography and ultra-wide field fluorescein angiography for detecting non-perfusion areas and retinal neovascularization in eyes with diabetic retinopathy. *Graefes Arch Clin Exp Ophthalmol* 2018;256(7):1275-80
19. Pellegrini M, Cozzi M, Staurenghi G, Corvi F. Comparison of wide field optical coherence tomography angiography with extended field imaging and fluorescein angiography in retinal vascular disorders. *PLoS ONE* 2019;14(4):e0214892
20. Couturier A, Mané V, Bonnin S, et al. Capillary plexus anomalies in diabetic retinopathy on optical coherence tomography angiography. *Retina* 2015;35(11):2384-91
21. Alibhai AY, De Pretto LR, Moulton EM, et al. Quantification of retinal capillary nonperfusion in diabetics using wide-field optical coherence tomography angiography. *Retina* 2020;40(3):412-20
22. Mastropasqua R, D'Aloisio R, Di Antonio L, et al. Widefield optical coherence tomography angiography in diabetic retinopathy. *Acta Diabetol* 2019;56(12):1293-303
23. Russell JF, Shi Y, Hinkle JW, et al. Longitudinal wide field swept source OCT angiography of neovascularization in proliferative diabetic retinopathy after panretinal photocoagulation. *Ophthalmol Retina* 2019;3(4):350-61
24. Couturier A, Rey P-A, Erginay A, et al. Widefield OCT-angiography and fluorescein angiography assessments of nonperfusion in diabetic retinopathy and edema treated with anti-vascular endothelial growth factor. *Ophthalmology* 2019;126(12):1685-94
25. Russell JF, Al-kharsan H, Shi Y, et al. Retinal nonperfusion in proliferative diabetic retinopathy before and after panretinal photocoagulation assessed by wide field OCT angiography. *Am J Ophthalmol* 2020;213:177-85
26. Lupidi M, Gujar R, Cerquaglia A, et al. OCT-angiography as a reliable prognostic tool in laser-treated proliferative diabetic retinopathy: the RENOCTA Study. *Eur J Ophthalmol* 2021;31(5):2511-9

4. Clinical cases

The three clinical cases that follow are representative examples of patients with diabetic retinopathy (DR), with or without diabetic macular edema (DME), encountered in clinical practice. The three patients, aged from 20 to 57 years, had a >10-year history of type 1 diabetes. Due to the severity of their retinopathy (presence of DME in case 1, proliferative DR in case 2, and rapid worsening of disease in case 3), they were all eligible for treatment with an anti-vascular endothelial growth factor (VEGF) agent. Anti-VEGF therapy (combined with photocoagulation in case 2) was associated with improvements detectable by multimodal retinal imaging already after 1 month. The benefits of the therapy were sustained and the patient of case 3 could be switched to a pro re nata regimen of anti-VEGF, after 1 year

Clinical case 1

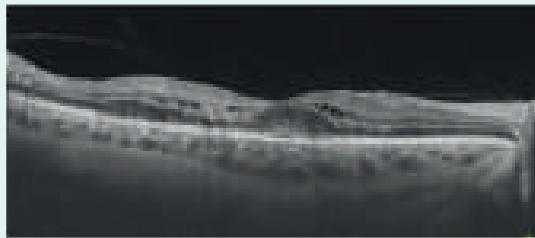
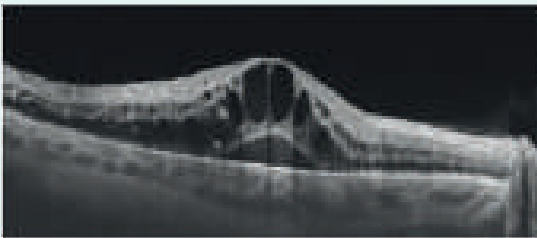
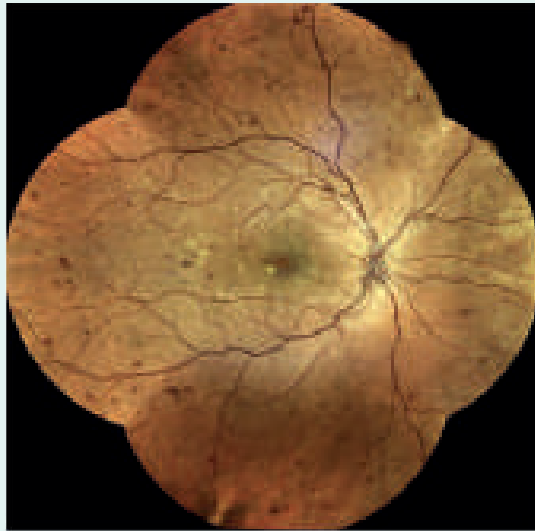
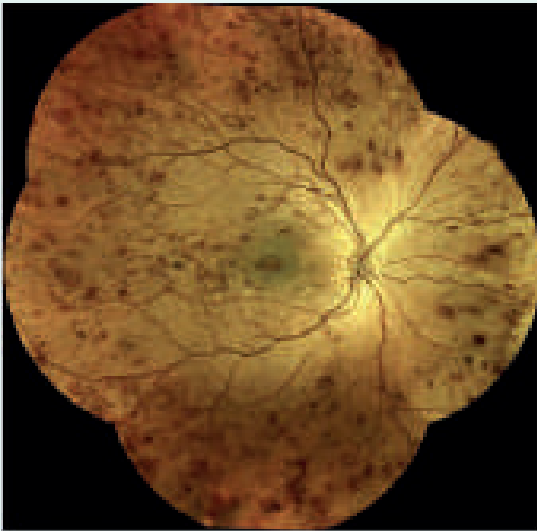
The 37-year old female patient of this case had a 20-year history of type 1 diabetes mellitus and presented with DME affecting both eyes (glycosylated hemoglobin, HbA1c, at presentation, 8.9%). DME was characterized by the presence of subretinal fluid and a few hyperreflective foci (HRF) on optical coherence tomography (OCT) scans. DR manifested with hemorrhage at multiple sites. At presentation, best corrected visual acuity (BCVA) was 20/50 for both eyes; central retinal thickness (CRT) was 818 μm at the right eye and 729 μm at the left eye. Both eyes

were phakic. Treatment of both eyes with an anti-VEGF agent was initiated as recommended for DME (one monthly injection for five times, followed by one injection every two months). Treatment was associated with edema resolution and a substantial improvement of visual acuity. After 12 months of treatment, BCVA had improved to 20/32 in the right eye and 20/20 in the left eye; CRT had decreased, respectively, to 311 μm and 287 μm . As shown in the color fundus photographs of **Figure 1**, DR also improved considerably with anti-VEGF treatment in both eyes.

Right eye

Baseline
BCVA 20/50; CRT 818 μm

12 months
BCVA 20/32; CRT 311 μm



Left eye

Baseline
BCVA 20/50; CRT 729 μm

12 months
BCVA 20/20; CRT 287 μm

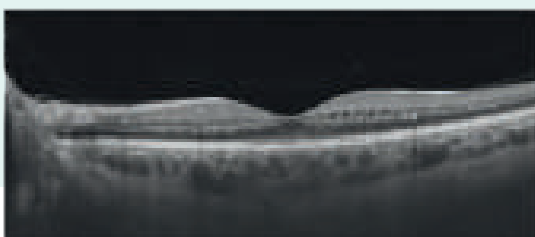
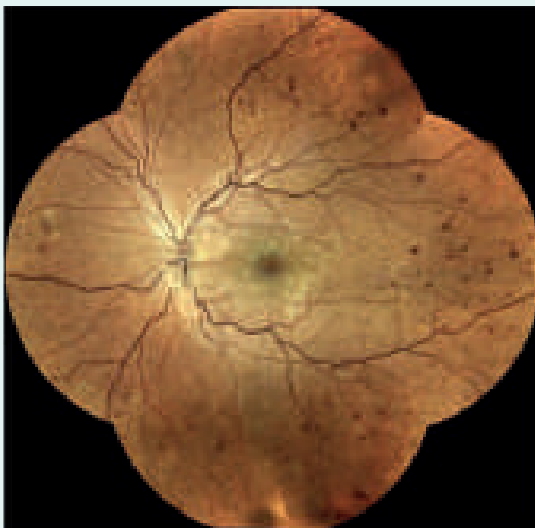


Figure 1. Color fundus photographs (upper panels) and OCT scans (lower panels) of the right and left eyes at presentation and after 12 months of intravitreal anti-VEGF treatment.

Clinical case 2

Figure 2 shows ultrawide-field (UWF) color fundus photographs and wide-field optical coherence tomography angiography (WF OCTA) images of both eyes of a 57-year old man presenting with uncontrolled type 1 diabetes (HbA1c, 12.9%). These photographs taken at presentation revealed the presence of proliferative DR without DME in both eyes (**Figure 2A** and **B**). WF OCTA (15×9 mm² montage) showed the presence of new vessels appearing as multiple, tangled flow signals associated with non-perfusion retinal areas

in both eyes (**Figure 2C** and **D**). The patient received a combined treatment with intravitreal anti-VEGF therapy and pattern panretinal photocoagulation. After 1 month of this regimen, UWF fundus photography and WF OCTA showed partial disease resolution in the right eye (**Figure 3A** and **C**) and complete disease resolution in the left eye (**Figure 3B** and **D**). Of note, WF OCTA imaging was able to visualize persistent areas of retinal non-perfusion in both eyes also after treatment (**Figure 3C** and **D**).

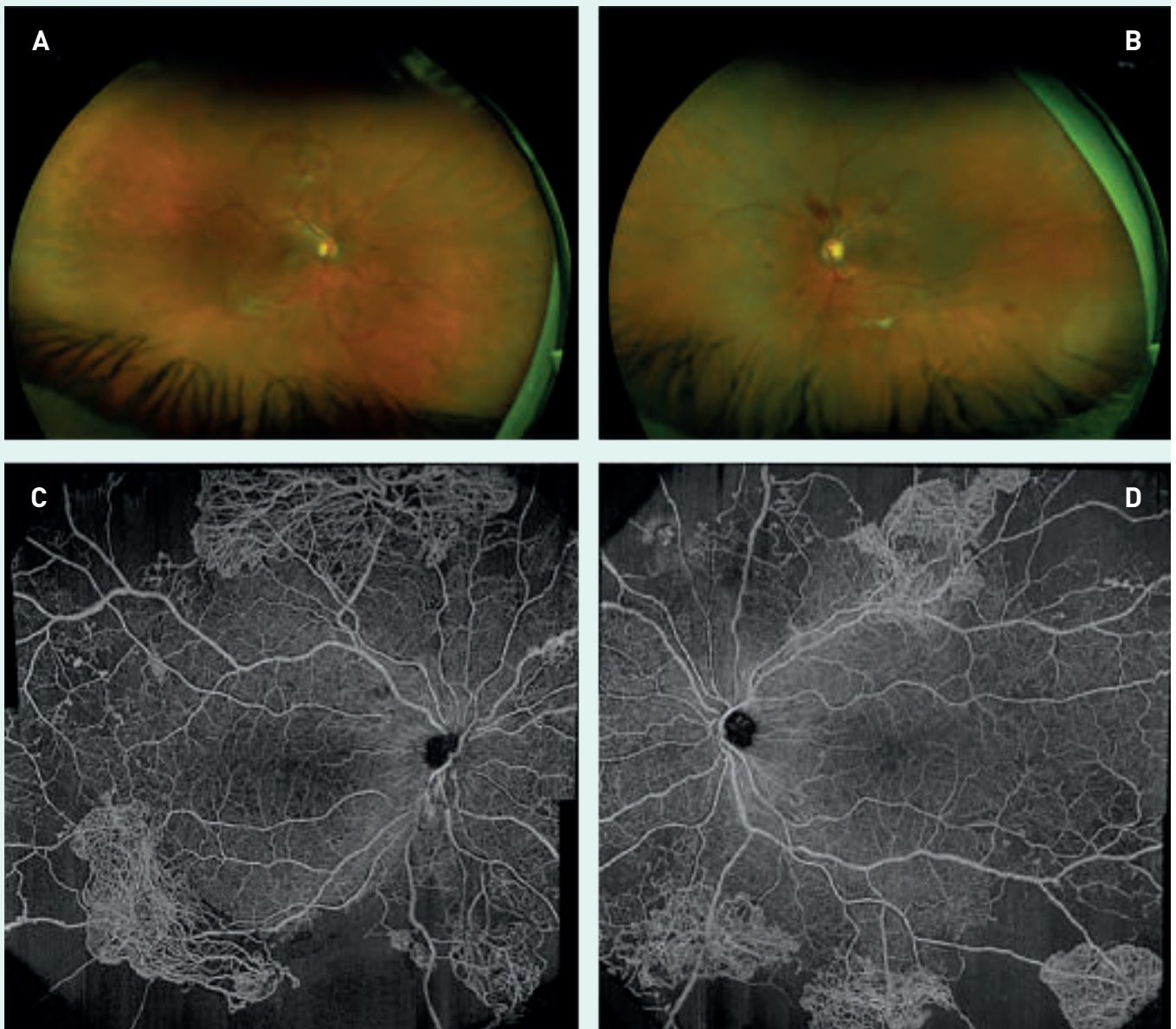


Figure 2. UWF color fundus photographs of the right (A) and left (B) eyes and WF OCTA of the right (C) and left (D) eyes at presentation.

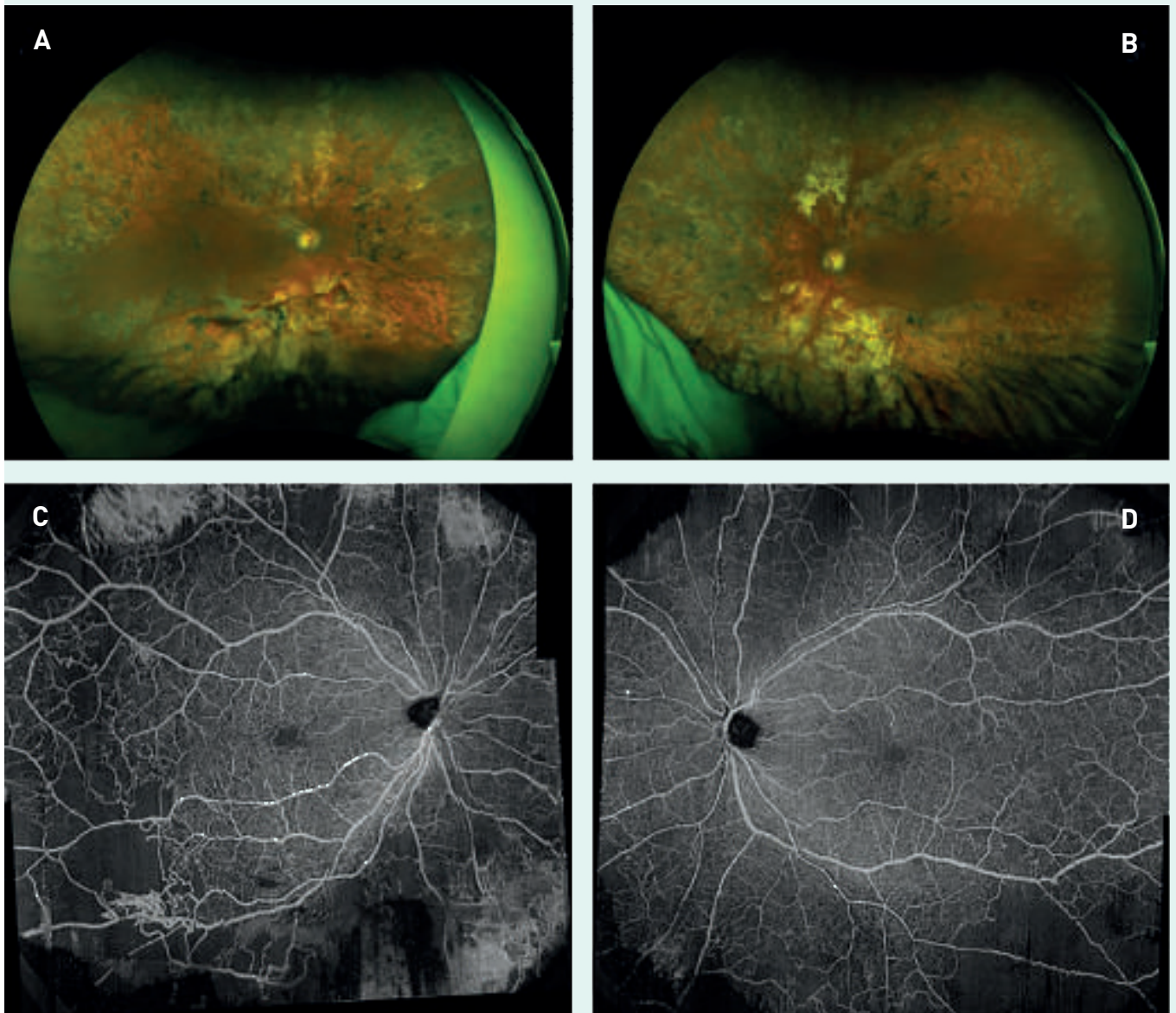


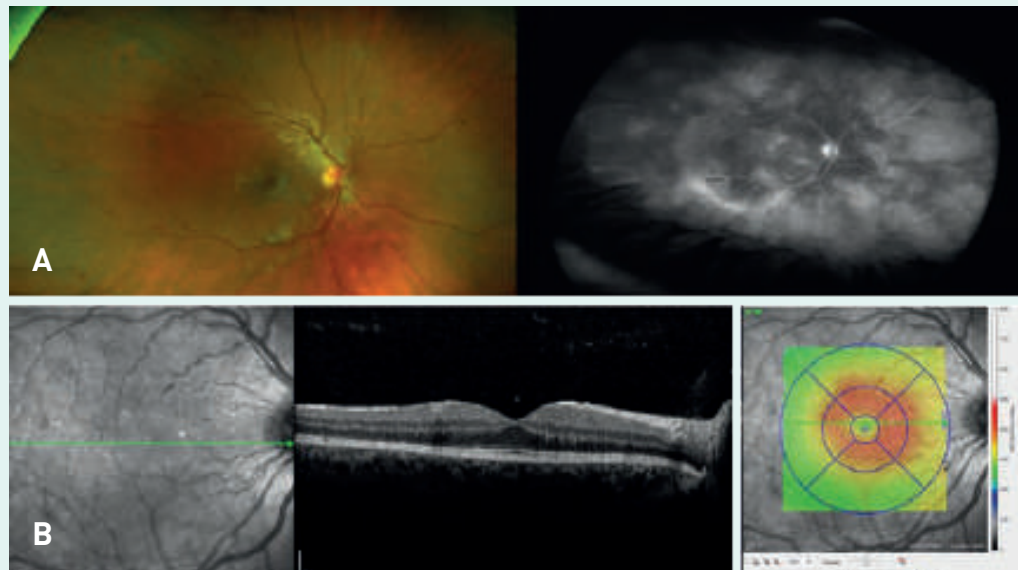
Figure 3. UWF color fundus photographs of the right (A) and left (B) eyes and WF OCTA of the right (C) and left (D) eyes after 1 month of combined treatment with anti-VEGF and pattern panretinal photocoagulation.

Clinical case 3

This patient was a 20-year old woman with type 1 diabetes and systemic hypertension. The patient had been diagnosed with diabetes at the age of 10 years. She had been using an insulin infusion pump for 3 years. At presentation, her HbA1c was 7.5%. Both eyes were phakic and intraocular pressure was normal (14 mmHg in the right eye and 12 mmHg in the left eye). BCVA was 10/10 for the right eye and 8/10 for the left eye. CRT was 332 μm in the right eye and 394 μm in the left eye. Color fundus photography and fluorescein angiography (FA) revealed signs of severe non-proliferative DR in the right eye and proliferative DR in the left eye with neovascularization on the optic disc. OCT scans showed foveal thickness increase (more pronounced in the left eye) with a small amount of intra- and subretinal fluid (Figure 4). One month after presentation, OCT and other parameters indicated a substantial disease worsening in the left eye (BCVA 6/10, CRT 725 μm) (Figure 5). Intravitreal anti-VEGF therapy was therefore initiated in the left eye as recommended (one monthly injection for five times, followed by one injection every two months). One month following the first five intravitreal injections of anti-VEGF, OCT showed a substantial improvement of the left eye (Figure 6), paralleled by improved BCVA

(10/10) and decreased CRT (317 μm). These improvements were sustained with the bi-monthly regimen of anti-VEGF (BCVA 10/10, CRT 315 μm) associated with a regression of the neovascularization of the optic disc, while imaging and clinical parameters of the right eye remained stable (Figure 7). After 1 year, anti-VEGF therapy was administered according to a pro re nata regimen for 2 years (BCVA 10/10, CRT 275 μm at 2 years) (Figure 8).

Right eye



Left eye

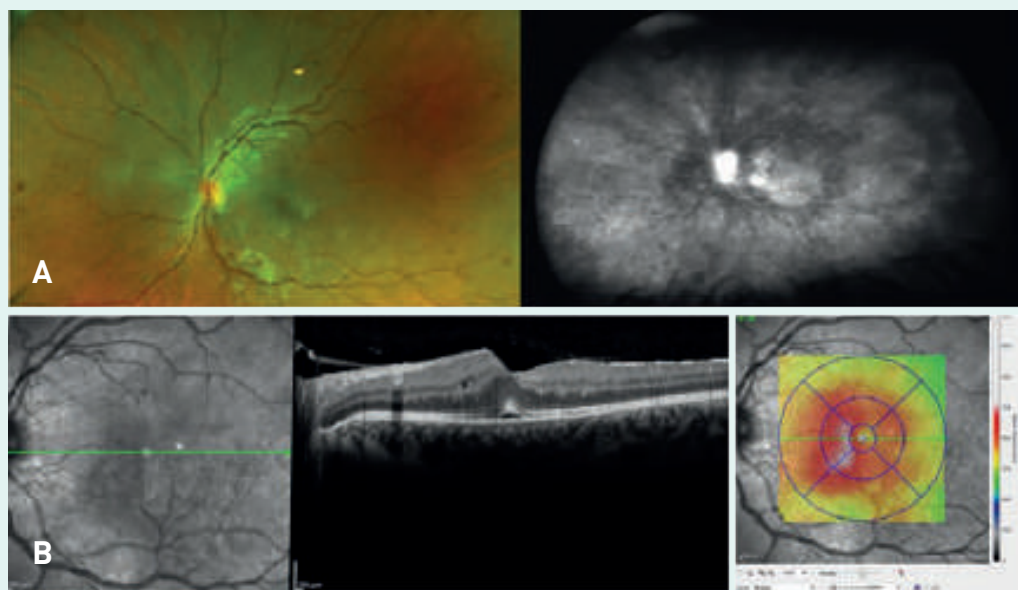


Figure 4. Right and left eyes at presentation. A, UWF fundus photography and UWF FA; B, OCT.

Left eye

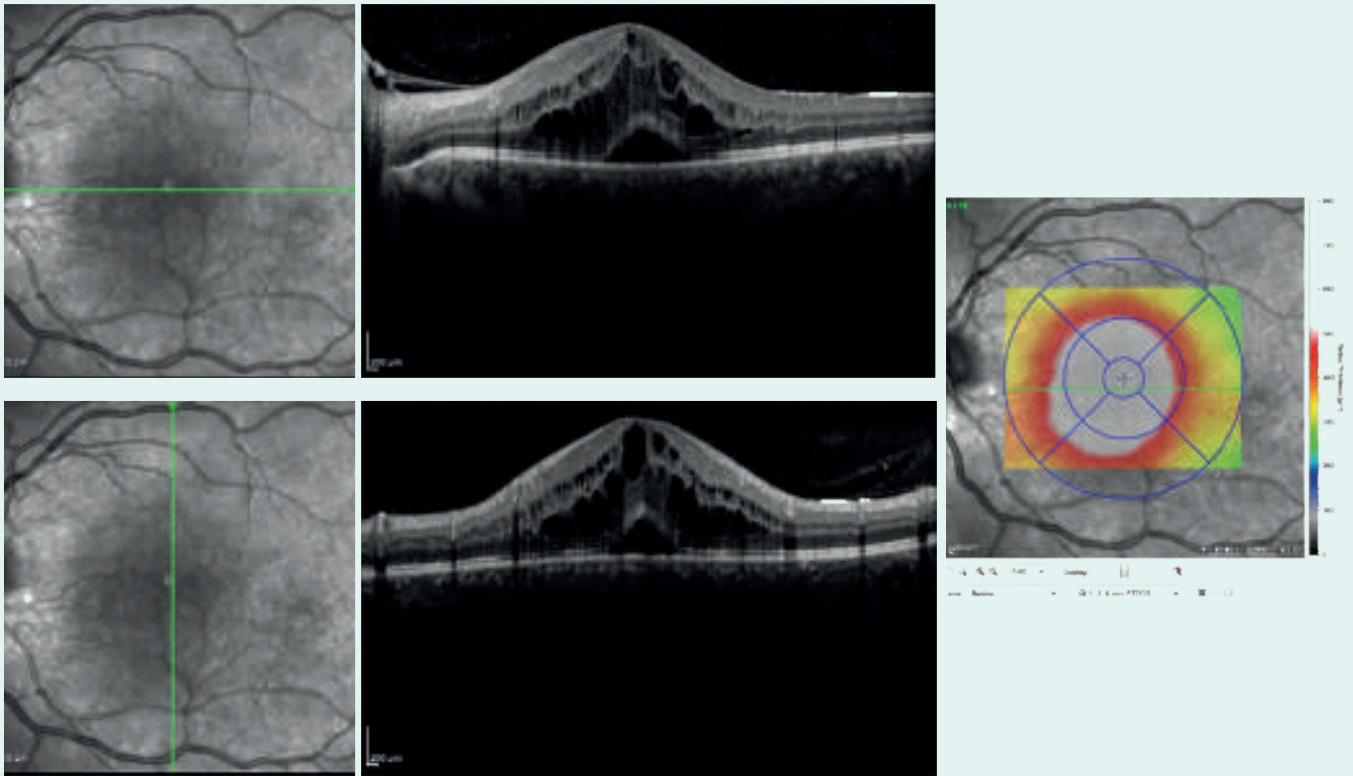


Figure 5. OCT of left eye 1 month following presentation.

Left eye

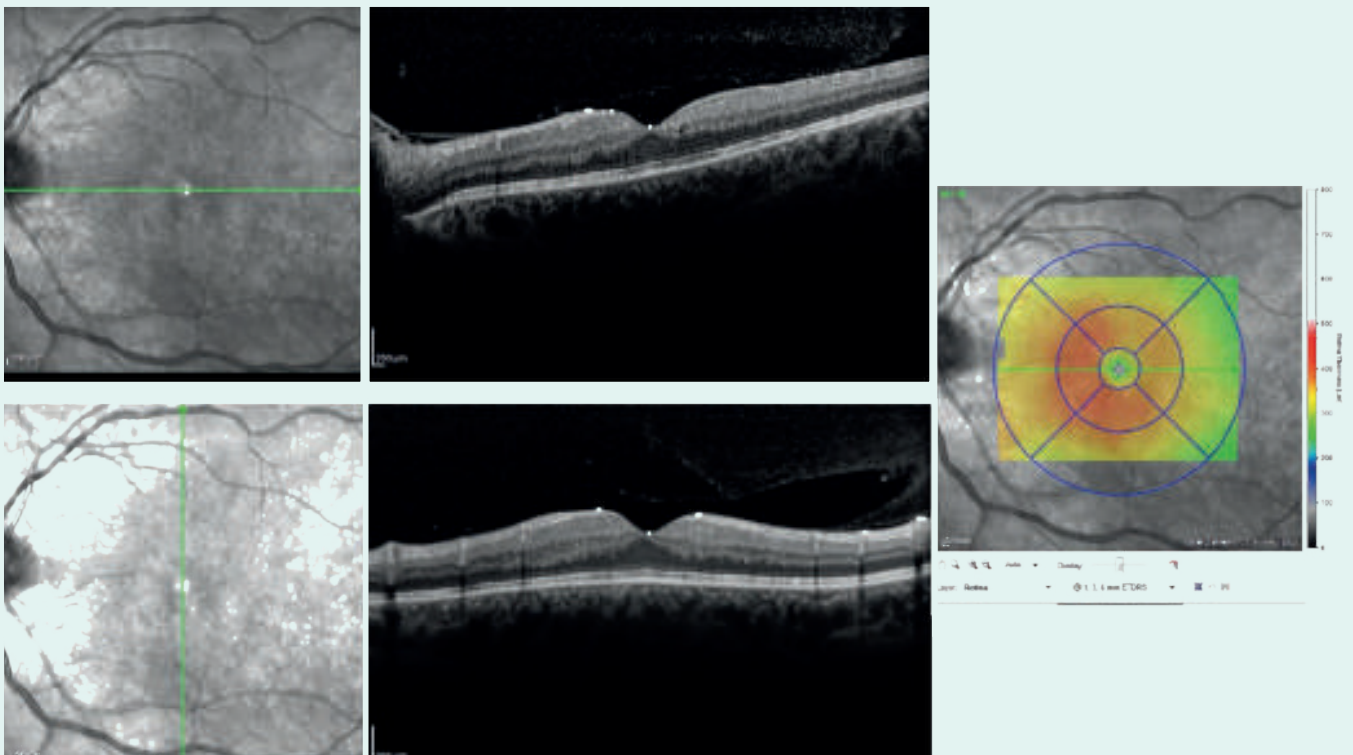


Figure 6. OCT of left eye at 1 month after five monthly anti-VEGF intravitreal injections.

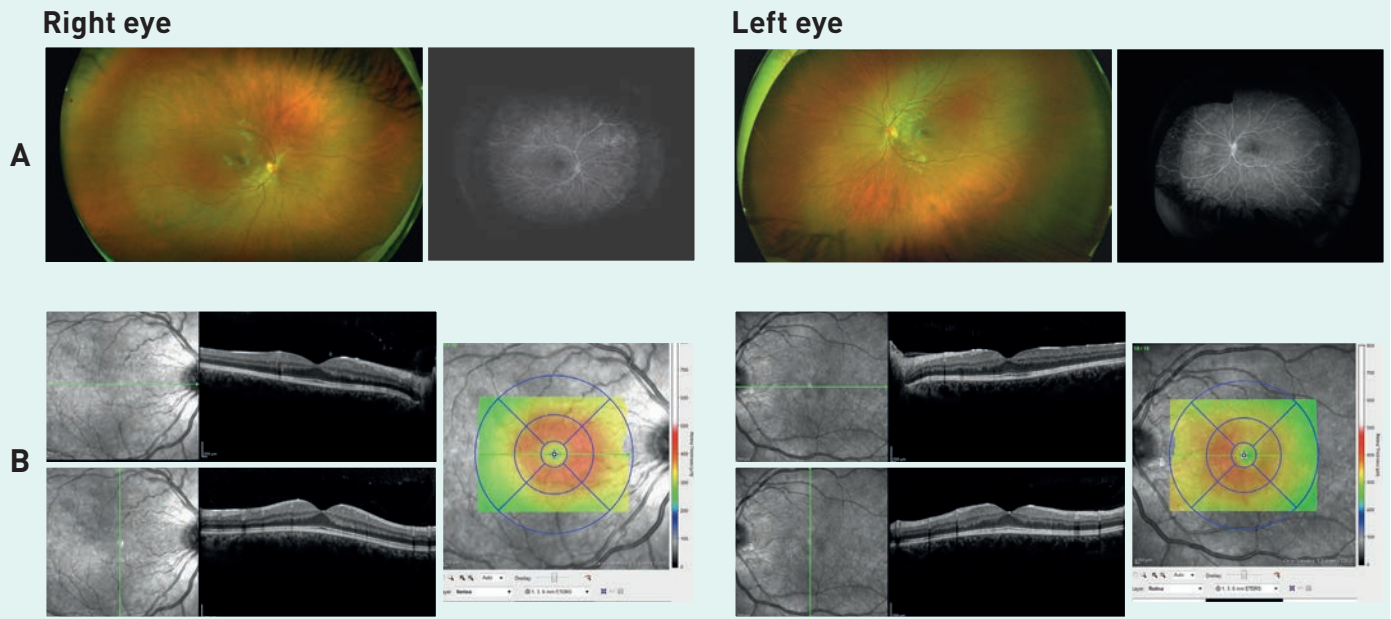


Figure 7. Imaging of right and left eyes 1 year after treatment (loading phase and q8) to the left eye. A, UWF fundus photography and UWF FA; B, OCT.

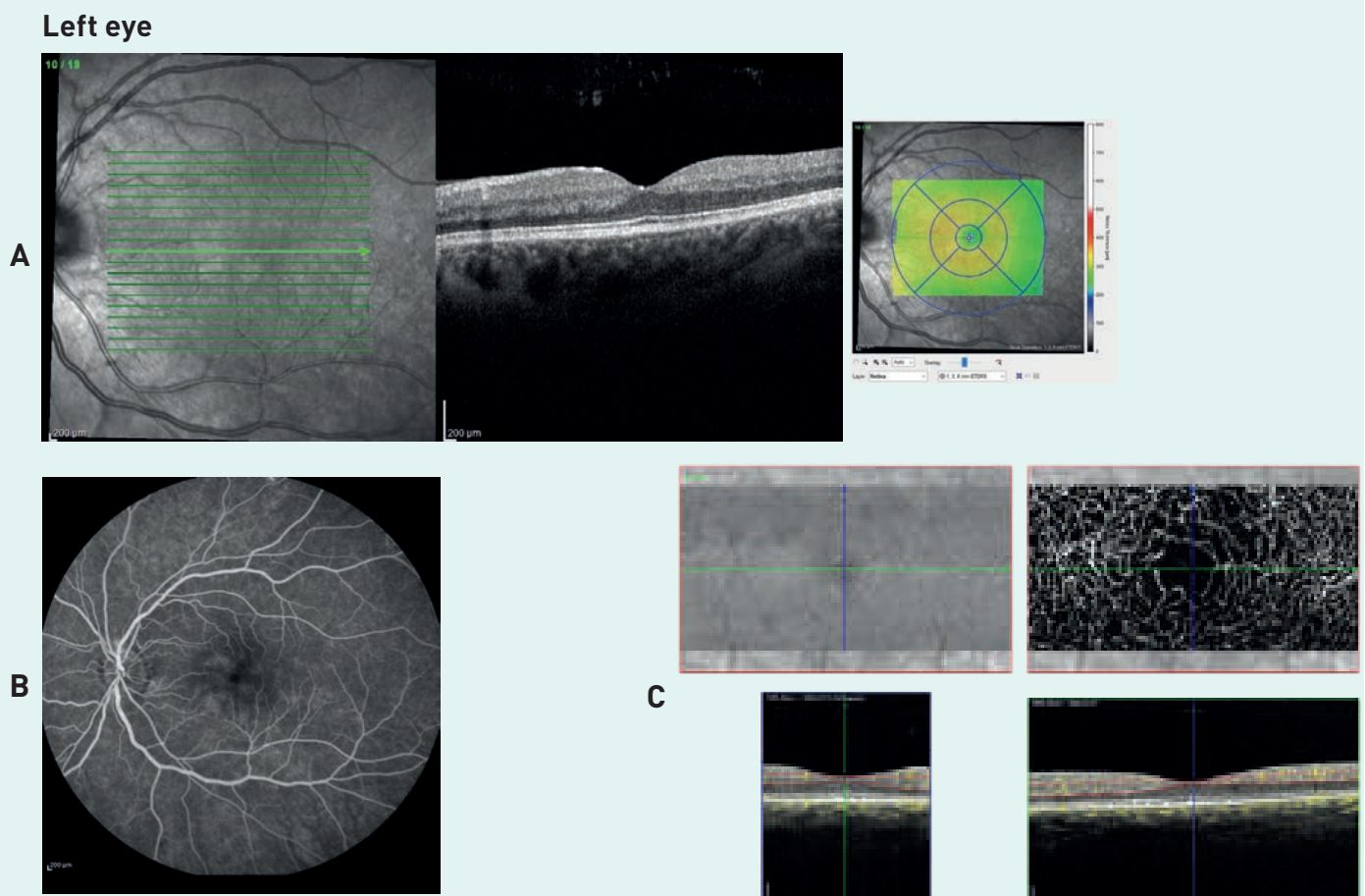


Figure 8. Imaging of left eye at 2 years of follow-up. A, OCT; B, FA; C, OCT angiography en-face images (upper panels) and corresponding B-scans with flow (lower panels).

5. Future perspectives

In this final chapter we provide an overview of the most relevant developments in the management of diabetic retinopathy (DR) and diabetic macular edema (DME) that can be expected in the near future

Artificial Intelligence applications for diabetic retinopathy and diabetic macular edema

Screening for DR coupled with early referral and treatment has proven a valuable strategy for preventing vision loss and blindness. Thus, retinopathy screening programs have been instituted worldwide. DR screening can be performed by different healthcare professionals (ophthalmologists, general practitioners, optometrists, medical technicians, and medical photographers) and is usually based on color fundus photographs that can be acquired with different methods^[1]. Evidence indicates, however, that the adherence to the recommended screening schedule is far from optimal for a variety of reasons, including high costs and low accessibility to eye examination services^[2]. In addition, the global prevalence of diabetes has dramatically increased over the past few decades. This trend is expected to continue in the future due to the aging population and the epidemic of obesity worldwide, posing a serious challenge to the feasibility of conventional screening programs^[2]. Therefore, there is an urgent need to improve DR screening in terms of accessibility, efficiency, rapidity, and optimization of resource use. Telemedicine and automated eye exams based on AI are attracting considerable attention as key strategies for potentiating current DR screening programs^[3,4] (**Figure 1**).

The major advances in digital and telecommunication technologies in recent years are no doubt contributing to the implementation of telemedicine in routine clinical practice and

the development of AI-based medical assessments^[4]. Telemedicine, defined as the delivery of medical care using communication technologies that allow physicians to visit their patients remotely, has been practiced for several decades but the global healthcare crisis caused by the pandemic of coronavirus disease 2019 (COVID-19) has renewed the interest for it. The unprecedented crisis of the past two years has indeed forced healthcare systems worldwide to adopt innovative technologies for the remote delivery of medical services.

The concept of “artificial intelligence” was introduced in the late ‘50s and refers to the development of computational machines that mimic neural networks and replicate human intelligence to perform complex tasks^[1,3,5]. Machine learning is an AI process in which a machine is capable of programming itself and learning how to perform a task like, for example, distinguishing fundus photographs of DR from fundus photographs of eyes with no DR. The learning process involves training the machine by submitting to it a large number of fundus images (the training dataset) previously annotated by experts as DR or non-DR. Based on the training dataset, the machine learns to produce its own answers; these are checked by the machine against the correct ones and the learning process is repeated until a pre-defined level of correct answers is achieved^[3]. Deep learning is a type of machine learning technology, which was developed in the early 2000s and is frequently used in current AI-based devices. The term “deep” refers to the fact that the artificial neural network has multiple layers with distinct functions, which ensures greater accuracy compared with other AI methods and allows the performance of demanding tasks^[3,5].

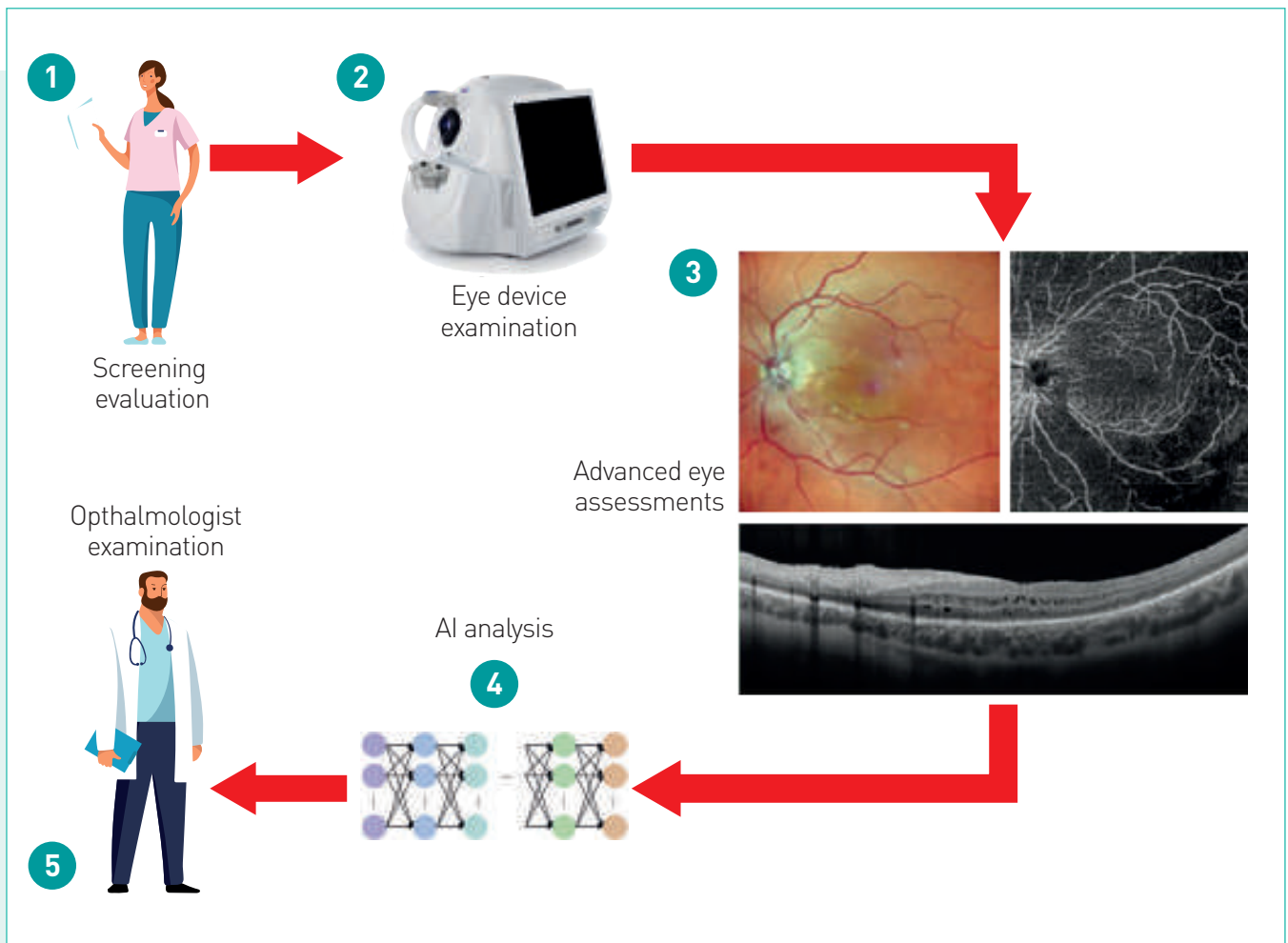


Figure 1. Steps involved in telemedicine- and AI-based screening of DR.

In medicine, the main application of deep learning has so far been in specialties that are strongly based on imaging analysis, including radiology, pathology, dermatology, and ophthalmology^[6]. Deep learning systems have been successfully used for the diagnosis of tuberculosis from chest X-ray images, malignant melanoma on skin photographs, and lymph node metastases on biopsies of breast cancer patients^[1]. Ophthalmology is also witnessing diagnostic innovations brought about by AI^[1,3,4]. Of note, the first fully automated AI system to be granted approval by the FDA in any field of medicine was a tool for the detection of DR^[7]. Deep learning-based techniques have been developed for the detection of DR, glaucoma, AMD, and retinopathy of prematurity, mostly on fundus photographs^[1]. Studies describing the application of deep learning to the analysis of optical coherence tomography (OCT) scans of

patients with various ocular conditions have also been reported^[1].

In recent years, several AI-based algorithms for automated DR screening using fundus photographs have become commercially available and, since 2016, several validation studies have been published^[8-11]; reviewed in^[1,3,4]. These studies have consistently shown that deep learning systems are capable of detecting DR on color fundus photographs with high sensitivity and specificity comparable to that of human graders, suggesting the potential of AI for reliable and efficient DR screening. The prospective pivotal trial, that led to the US FDA authorization of the first AI-based tool for clinical use, enrolled 900 diabetes patients with no history of retinopathy and compared the diagnostic performance of the system to an independent, high-quality standard that included fundus imaging and OCT scans^[7]. With

a sensitivity of 87.2% and a specificity of 90.7% in detecting referable DR, the system met the pre-specified superiority endpoints and demonstrated that fully automated AI-based screening of DR is feasible in the setting of primary care^[7]. A recent meta-analysis of 60 studies (and 445,175 interpretations) of machine learning-based systems for DR detection on fundus photographs confirmed that automated systems provide accurate diagnosis of referable disease^[2].

Given the importance of multimodal imaging for the early diagnosis of DR and DME, as discussed in the previous Chapters of this book, it is not surprising that deep learning has been implemented also for the automated interpretation of OCT scans^[1,4]. OCT provides a detailed view of retinal layers that are not visible on fundus photographs, and it is crucial for the detection and management of DME. Several studies have evaluated the applicability of deep learning to OCT scans for the identification and classification of DME and other ophthalmologic conditions, and have suggested the feasibility of AI-based OCT interpretation in clinical practice^[12-16] (reviewed by Ting et al.^[1] and Li et al.^[4]). In a recent study, an ensemble AI system, which consisted of multiple deep learning and classical machine learning models, was shown to accurately predict post-treatment central foveal thickness and best-corrected visual acuity based on OCT scans^[17]. Thus, AI may be useful also for predicting the efficacy of anti-VEGF therapy.

The results emerging from studies on deep learning-based diagnostic and prognostic systems are no doubt promising, but several issues surrounding this approach and its implementation in clinical practice have been raised, including: quality of dataset used for machine training and algorithm validation; algorithm transparency; data security and privacy; acceptance by patients and clinicians; regulatory and medico-legal questions (including liability and patient safety)^[1,5]. The accuracy of diagnosis relies heavily on the annotated data used for machine training as well as for algorithm validation. The quality of the images to be diagnosed is also important. A recent study compared the diagnostic performance of an automated AI-based DR algorithm on images taken with

two different technologies, a conventional flash fundus camera and a LED confocal scanner^[18]. The latter system had previously demonstrated higher diagnostic accuracy than fundus photography^[18]. The AI-automated system achieved significantly greater sensitivity and specificity on images acquired with the LED confocal scanner than with the conventional flash fundus camera^[18].

Data standardization and transparency of AI-based techniques will be crucial to ensure high quality and patient safety. Transparency is relevant also for explaining the diagnostic results. Current deep learning systems are inscrutable black-boxes and for most of them it is unclear how a certain diagnostic decision was made. The inability to understand the processes underlying the diagnostic algorithm may have a negative impact on its acceptance by patients and clinicians. Great efforts are being made by health authorities worldwide to define the regulatory framework for AI use in medicine^[19]. According to the US FDA, AI-based technologies are distinct from conventional medical devices. In a joint effort with the International Medical Device Regulators Forum (IMDRF), the FDA has defined a new category called Software as Medical Device (SaMD). A formal definition of SaMD and an updated framework regulating this new category have been issued by the IMDRF^[20]. IMDRF guidance on AI is continuously updated based on real-world performance data^[21]. According to the European Commission, “software programs created with the clear intention to be used for medical purposes are considered medical devices”^[22,23]. AI-based technologies appear to meet this definition. The General Data Protection and Regulation (GDPR) issued by the European Union and effective since 2018 states, in one of its articles, the right of citizens to receive an explanation for algorithm decisions. It has been pointed out that this statement may potentially limit the use of current black-box algorithms and slow down the implementation of AI in clinical practice^[6,24]. In the long-term, however, regulations that promote transparency, patient trust and engagement may improve implementation and acceptance of AI strategies in healthcare^[6].

The future of multimodal imaging for the management of DR and DME will certainly in-

clude AI-based tools, which are expected to revolutionize the management of ophthalmologic diseases. Deep learning systems have proven capable of interpreting large sets of fundus photographs and OCT scans, providing accurate diagnosis and classification of DR and

DME. These systems should therefore contribute to improving screening programs and DME management. Further research is required to establish whether the implementation of AI in clinical practice will also improve the outcomes of patients with DR.

REFERENCES

1. Ting DSW, Pasquale LR, Peng L, et al. Artificial intelligence and deep learning in ophthalmology. *Br J Ophthalmol* 2019;103:167-75
2. Wu J-H, Liu TYA, Hsu W-T, et al. Performance and limitations of machine learning algorithms for diabetic retinopathy screening: meta-analysis. *J Med Internet Res* 2021;23(7):e23863
3. Hogarty DT, Mackey DA, Hewitt AW. Current state and future prospects of artificial intelligence in ophthalmology: a review. *Clin Exp Ophthalmol* 2019;47:128-39
4. Li J-PO, Liu H, Ting DSJ, et al. Digital technology, tele-medicine and artificial intelligence in ophthalmology: a global perspective. *Prog Retin Eye Res* 2021;82:100900
5. Grzybowski A, Brona P, Lim G, et al. Artificial intelligence for diabetic retinopathy screening: a review. *Eye* 2020;34:451-60
6. He J, Baxter SL, Xu J, et al. The practical implementation of artificial intelligence technologies in medicine. *Nat Med* 2019;25(1):30-6
7. Abramoff MD, Lavin PT, Birch M, et al. Pivotal trial of an autonomous AI-based diagnostic system for detection of diabetic retinopathy in primary care offices. *npj Digital Med* 2018;1:39
8. Gulshan V, Peng L, Coram M, et al. Development and validation of a learning algorithm for detection of diabetic retinopathy in retinal fundus photographs. *JAMA* 2016;316(22):2402-10
9. Ting DSW, Cheung CY-L, Lim G, et al. Development and validation of a deep learning system for diabetic retinopathy and related eye diseases using retinal images from multiethnic populations with diabetes. *JAMA* 2017;318(22):2211-23
10. Gargeya R, Leng T. Identification of diabetic retinopathy using deep learning. *Ophthalmology* 2017;124(7):962-9
11. Raumviboonsuk P, Krause J, Chotcomwongse P, et al. Deep learning versus human graders for classifying diabetic retinopathy severity in a nationwide screening program. *npj Digital Med* 2019;2:25
12. De Fauw J, Ledsam JR, Romera-Paredes B, et al. Clinically applicable deep learning for diagnosis and referral in retinal disease. *Nat Med* 2018;24(9):1342-50
13. Kermany DS, Goldbaum M, Cai W, et al. Identifying medical diagnoses and treatable diseases by image-based deep learning. *Cell* 2018;172:1122-31
14. Schlegl T, Waldstein SM, Bogunovic H, et al. Fully automated detection and quantification of macular fluid in OCT using deep learning. *Ophthalmology* 2018;125(4):549-58
15. Kapoor R, Whigham BT, Al-Aswad LA. Artificial intelligence and optical coherence tomography imaging. *Asia Pac J Ophthalmol* 2019;8:187-94
16. Wu Q, Zhang B, Hu X, et al. Detection of morphologic patterns of diabetic macular edema using a deep learning approach based on optical coherence tomography images. *Retina* 2021;41:1110-7
17. Liu B, Zhang B, Hu Y, et al. Automatic prediction of treatment outcomes in patients with diabetic macular edema using ensemble machine learning. *Ann Transl Med* 2021;9(1):43
18. Sarao V, Veritti D, Lanzetta P. Automated diabetic retinopathy detection with two different retinal imaging devices using artificial intelligence: a comparative study. *Graefes Arch Clin Exp Ophthalmol* 2020;258(12):2647-54
19. European Commission. White paper. On artificial intelligence - a European approach to excellence and trust. https://ec.europa.eu/info/publications/white-paper-artificial-intelligence-european-approach-excellence-and-trust_en
20. IMDRF SaMD Working Group. Software as a Medical Device (SaMD): Key Definitions (International Medical Device Regulators Form, 2013). <https://www.imdrf.org/sites/default/files/docs/imdrf/final/technical/imdrf-tech-131209-samd-key-definitions-140901.pdf>
21. Software as a Medical Device Working Group. Software as a Medical Device (SaMD): Clinical Evaluation (United States Food and Drug Administration, 2017). <https://www.fda.gov/regulatory-information/search-fda-guidance-documents/software-medical-device-samd-clinical-evaluation>
22. European perspective on AI medical devices. <https://bg.legal/en/europese-perspectieven-op-ai-medische-hulpmiddelen>
23. Cohen GI, Evgeniou T, Gerke S, Minssen T. The European artificial intelligence strategy: implications and challenge for digital health. *Lancet Digit Health* 2020;2(7):e376-e379
24. Goodman B, Flaxman S. European Union regulations on algorithmic decision-making and a "right to explanation". *AI Mag* 2017;38(3):50-7

